UNIVERSIDADE D
COIMBRA

Francisco José Dias Roque

CODE-MODULATED VISUAL EVOKED POTENTIALS FOR BCI AND BIOMETRIC AUTHENTICATION

Dissertação no âmbito do Mestrado Integrado em Engenharia Eletrotécnica e de Computadores, na especialização de Automação, orientada pelo Professor Doutor Urbano José Carreira Nunes e pelo Professor Doutor Gabriel Pereira Pires e apresentada ao Departamento de Engenharia Eletrotécnica e de Computadores da Faculdade de Ciências e Tecnologias da Universidade de Coimbra.

Outubro de 2020

1 2  9 0

UNIVERSIDADE D
COIMBRA

Code-Modulated Visual Evoked Potentials for BCI and Biometric Authentication

Francisco José Dias Roque

Coimbra, October of 2020

FACULDADE DE
CIÊNCIAS E TECNOLOGIA
UNIVERSIDADE D
COIMBRA

Code-Modulated Visual Evoked Potentials for BCI and Biometric Authentication

Dissertation supervised by Professor Doctor Urbano José Carreira Nunes and Professor Doctor Gabriel Pereira Pires and submitted to the Electrical and Computer Engineering Department of the Faculty of Science and Technology of the University of Coimbra, in partial fulfillment of the requirements for the Degree of Master in Electrical and Computer Engineering, specialization in Automation.

Supervisors:

Prof. Dr. Urbano José Carreira Nunes

Prof. Dr. Gabriel Pereira Pires

Jury:

Prof. Dr. Fernando Manuel dos Santos Perdigão

Prof. Dr. Paulo José Monteiro Peixoto

Prof. Dr. Urbano José Carreira Nunes

Coimbra, October of 2020

Acknowledgments

O trabalho que aqui é apresentado não seria possível sem o apoio de todos aqueles com quem convivo diariamente. Há no entanto que endereçar um agradecimento especial a todos os professores com que me cruzei durante o meu percurso académico.

Gostaria de começar por agradecer aos meus orientadores toda a sua ajuda, as discussões enriquecedoras e os conhecimentos que foram fundamentais para a concretização deste trabalho, induzindo à curiosidade e entusiasmo ao longo do projeto.

A toda a equipa do laboratório, em especial ao João Perdiz, ao Luís Garrote e à Mine Yasemin a constante disponibilidade e ajuda. Um especial agradecimento a todos os participantes nos testes da minha tese pela boa vontade sempre que era pedido.

A toda a minha família, que foram o meu pilar ao longo de todos os momentos nestes últimos anos. Em especial à minha Mãe, ao meu Pai, à minha Irmã e aos meus Avós* por todo o apoio, carinho e força ao longo de toda a minha vida.

Aos meus amigos de curso, um grande obrigado por todos os momentos vividos ao longo dos últimos 5 anos, obrigado pela amizade, pelo apoio, pelos momentos de entreajuda que foram fundamentais para ultrapassar os momentos menos fáceis.

À Inês, um grande obrigado pelo apoio, motivação e estares sempre presente quando era necessário.

A todos aqueles que fizeram parte deste percurso e não foram mencionados até aqui! À cidade que é Coimbra!

A todos, um muito obrigado!

Esta dissertação foi realizada no âmbito do projeto
B-RELIABLE:PTDC/EEI-AUT/30935/2017,
sendo financiados pelo FEDER através dos programas CENTRO2020 e a Fundação para a Ciência e a Tecnologia (FCT).

Esta dissertação foi desenvolvida em colaboração com:

1 2 90 UNIVERSIDADE D COIMBRA
deer.uc DEPARTAMENTO DE ENGENHARIA ELETROTÉCNICA E DE COMPUTADORES
INSTITUTE OF SYSTEMS AND ROBOTICS UNIVERSITY OF COIMBRA
FCT Fundação para a Ciência e a Tecnologia
CENTRO 2020
PORTUGAL 2020
UNIÃO EUROPEIA Fundo Social Europeu

Abstract

A Brain-Computer Interface (BCI) provides a direct communication pathway between the brain and an external device. BCI systems have improved significantly in recent years, but are still unsuitable for many applications and not prepared for contexts out of the lab. BCI has been researched primarily as a communication device for people with severe motor disabilities, but a wide range of new areas of application is emerging. One of these areas is personal identification/recognition in security systems.

The goal of this dissertation was to explore the use of Code-modulated Visual Evoked Potentials (C-VEP) in two different contexts: as a BCI system for interaction, and as user identifier. The C-VEP is a neural mechanism that results from a visual stimulus modulated by a given bit pattern called pseudorandom binary sequence (PRBS). The use of EEG and in particular C-VEP has been relatively unexplored in the context of user identification. To evaluate the feasibility of these approaches, we tested an extensive set of feature extraction methods (spatial domain and time domain), combined with different normalization methods.

In addition to these methods, the first and second derivatives of the EEG data were also proposed as a preprocessing step, to explore the effect of different dynamics of the signal. Initially, the methods were applied and tested with public benchmark datasets and after with data gathered with our framework and acquisition setup. We proposed and validated our own binary stimulation sequence, and we tested several methods of complexity to analyse the correlation between complexity and accuracy. Task-Related Component Analysis (TRCA) was the feature extraction method that attained the best accuracy, 96%, with our proposed binary sequence, in the context of user identification in a database of 10 participants. The use of EEG data derivative form showed that the first derivative of the acquired C-VEP signals improves user identification performance.

The results were promising, showing as a proof-of-concept the possibility of using C-VEP for identification and authentication systems, which might allow to develop alternative security systems in the future.

Keywords : Brain-Computer Interface (BCI), Electroencephalography (EEG), Code-modulated

Visual Evoked Potentials (C-VEP), Visual Evoked Potentials (VEP), Biometric Identification, M-Sequences, Complexity Analysis.

Resumo

Uma interface cérebro-computador (ICC) providencia uma via de comunicação direta entre o cérebro e um dispositivo externo. Os sistemas ICC têm melhorado significativamente nos últimos anos mas ainda são insuficientes para muitas aplicações e não se encontram preparados para serem aplicados a situações fora do laboratório. ICC tem sido investigado primariamente como dispositivo de comunicação para pessoas com deficiência motora grave, mas um vasto grupo de novas áreas para esta aplicação tem vindo a ser desenvolvida. Uma destas áreas é a identificação/reconhecimento pessoal nos sistemas de segurança.

O objetivo desta dissertação foi explorar o uso do Código modulado por Potenciais Visuais Evocados (C-VEP) em dois contextos diferentes: como um sistema ICC para interação e como um identificador de utilizadores. O C-VEP é um mecanismo neuronal que resulta do estímulo visual modulado por um padrão de bits denominado sequência binária pseudoaleatorizada. O uso do EEG e em particular do C-VEP tem sido relativamente inexplorado no contexto da identificação de utilizadores. Para avaliar a exequibilidade destas abordagens, testámos um extenso grupo de métodos de extração de características (domínio espacial e domínio temporal), combinado com diferentes métodos de normalização.

Em adição a esses métodos, as primeiras e segundas derivadas dos dados do EEG foram propostas como etapas de pré-processamento, de forma a explorar o efeito das diferentes dinâmicas do sinal. Inicialmente, os métodos foram aplicados e testados utilizando bases de dados públicas e posteriormente com dados coletados do nosso sistema de aquisição implementado. Nós propusemos e validámos a nossa própria sequência de estimulação binária e testámos vários métodos de complexidade para analisar a correlação entre complexidade e precisão de identificação. A Análise de Componentes Relacionados com Tarefas (TRCA) foi o método de extração que conseguiu melhor precisão, 96%, com a nossa sequência binária proposta, no contexto de identificação de utilizadores numa base de dados de 10 participantes. A utilização da forma derivada dos dados EEG revelaram que a primeira derivada dos sinais C-VEP adquiridos melhora a performance de identificação de utilizadores.

Os resultados são promissores ilustrando a prova de conceito da possibilidade de uti-

lização de C-VEP para sistemas de identificação e autenticação, o que pode permitir desenvolver sistemas de segurança alternativos no futuro.

Palavras − chave : Interface Cérebro-Computador (ICC), Eletroencefalografia (EEG), Código modulado por Potenciais Visuais Evocados (C-VEP), Identificação Biométrica, M-Sequências, Análise da Complexidade.

"There are many hypotheses in Science that are wrong.
That's perfectly alright; it's the aperture to finding out what's right."
Carl Sagan

Contents

List of Acronyms

BCI Brain Computer Interface

CCA Canonical Correlation Analysis

C-VEP Code-modulated Visual Evoked Potentials

EEG Electroencephalography

ERP Event Related Potential

ITCCA Individual Template-Canonical Correlation Analysis

ITR Information Transfer Rate

LFSR Linear-Feedback Shift Register

PRBS Pseudorandom Binary Sequences

SSVEP Steady State Visual Evoked Potential

TRCA Task-Related Component Analysis

VEP Visual Evoked Potentials

List of Figures

List of Tables

1

Introduction

This chapter presents the context and motivation of the developed work, as well as the main goals and key contributions.

1.1 Motivation and Context

In recent years, the area of Brain-Computer Interfaces (BCI) based on electroencephalography (EEG) has grown exponentially due to its enormous potential for different applications. BCI can be used to facilitate communication for people with severe motor disabilities. Particularly for people in complete locked-in state (CLIS) who have lost all motor control ability but are consciously aware, BCI may represent the single available communication channel with the external world. Moreover, BCI is being researched in many different contexts expanding the number of people who can take advantage of a BCI in areas such as neurorehabilitation (motor, cognitive, social and development disorders), driver attention and fatigue monitoring, gaming and virtual reality applications, interaction/control augmentation, education, security and other non-medical applications, such as smart houses or workplaces with the cooperation between AI (Artificial Intelligence) and IoT (Internet of Things) [1, 23]. An emergent BCI topic, explored in this dissertation, is is the use of EEG for user identification/recognition. EEG can be used to fight vulnerabilities existing in actual security and authentication systems, since it cannot be acquired by external observers and is difficult to recreate by a computer [14].

The Institute of Systems and Robotics – University of Coimbra (ISR – UC), in particular in the Human-Centered Mobile Robotics (HCMR) laboratory, has been working in many Research and Development (R&D) projects that are researching methods to improve several aspects regarding the information transfer rate, reliability, control methods and the general usability of BCI systems. One of the ongoing projects is "B-RELIABLE[1]: Boosting reliability and interaction on brain-machine interface systems integrating automatic error-detection", whose main goals are to increase the reliability of brain-machine/computer interfaces (BMI/BCI) intended to people with severe motor disabilities in communication and collaborative control applications, and to design new and more natural forms

[1]B-RELIABLE Project Link: https://sites.google.com/view/b-reliable/

of human-machine interaction (HMI) and new paradigms for neurofeedback intervention, based on the automatic detection of system/user errors from brain activity.

BCI systems face many limitations that reduce their effectiveness and use in possible applications. Two such limitations are the low reliability and low wearability of BCI systems, which make them unsuitable for many applications and not prepared for out of lab contexts (e.g., issues related to wearability, portability, and standalone computational processing and calibration) [40]. Low Information Transfer Rate (ITR) is another limitation of BCI systems, as it is only possible to detect a few commands per minute, which limits the type of applications that can be controlled (i.e., applications usually need to be adapted and simplified). Research is being carried out to overcome these limitations and to expand the range of BCI applications.

There are several neural mechanisms currently used in EEG-based BCI namely, Event Related Desynchronization (ERD) related to motor imagery, Slow Cortical Potentials (SCPs), P300 Event Related Potentials (ERP) and Visual Evoked Potentials (VEP). The ERPs result from selective attention to external events that can be visual, auditory or tactile, while VEPs are automatic responses of the visual cortex to visual stimuli gazed by the subject. Motor imagery and SCP are internally induced and depend on user's mental strategies. VEPs can be grouped into two approaches, Steady-State Visual Evoked Potential (SSVEP) and Code-modulated Visual Evoked Potential (C-VEP). C-VEP was the neural mechanism researched in this dissertation in two different contexts: target selection and user identification. C-VEP approaches have several advantages over ERP and motor imagery, particularly, they allow for a higher number of possible commands, leading to a higher information transfer rate (ITR), they provide higher communication speed, and usually they do not require training [9]. However, VEP-BCIs depend on eye movements to gaze the stimulus and cause some eye discomfort due to the strong flickering. In a C-VEP based BCI, the external stimulus is a flicker coded by a number of bits called pseudorandom binary sequence (PRBS). A C-VEP signal is evoked in the occipital area, containing the visual target information. Then, the BCI system executes the signal processing algorithms translating the target that the person is gazing.

1.2 Goals and Contributions

The main objective of this dissertation was the use of Code-modulated Visual Evoked Potential (C-VEP) in two different contexts:

1. **C-VEP BCI:** development of a C-VEP based BCI for computer interaction and control of home devices. Using different stimulation sequences, each one associated with a command, we applied a C-VEP decoder to discriminate different commands;

2. **C-VEP identification:** use C-VEP as a security system for people identification. Here, using a single sequence stimulation we analyzed the subjects' unique digital

signatures from EEG to allow the identification of people whose EEG data were previously recorded in a database.

The methods were tested and validated using public datasets, and the best methods were tested later with data collected with the EEG setup (g.USBamp and Unicorn) and framework developed in the HCMR-ISR laboratory.

Figure 1.1 shows the general pipeline of the BCI system that was implemented for the two approaches (SSVEP/C-VEP BCI and C-VEP user identification), which share most of the methods. The blocks in black (EEG Signal Acquisition, Preprocessing and Feature Extraction Methods) represent the BCI system modules common to both approaches.

The visual stimuli are synchronized with the EEG signal acquisition system. This is a crucial requirement because visual evoked potentials are time and phase-locked with the stimuli.

For the EEG preprocessing, basic filtering was applied and then the signal was normalized following different approaches. The application of the first derivative of the EEG signals was also proposed as a preprocessing step contributing to an improvement in the classification accuracy for most of the feature extraction methods.

The implemented feature extraction methods followed two approaches, namely, methods that explore the spatial correlation of EEG data (Individual Template CCA and Task-Related Component Analysis) and methods based on the distance or correlation between time series of EEG signals (Pearson Correlation Coefficient, Cosine Similarity and Dynamic Time Warping). Additionnaly, the Welch and Cepstrum methods were implemented for SSVEP detection. The SSVEP paradigm was used in the initial phase of the project, as a preliminary step to move forward to C-VEPs detection. Since SSVEP is a much more established approach in BCI, but sharing many methodological and implementation features with C-VEP, we used it to validate the initial frameworks, setups and some signal processing methods.

The output of the implemented feature extraction is a single value and not a vector of characteristics. Therefore, a threshold-based decision-maker was implemented, which indicates the identified target or subject.

The following specific developments were carried out:

- Extensive implementation and validation of feature extraction methods for SSVEP (Welch, Cepstrum, CCA, ITCCA and TRCA) and for C-VEP (ITCCA, TRCA, Correlation Coefficients, Cosine Similarity and Dynamic Time Warping). These methods were tested and validated in two public datasets;
- Implementation and comparison of different methods of EEG signal normalization, aiming to optimize the results obtained with the above feature extraction methods;

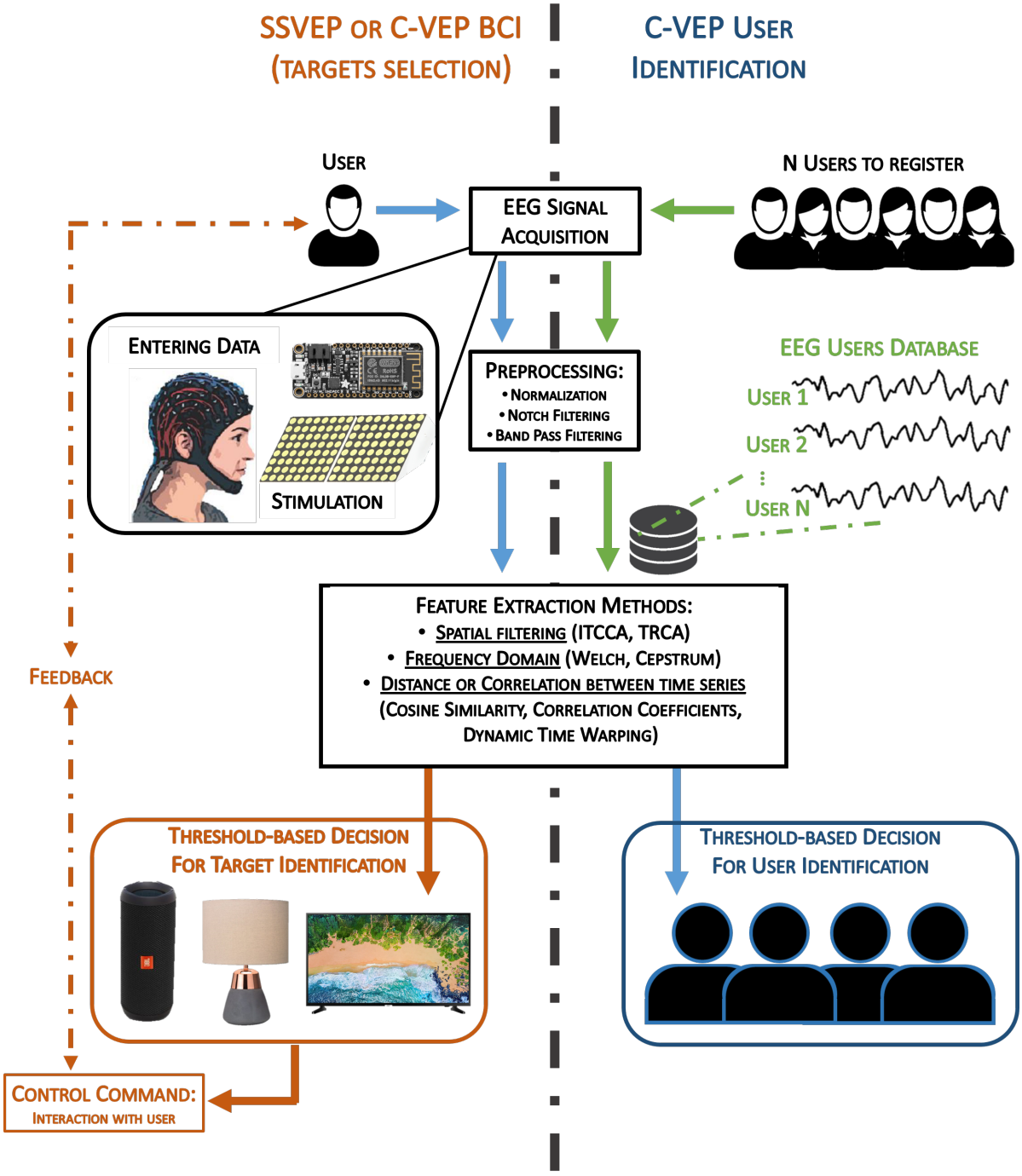

Figure 1.1: Architecture of BCI interface used for computer interaction, control of home appliances and subject identification.

- Proposal of a signal derivative approach, as a preprocessing step, applied before feature extraction in C-VEP;
- Deep analysis of how Pseudorandom Binary Sequences (PRBS) are generated. This allowed us to propose our own PRBS. Moreover, an analysis of the complexity of PRBS was carried out to analyse the correlation between complexity and accuracy;
- Development of a stimulation and EEG acquisition framework to implement C-VEP BCI and C-VEP identification. The approaches that obtained the best classification results with the public datasets were implemented pseudo-online and tested with our setup.

The course flow of this dissertation and content of each chapter are the following:

- Chapter 2 reviews the state of the art on the C-VEP paradigm with different stimulation devices, different types of stimulation sequences and different feature extraction and classification methods, as well as the various studies that use biometric identification and authentication with different visual paradigms;
- Chapter 3 presents the general concepts about C-VEP as well as the signal processing methods studied in this work;
- Chapter 4 describes the entire architecture of the identification pipeline used for the proposed architecture with C-VEP and the implementation of the signal processing methods;
- In chapter 5, the results obtained are presented and discussed;
- Chapter 6 draws some conclusions, as well as some proposals for future work.

The following manuscript is being prepared for submission:

- Francisco Roque, João Perdiz, Gabriel Pires, Urbano Nunes - An extensive evaluation of methods for C-VEP detection in the context of user-identification.

2

State of the art

In the last years, the number of publications focused on C-VEP based BCI has been increasing exponentially. In this chapter, we present the most relevant applications and methods related to C-VEP, and we introduce the use of EEG for identification/authentication of people.

Appendix D presents more information regarding some basic EEG concepts (the EEG International 10-20 System that defines the location of scalp electrodes and additional information about the sub-bands of the EEG waves).

2.1 Code-Modulated Visual Evoked Potentials (C-VEP)

There are many research works based on the C-VEP paradigm, however, the diversity of applications is still reduced. C-VEP has been applied mainly in communication Spellers with stimuli encoded by binary sequences using LCD screens. The targets are usually arranged in a matrix layout that allows for target selection and to provide feedback indicating the target selected by the user. In a C-VEP visual paradigm, it is important that the subject gazes the stimulus he/she wants to select. For a given selection, this stimulus is called the 'target stimulus' and the others are called the 'non-target stimuli' (each target is modulated with one binary sequence called m-sequence).

The first BCI based on C-VEP was proposed by Erich Sutter [69] in 1984, to control a communication speller, and eight years later it was tested in a patient with amyotrophic lateral sclerosis, using an invasive approach (four platinum electrodes implanted into the epidural space through a small hole in the skull). The subject was able to write 10 to 12 words/min [70]. Despite of these promising results it was only in 2008 that C-VEP was researched again.

BCI applications based on C-VEP have very high classification accuracy and ITR. This is partly due to a couple of methods that have proven to be very effective for feature extraction, such as template matching and canonical correlation analysis (CCA) [10]. The output of these feature extraction methods is usually a single value (single feature), and therefore the decision is based on the definition of a threshold (or selecting the maximum

value) without needing the use of a classifier. In cases where the feature extractor returns a vector of features, a classifier is required, such as Support Vector Machine (SVM), One-Class SVM (OCSVM) and Linear Discriminant Analysis (LDA) [66].

The implementations of C-VEP differ mainly in three aspects: 1) Stimulation devices and properties, 2) Sequences used to encode the stimuli; and 3) Signal processing and classification methods. In terms of applications, C-VEPs have been tested mostly as a BCI for communication/control. More recently, it has been researched for biometric identification/authentication.

2.2 Stimulation Devices and Properties

2.2.1 LED Matrices

Stimulation based on LEDs are usually organized in a matrix and driven from a microcontroller board acting as a generator, such as an Arduino or Raspberry [3]. Using LEDs it is possible to generate stimuli at higher frequencies than LCDs, and in a much cheaper way. With higher frequencies it is possible to shorten the time of sequences and therefore increase the information transfer rate (ITR). While in SSVEP the stimulus is a flickering frequency with a given frequency, in C-VEP the stimulus is encoded by a binary pattern [6, 43, 45]. Generally, each of the target LEDs used in a C-VEP protocol has an associated m-sequence (a shifted sequence or a new sequence). Despite the need for additional hardware and software to generate different frequencies and sequences, LEDs have proven to be the most suitable choice for visual stimuli, as they present low energy consumption, greater contrasts, allow multi-chromatic function and support a wider frequency range. However, LEDs have limitations in terms of shape, colour and patterns that can be reproduced [44]. The main applications in which LEDs have been used are in the control of external devices and home automation.

LED stimuli typically use different colors and patterns, being the most used the monochrome colors (black and white stimuli) [25, 27, 67]. More recently, frameworks that used multi-chromatic stimuli were implemented (stimuli with different colors depending on whether the bit is '0' or '1') [3, 4, 75]. More specifically, blue-green LEDs with four high-frequency green-blue chromatic flashing stimuli was implemented by Aminaka *et al.* [3]. In [4], monochromatic stimuli at 30Hz and 40Hz and stimuli with green-blue colors with the same frequencies were used, to compare accuracy with the four types of visual stimulation but the results were inconclusive regarding the best stimulation. The main applications in which LEDs have been used are in the control of external devices and home automation.

2.2.2 LCDs

LCDs are the most used approach in C-VEP [39, 47, 26]. LCDs have been shown as capable visual stimulators by changing a selected of the screen managed by software. Using

Figure 2.1: Interface of the QWERTZ speller. The n-gram based word suggestions were provided in the lowest row. Source: [25]

a computer screen provides high flexibility to design the form and select the colour of the visual stimuli compared to LEDs. However, the LCD screen has a restriction related to its limited refresh rate which results in issues related to frequency modulation. The C-VEPs based on LCD are mostly used in communication spellers, some of them presented below.

The interface proposed in [25] uses 32 rectangular boxes, consisting of 26 letters of the alphabet, two signs, 3 suggested words (updated after each selection) and the back-space button. For this protocol, only one sequence was used and for the remaining boxes a 2-bit shift of the original sequence was used. A screenshot of the paradigm is shown in Fig. 2.1, showing the organization of the different buttons.

Another possibility for using a Speller interface with C-VEP is shown in Fig. 2.2 [28]. Contrary to the previous one, there are only eight targets, organized in a 2x4 matrix, which are selected several times by steps. Each target in the upper line has up to seven letters of the alphabet and if you choose one of these targets, a second step is presented that allow to choose the desired letter. In the bottom line of the first layer, the suggested words are presented to facilitate the choice. In the center of the screen, between the two lines, the chosen letters are displayed.

Figure 2.3 presents an example of a visual representation of the described target arrangement organized in matrix is used, surrounded by non-target stimuli. Each target was periodically modulated by a 63-bit binary m-sequence. This representation satisfies the condition for the C-VEP BCI of the equivalent neighbours. With the inclusion of complementary non-targets, a peripheral target is surrounded by other targets and also by non-complementary targets, just as it happens with a central target that is surrounded by eight targets.

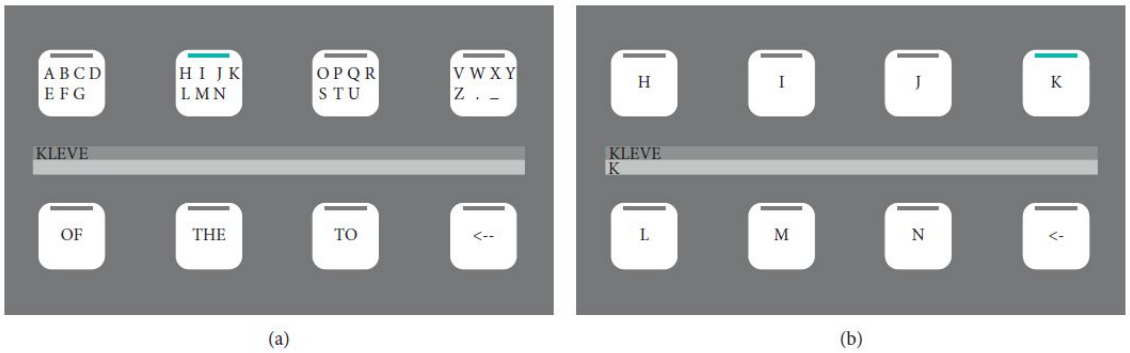

Figure 2.2: Graphical user interface of the C-VEP-based eight-target speller. By selecting a group of letters (e.g., H–N), a second layer containing individual letters was displayed. In the example, the letter K was selected. In addition to letter groups, the first layer of the interface also presented three word suggestions based on an integrated dictionary function. The lower right target represent an undo function. Source: [28]

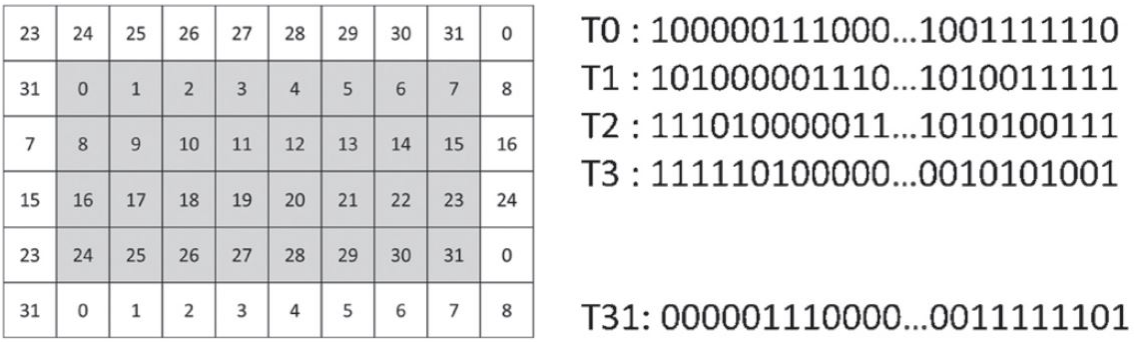

Figure 2.3: In left, the target arrangement of the C-VEP-based BCI, illustrating the 32 targets distributed as a 4x8 array (the gray area in the center of the screen) surrounded by 28 complementary flickers (white background). In right, an example of modulation sequences of 32 targets in one stimulation cycle, with two-frame time lag between two consecutive targets. Source: [10]

Another existing target arrangement uses 64 targets organized in a stimulus matrix of 8x8 size, being divided into four groups of 16 targets (4x4 size stimulus matrix), thus allowing to increase the number of existing targets [39]. Figure 2.4 presents a visual representation of the described target arrangement. Each group of stimuli is modulated by a distinct binary sequence (the original and the repetitive sequences with circularly shifting).

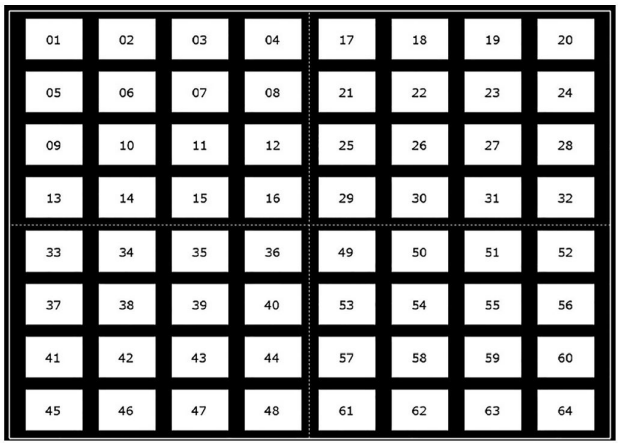

Figure 2.4: The visual stimulator consisting of four groups of stimulus targets. From left to right and from up to bottom, the number of the four target groups is 1, 2, 3 and 4 respectively. Each group contains 16 stimulus targets arranged in a 4x4 stimulus matrix. Source: [39]

2.3 Encoding Sequences

Most of the studies apply directly the binary patterns (m-sequences) and their shifted version, as detailed in section 3.2.1 [75, 3, 67, 25]. However, some researchers have explored different approaches to build variants of the m-sequences. Two relevant approaches are the quintary m-sequences and the periodicity detection presented in the following.

2.3.1 Quintary m-Sequences

Quintary m-sequences is an adaptation of the m-sequences, changing the states between five different shades of grey, replacing the switching between black and white of the commonly used binary stimulation patterns [28]. For the modulation of these stimuli, the alpha blending process was used, which allows changing the transparency effect by applying a two-color convex combination. With this process, the two colours combined were black and white, creating the different shades of grey. The degree of translucency, α, contained in the range from 0.0 to 1.0. The degree of translucency of the stimuli was updated every bit of the sequence and this values were derived from the code pattern. For the quintary m-sequences, the quintary digits 0, 1, 2, 3, and 4 were mapped to the corresponding α-values 0, 0.25, 0.5, 0.75, and 1. Figure 2.5 shows an example of a binary sequence with 63 bits and a quintary sequence with 124 bits. The average accuracy of the eighteen participants of the experiment was 97.7% for the binary sequences and 98.7% for the quintary sequences at 60Hz.

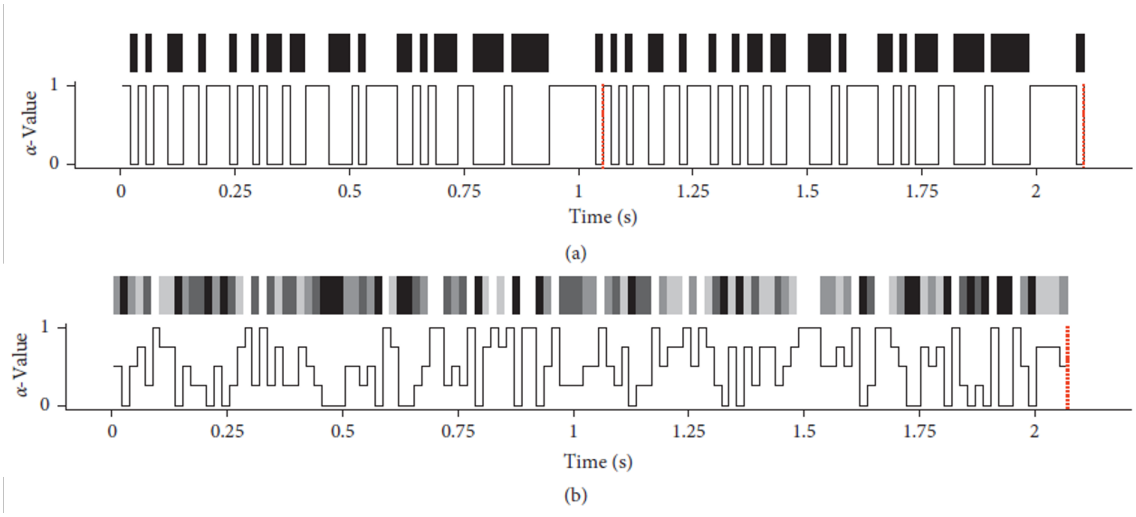

Figure 2.5: α-Values of the stimulation object for two tested flickering patterns. The α-values range from 0 (fully transparent) to 1 (fully opaque), with a 0.25 gap between the α-values. (a) Stimulus pattern of the binary 63-digit m-sequence. (b) Stimulus pattern of the quintary 124-digit m-sequence. Adapted from [28].

2.3.2 Periodicity Detection

In periodicity detection, periodic binary codes are used [47]. The periodicity of EEG signals is obtained from periodic sequences in addition to non-periodic sequences used in the BCI application with C-VEP, as exemplified in Fig. 2.6. Using this periodicity it is also possible to identify several targets using the respective circular-shifted periodic codes.

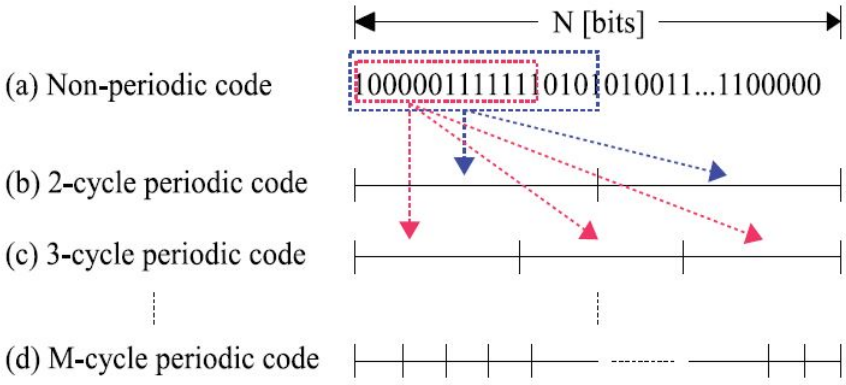

Figure 2.6: Example of modulation codes. (a) Non-periodic modulation code. (b) Two-cycle periodic modulation code.(c) Three-cycle periodic modulation code. (d) M-cycle periodic modulation code. Source: [47]

Table 2.1 shows a summary of relevant studies of features extraction methods and interfaces for C-VEP based BCI detection, including also the signal processing methods applied.

2.4 Signal Processing and Classification Methods

There are several processing methods to extract features and classifying C-VEP. The feature extraction methods that provide best results are the Individual Template Canonical Correlation Analysis (ITCCA) [25, 10, 28, 83], the Task-Related Component Analysis (TRCA) [83, 47, 48] and the Spatiotemporal Beamformer Decoding (SBD) [77].

Several methods of machine learning classification are also used when the feature extractor returns more than a single value, for example, Support Vector Machine (SVM) [4, 67], Linear Discriminant Analysis (LDA) [32] and Convolutional Neural Network (CNN) [46, 80]. However most of successful approaches don't use classifiers. For example, Wittervrongel *et al.* [77] compared a decoding algorithm based on SBD which achieved high results with the implementation of an SVM-based classifier in a framework with 32 targets for a reduced number of repetitions of the m-sequence, reaching a maximum average ITR of 172.87 bits per minute (bpm).

In Gembler *et al.* [28], the authors use a template-matching method using spatial filters generated using Canonical Correlation Analysis (CCA). The average accuracy of the eighteen participants in a two-step target selection with eight targets at each step used in the experiment was 97% and the ITR was 64 bits/min, approximately. Also, in [25], the same authors designed a filter bank based on alpha, beta and gamma sub-bands and use the CCA method to obtain results of 97% for accuracy and 93.1 bpm using a framework with 32 targets.

In Zhao *et al.* [83], the authors used the CCA and TRCA methods, using a filter bank to decompose the EEG signals into multiple components of sub-bands. The proposed system obtained results of 100% for the correct recognition rate (CRR) using 5.25 seconds of stimulation.

Sato *et al.* [65] compared the linear (with least mean square error) and nonlinear (with a Neural Network) spatio-temporal inverse filtering methods, exhibiting better decoding performance, and higher classification accuracies than conventional CCA spatial filtered.

In Zúquete *et al.* [60], the authors use two different one-class classifiers by subject (K-Nearest Neighbor and Support Vector Data) and allowed to obtain accuracy results with values between 75% and 99% on the 70 subjects tested, with eight channels in the occipital zone. In Das *et al.* [18], the authors obtain a classification accuracy between 75% and 88% for LDA performance and between 91% and 94% for the SVM performance.

In Das *et al.* [19], the authors applied a Convolutional Neural Network (CNN) to improve the accuracy values obtained in the extraction of features with this protocol. In this experiment, the EEG was acquired from two different sessions with a week interval from 40 subjects, allowing to obtain results between 80% and 100% for accuracy parameters.

Table 2.1: State of art to C-VEP based BCI

Art	Acquisition System - Portability	Feature Extractor Methods	Interface	Accuracy (%)	ITR (bpm)	Nº users
[25]	g.USBamp - No	CCA	LCD Speller	97-100	93.1-149.3	18
[26]	g.USBamp - No	CCA	LCD	75.89-77.68	37.22-38.16	8
[27]	g.USBamp - No	CCA	LCD Speller	94-98	57	12
[34]	Intelligent Hearing System - No	Means	LED based black and white lines	76-98	-	8
[39]	SynAmps2 EEG system, Neuroscan,Inc. - No	CCA	LCD	88.36	184.6	8
[46]	g.USBamp - No	OCSVM	LCD Speller	95.39	-	24
[62]	g.USBamp - No	CCA; Linear SVM.; OCSVM	3D kitchen scenario	23	37-68	10;6;5
[67]	g.USBamp - No	CCA; OCSVM	LCD	96	144	6
[10]	SynAmps2 EEG system - No	CCA	LCD	80-95	avg 108+-12	5

2.5 Biometric Identification and Authentication

A biometric authentication system is a pattern recognition system that makes a personal identification by determining the authenticity of specific physiological characteristics of a person [55]. The objective of a person authentication is to accept or to reject a person requesting an identity (one-to-one matching), (i.e. comparing a biometric data to templates), while the goal of person identification is to match the biometric data against all the records in a database (one-to-N matching).

The use of biometrics to identify or authenticate a person requires to measure some physical and behavioral characteristics and presents several advantages in comparison with traditional identification methods like passwords or key cards, establishing a strong bond between an individual and his identity. Within the biometric options, brain activity may represent a good alternative for user identification/authentication, although not in the near future, since it provides high confidentiality, is difficult to copy and steal. Brain signals have all the necessary properties to be used for identification/authentication, namely [16, 15]:

- **Universality:** once all of the human brains are composed with neurons that produce electrical activity, which can be read as EEG signals, possessing physical and behavioral characteristics;
- **Distinctiveness:** because two different individuals have different biometric representations;
- **Stability:** brain signals are relatively stable over time but can be affected by signal recording conditions (e.g. setup) or emotional conditions of the person;
- **Collectability:** since brain signals can be collected through several modalities being EEG the most suitable (dry electrodes should be considered to increase usability);
- **Acceptance:** the acceptance is mostly related with the constraints of brain signal acquisition setups, which are currently not very wearable and aesthetic.
- **Circumvention:** EEG is difficult to circumvent once EEG can not be easily falsified, unlike fingerprints, voice and faces that can be artificially reproduced or recorded. Additionally, if a person is coerced into accessing the system, stress changes will have an effect on EEG leading to failure on identification/authentication.
- **Performance:** currently, performance depends heavily of the approaches being followed but several proofs of concept have shown promising results in terms of accuracy. Performance is also influenced by operational and environmental changes.
- **Friendly Privacy:** in a EEG database it is more difficult to find the true identity of an individual if the database has been compromised.

We summarize below some of the challenges in the area of EEG-based biometric recognition that need to be addressed to improve the usability of the system [15]:

- **Robustness to Psychological and Physiological Changes:** The system must be robust to people under pain, diseases, mental states, emotional states, stress and other emotions, allowing the access of the subjects even when they are in these conditions.
- **User Databases:** The databases must consider the number of users that tends to grow more and more; the variations between the subjects (gender and age, for example); the individual variations of each subject in each train and test (must have stable features with long durations); consider intruders (people who have no information in the database and must be rejected by the system).
- **Protocol Design:** design suitable protocols that can evoked reliable and stable EEG features. Evoked potentials have been considered particularly suitable.
- **Performance Evaluation:** the testing data must be (almost) independent of the training data in order not to influence the system.

The first biometric identification system based on EEG was implemented in 1980 by Hans Stassen [68]. In this research, the identification was based on spectral patterns when participants were with closed eyes. The experiment with 82 participants achieved 90% confidence. Despite these results, it was only in the last few years that new works have appeared in this area [14].

EEG-based approaches are mainly based on: 1) mental and cognitive tasks (e.g., motor imagery) [20] and 2) visual evoked potentials. One of the most recent approaches is based on VEP stimuli. Given its relationship with the work carried out in this dissertation, we will focus more on this last approach.

The first biometric identification system using VEP was based on pictures and objects stimuli [52] was implemented in 2003 by Palaniappan *et al.*, obtaining an average rating of 94% for the identification of 20 subjects. Current approaches include visual tasks with: Visual tasks with images, with geometric shapes, letters and numbers, visual flickering stimuli (to evoke SSVEP) and bit patterns visual stimuli (to evoke C-VEP), although applications for C-VEP identification and authentication are very few.

2.5.1 VEP based on Image Recognition

This stimulation technique is based on the presentation of images of objects or faces, which appear over a short period of time. With this type of stimulus, the subject has to focus on the image and must recognize what is represented in that image, which is expected to evoke a VEP. Figures 2.7 and 2.8 shows two examples of a visual representation procedure from [60] and [18]. In [60], using a dataset with the EEG from 70 subjects, it

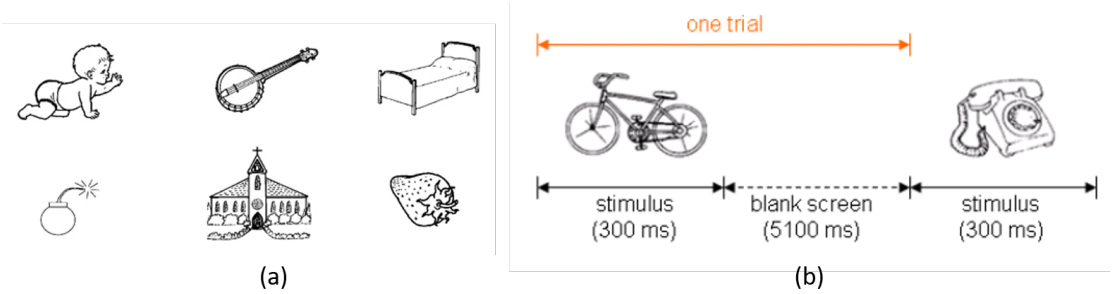

Figure 2.7: (a) Examples of pictures of the Snodgrass & Vanderwart standard 260 picture set. (b) Stimuli visualization procedure. The visual stimuli used in the experiment are in the form of presentation of black and white image sequences from the Snodgrass & Vanderwart picture set. Source: [60]

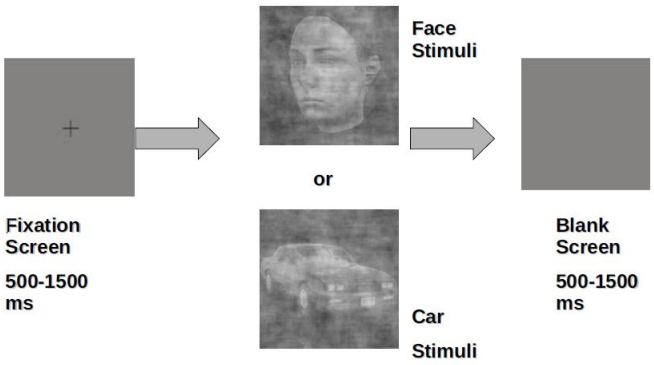

Figure 2.8: Illustration of experiment with images from the Max Planck Institute for Biological Cybernetics face database. Source: [18]

was possible to achieve various results of recognition, while in [18] the EEG of 20 subjects was acquired to achieve a performance between 75% and 94%.

2.5.2 VEP based on Geometric Shapes

In this stimulation method, images of eight different geometric shapes are presented, with the circle formula being the target stimulus, while the remaining seven geometric shapes (triangle, rectangle, square, pentagon, hexagon, octagon and diamond) are the non-target stimuli displayed on an LCD monitor [21]. The stimuli are organized in a matrix m x n. The subject has to focus on the target stimulus occurrence on the screen and ignore the occurrence of the other stimuli. A VEP signal is evoked from the subject when the target image is shown. In [21] was possible to achieve an equal error rate of 20-23% employing EEG data of 50 subjects.

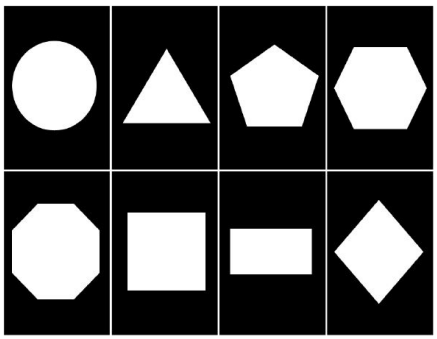

Figure 2.9: Shapes employed for the geometric shapes protocol. Source: [21]

2.5.3 VEP based on letters and numbers

This process uses 62 images as a visual stimulus (26 lowercase letters, 26 uppercase letters and 10 digits between 0 and 9), with the numbers being the target stimuli and the letters being the non-target stimuli [22]. The objective is the subject to focus on targets (numbers) at the moment they appear and ignore non-targets (letters). The target images are randomly shown for a total of 60 times and the letters are randomly displayed 660 times. Each image is shown during 250 ms and a black screen between two images during 450 ms. The total acquisition time is 8 minutes and 24 seconds with the presentation of 720 stimuli. In [22] was possible to achieved a performance of the equal error rate of 10-22% with the EEG signals from 50 subjects.

2.5.4 SSVEP

This protocol intends to extract discriminative features through SSVEP. Usually, subjects are asked to focus on a flickering target for a certain time for each of the stimulus frequencies considered. Piciucco *et al.* [58] propose a biometric recognition system based on the SSVEP paradigm using frequencies with values of 6, 12, 18 and 24 Hz. Yu *et al.* [80] use frequencies between 8 and 15.8Hz and Phothisonothai *et al.* [57] use frequencies between 6 and 9Hz. In [58] the database is composed by EEG signals from 25 subjects and it was possible to have a correct recognition rate of 95%; in [80] achieved 97% accuracy of user authentication using 8 subjects, and in [57] was possible to achieve a performance between 60-100% testing 5 subjects.

2.5.5 C-VEP

The use of C-VEP for biometric identification is very recent, and it is still a very emerging area. The only work that uses C-VEP for biometric identification was proposed by Zhao *et al.* [83]. In this paper, different stimulation patterns with 63-bit sequences displayed on an LCD are compared. The EEG database consisted of 25 subjects. The detection approach was based on a filter bank followed by the ITCCA or the TRCA methods. The approaches were validated in intra-session and cross-session scenarios achieving

a performance of 97-100%, which are very promising results.

Our proposed approach is very close to this implementation. We tested TRCA and ITCCA methods but without the application of a filter bank. However, we used LED stimulation, modulated by 31-bit sequences. Moreover, we tested several other detection methods and their combination with different normalization and preprocessing techniques.

3

Background Material

This chapter presents the background material required to understand the approaches and methods that have been developed in this dissertation. The chapter is organized as follows: BCI introductory concepts, Code-Modulated VEP concepts, signal processing methods that were considered for C-VEP detection, and description of the public datasets used for methods validation.

3.1 Introduction to BCI

A BCI measures electrical, magnetic or other physical signals from brain activity and translates these into commands to control a computer or other device [41]. In this dissertation we focus on methods based on electroencephalography (EEG), a technique that measures electrical activity at the surface of the scalp using electrodes [12].

Electrical signals generated by a EEG-based BCI system can be divided into two different approaches: evoked potentials (EP) (transient waveforms or perturbations in the ongoing activity, phase-locked to an event like a visual stimulation) and event-related desynchronization/synchronization (ERD / ERS) which occurs in response to specific internal events induced by mental tasks (motor imagery, mental arithmetic, mental object rotation). ERD/ERS does not need external stimulation but requires extensive training that may take several weeks.

In EP approach, subjects receive a set of visual or auditory stimuli [23]. EP can be divided into two classes: the steady-state evoked potential (SSEP) (where the signals are evoked by a visual stimulus modulated at a fixed frequency, eliciting an increase in EEG activity at the stimulation frequency) and event related potentials (ERPs) which are evoked by a relevant external event (visual auditory or tactile) with a sensory or cognitive meaning, and usually requiring selective attention [78]. The most well studied ERP is the P300, a peak usually occuring 300 ms after a relevant target in an oddball paradigm [24].

Visual Evoked Potentials (VEP) are evoked by sensory stimulation of a subject's visual field and reflect visual information processing mechanisms in the brain. VEPs can be modulated in different ways [66, 9]:

- Time modulation in event related potentials (oddball P300 paradigms);
- Frequency modulation (SSVEP);
- Frequency and phase modulation (P-SSVEP);
- Code modulation (C-VEP).

Generically, an EEG-based BCI system consists of four modular subsystems. The first subsystem is the signal acquisition which acquires the EEG signals from the scalp. The second module processes these signals and extract features that are classified and translated to an output command that controls a computer application or a device. This dissertation will focus on C-VEP approaches.

3.2 Code-Modulated Visual Evoked Potentials (C-VEP)

Instead of using visual stimulus with a constant frequency like in SSVEP, C-VEP is the response to visual stimulation modulated by a pseudorandom code (binary sequence pattern) sequences [11].

3.2.1 C-VEP sequences

In a C-VEP system, there is a special category of pseudorandom binary sequences (PRBS) called m-sequences which proved to be effective for BCI, due to their low autocorrelation and shifted versions nearly orthogonal. The main sequence can be used to generate other shifted versions of the m-sequence, which can then be associated to different targets/commands of a BCI. To identify a target that has been modulated by a given sequence, the basic approach consists in matching the VEP with a pre-recorded user's template [26, 25]. The m-sequences with non-periodic binary code can be generated using maximal linear feedback shift registers (LFSR) (i.e., a shift register where the input bit is the result from a linear function of the previous state - linear recursion) [66, 28]. M-sequences are used in several areas, such as the creation of pseudorandom sequences for communications (Cyclic Redundancy Check, ATM Networks), for cryptography, for impedance spectroscopy, acoustic pulse reflectometry and also in the design of some experiments using Functional Magnetic Resonance Imaging (fMRI) [56, 13, 63, 36].

Figure 3.1 shows an example of an LFSR with N bits. The output bit is the rightmost bit of the LFSR and the taps are the bits that modify the next state of the LFSR. The coefficients of the general polynomial must be $'0'$ or $'1'$. The generator polynomial of a LFSR is

$$g(x) = g_N x^N + g_{N-1} x^{N-1} + ... + g_2 x^2 + g_1 x + g_0 \qquad (mod\ 2) \tag{3.1}$$

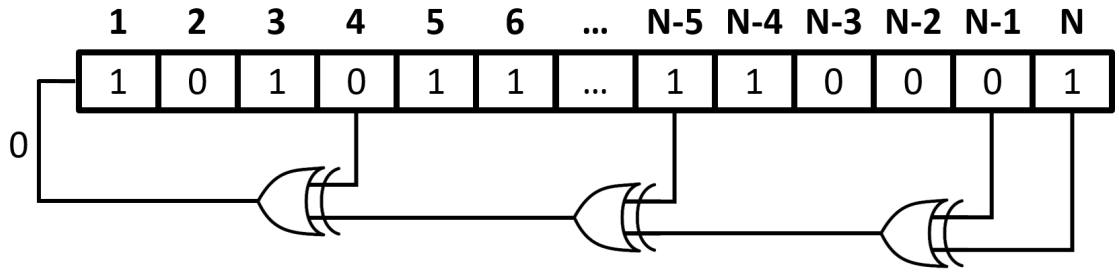

Figure 3.1: A basic LFSR architecture with N bits. In this diagram, the taps are $[N, N-1, N-5, 4]$, with the rightmost bit being the output bit of the sequence. The primitive polynomial of this diagram is $x(n) = x(n-N) \oplus x(n-(N-1)) \oplus x(n-(N-5)) \oplus x(n-4)$, where $x(n)$ is the n^{th} element of the sequence obtained by the exclusive-or (XOR) binary operation, denoted here by $\oplus$.

and the generator polynomial for the LFSR in Fig. 3.1 is

$$g(x) = x^N + x^{N-1} + x^{N-5} + x^4 + 1 \tag{3.2}$$

The initial N values of the sequence are called the seed, a non-zero sequence with an odd number of elements that obeys the following rules that starts the process of building the m-sequences. The seed can be generated randomly or selected using the bits that correspond to the degrees of the polynomial with a value of $'1'$ and the rest with a value of $'0'$. The rest of the sequence is created using the respective equation.

A primitive polynomial must be used to generate an m-sequence. A primitive polynomial must be irreducible of degree n, i.e., it cannot be written as the multiplication of two non-constant polynomials (of degree 0). The polynomial $x + 1$ is a primitive polynomial and all other primitive polynomials have an odd number of terms since if you have an even number of terms it is divisible by $x + 1$. Table 3.1 shows some primitive polynomials to generate m-sequences with a degree between 1 and 12 [73]. For example, considering the 10 degree polynomial in table 3.1, the polynomial taps are 10 and 3 and therefore a non-zero 10-bit seed will be needed, occupying positions 1 to 10 of the LFSR starting the process of the construction of m-sequence at the least significant bit that will give rise of the remaining sequence. The XOR operation between the 10^{th} and 3^{rd} bits will give rise to the new 0^{th} bit. After that, the sequence is shifted one position to the right so that the 0^{th} bit moves to position 1. This process can be repeated to generate 1023 bits.

Table 3.1: Examples of primitive polynomials up to degree N=12

Degree (N)	**Sequence Length** ($L = 2^N - 1$)	**Primitive polynomial**
1	1	$x + 1$
2	3	$x^2 + x + 1$
3	7	$x^3 + x + 1$
4	15	$x^4 + x + 1$
5	31	$x^5 + x^2 + 1$
6	63	$x^6 + x + 1$
7	127	$x^7 + x + 1$
8	255	$x^8 + x^7 + x^2 + x + 1$
9	511	$x^9 + x^4 + 1$
10	1023	$x^{10} + x^3 + 1$
11	2047	$x^{11} + x^2 + 1$
12	4095	$x^{12} + x^6 + x^4 + x + 1$

The length of an m-sequence is always an odd number, $2^n - 1$, where n is the number of bits used to generate the sequence. Despite that, in an m-sequence the difference between the numbers of zeros and the number of ones is always one, leading to a balanced stimulus with stability [50]. A run from a m-sequence is considered to be a consecutive subsequence consisting only of '0' or '1'. For any m-sequence, and considering r the maximum number of consecutive 'ones', there are [29]:

- One run of 'ones' of length r;
- One run of 'zeros' of length $r - 1$;
- One run of 'ones' and one run of 'zeros' of length $r - 2$;
- Two runs of 'ones' and two runs of 'zeros' of length $r - 3$;
- Four runs of 'ones' and four runs of 'zeros' of length $r - 4$;
- ...
- 2^{r-3} runs of 'ones' and 2^{r-3} runs of 'zeros' of length 1

In the context of C-VEP, m-sequences can be divided into two groups: one sequence give rise to several m-sequences using codes to circularly shifting; or different PRBS sequences with the same length, are used for each of the stimulation targets. The shifted versions of an m-sequence are almost orthogonal, so different shifts of a unique m-sequence can be used for numerous commands to the BCI system [50]. With this method, it is possible to create a template of all targets using only one target, decreasing the training time, with the possibility to back-shift the EEG-class to obtain a problem with a single one-class.

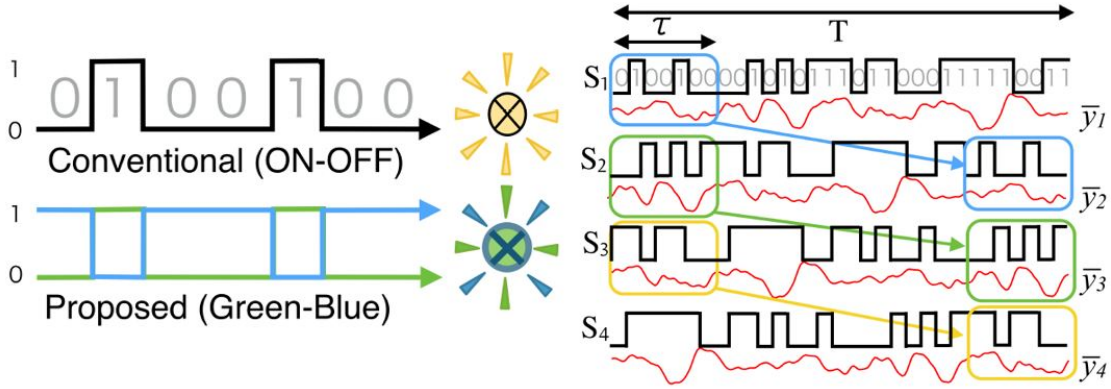

Figure 3.2: Example of a C-VEP implementation (adapted from [3]). At the left side, two types of possible stimulation are presented, conventional monochromatic (white–black;ON-OFF) and the proposed chromatic (green-blue) flickering patterns. At the right side are 4 sequences created from sequence 1, with a shift of $\tau = 7$ bits.

Though, the number of targets that can be used will be limited by the number of bits in the circular shift. If the BCI uses different sequences for different targets, a template for each sequence will be required [39].

Figure 3.2 (adapted from [3]) illustrates an example of the construction of PRBS used in the C-VEP paradigm. Each sequence with a total of 31 bits, is shifted by a value $\tau = 7$ bits, and it has a period of time with a value T. In this example, four different sequences called s_i (i = 1,2,3,4) were generated, creating the respective averaged EEG C-VEP responses, $\bar{y}_j$ (j = 1,2,3,4).

3.3 EEG Signal Processing

The preprocessing and the feature extraction are two of the modules of a BCI architecture, required to select the most relevant features.

3.3.1 Preprocessing

In the preprocessing stage, the recorded EEG data is filtered to remove muscle artifacts and the electrical noise, and to limit the signal to the band of interest, increasing the signal-to-noise ratio (SNR).

In general, at this stage, the EEG signals are filtered to remove the powerline interference at 50Hz, to remove the signal DC component and to remove the irrelevant band frequencies. However, only filtering the signal is not enough to increase the SNR to a level that allows C-VEP detection. The identification of patterns of interest require effective signal processing methods to extract discriminative characteristics.

3.3.2 Feature Extraction Methods

Feature extraction is one of the most important stages of a BCI architecture because it allows to find the most discriminative features to identify the signals of interest. This section describes methods to detect the two neural mechanisms considered in this dissertation, SSVEP and C-VEP. The methods presented here include: 1) approaches in the frequency domain (applied only for SSVEP); 2) methods based on the distance or correlation between time-series (applied only for C-VEP); and 3) methods that take advantage of the spatial correlation of EEG data (applied for SSVEP and C-VEP). It is worth to remember that, in SSVEP the main goal is to identify a frequency modulated by a stationary stimulus at a constant frequency, while in C-VEP the purpose is to identify a given pattern modulated by a binary code.

3.3.2.1 WELCH

The Welch's method was developed by Peter D. Welch in 1967 [76] and it is based on the averaged periodogram spectrum estimates that results of the conversion of a signal from the time domain to the frequency domain.

The method consists of dividing the signal into successive segments as described by:

$$x_m[n] \triangleq w[n]x[n + mR], \quad n = 0, 1, \ldots, M - 1, m = 0, 1, \ldots, K - 1, \tag{3.3}$$

where R is defined as the window hop size, and K denote the number of available frames. It is possible to use different types of windows, $w[n]$, such as rectangular, Hamming, Hanning, as well as different overlap percentages allowing to adjust power spectral resolution and standard deviation.

The periodogram of the m-th segment is defined by:

$$P_{x_m,M}(w_k) = \frac{1}{M}|FFT_{N,k}[x_m]|^2 \triangleq \frac{1}{M}\left|\sum_{n=0}^{N-1} x_m[n].e^{-j2\pi kn/N}\right|^2 \tag{3.4}$$

where N is the number of points of the Fast Fourier Transform (FFT). The Welch estimate of the power spectral density is defined by the average of periodograms across time, computed according to:

$$\hat{S}_x^W(w_k) \triangleq \frac{1}{K}\sum_{m=0}^{K-1} P_{x_m,M}(w_k). \tag{3.5}$$

3.3.2.2 Cepstrum

Cepstrum analysis was proposed by Bogert *et al.* in 1963 as the "power spectrum of the logarithm of the power spectrum" with the purpose of detecting echoes in seismic signals. The term "cepstrum" and "quefrency" are anagrams of "spectrum" and "frequency", respectively, changing the syllables of the two terms [51, 79]. This method is used to explore the periodic structures within frequency spectra and it is used in speech analysis and voice recognition, medical imaging and analysis of machine vibration on harmonic patterns like gearbox faults and turbine blade failures. This method was applied to explore the frequency nature of SSVEPs which are characterized by several harmonics.

The Cepstrum of a discrete-time signal neglects the information of phase, turning the convolution into sum, and it is defined by:

$$c[n] = IDFT\{log|DFT(x[n])|\} \equiv \frac{1}{2\pi}\int_{-\pi}^{\pi} log|X(e^{jw})|e^{jwn}\,\mathrm{d}w \tag{3.6}$$

where $log|X(e^{jw})|$ means the log-magnitude of the Discrete-Time Fourier Transform (DTFT) implemented with the FFT. The variable "n" in the $c[n]$ corresponds to the quefrency term of the frequency inversion, denoting the independent variable of this method [79].

Figure 3.3 shows a block diagram representing the Cepstrum computation. The sequence $x[n]$ is the digital signal applied to the input of the transformation system of the Cepstrum method, while $X[k]$ is its correspondence in the frequency spectrum. $X^*[k]$ characterizes the log-magnitude form of the frequency spectrum and $c[n]$ represents the Cepstrum at the output of the inverse discrete Fourier transform (IDFT) block.

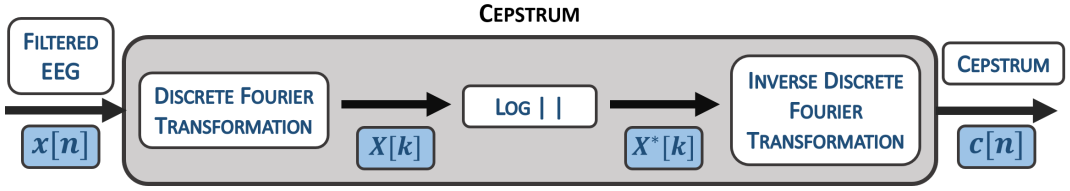

Figure 3.3: Diagram of Cepstrum estimation method.

3.3.2.3 Correlation Coefficients

The correlation between two random variables is a statistical measure of similarity between the relative movements of the two variables. There are several types of correlation measures and one of the most used is the Pearson product-moment correlation [8]. For N scalar observations for each variable, the Pearson correlation coefficient is defined by:

$$\rho(A,B) = \frac{1}{(N-1)}\sum_{i=1}^{N}\left(\overline{\frac{A_i-\mu_A}{\sigma_A}}\right)\left(\overline{\frac{B_i-\mu_B}{\sigma_B}}\right) \tag{3.7}$$

where μ_A, σ_A, μ_B and σ_B are the mean and standard deviation of A and the mean and standard deviation of B, respectively.

In a matrix form, the correlation coefficient matrix of two random variables is the matrix of the correlation coefficients for each combination of variables in pairs defined by:

$$R = \begin{pmatrix} \rho(A,A) & \rho(A,B) \\ \rho(B,A) & \rho(B,B) \end{pmatrix} = \begin{pmatrix} 1 & \rho(A,B) \\ \rho(B,A) & 1 \end{pmatrix} \tag{3.8}$$

The main diagonal of the matrix has values equal to one because the variables A and B are always directly correlated to themselves.

3.3.2.4 Time Series Similarity based on Distance

There are several metrics to calculate the distance, one of the most used is the Euclidean or l_2 metric. Considering X and Y two N-dimensional signals, then the distance between the m^{th} sample of X and the n^{th} sample of Y using the Euclidean metric is defined by:

$$d_{mn}(X,Y) = \sqrt{\sum_{k=1}^{N}(x_{k,m} - y_{k,n})^2} \tag{3.9}$$

Other metrics are the Manhattan or l_1 metric, the Square of the Euclidean metric and the Symmetric Kullback-Leibler metric (only for real and positive X and Y because of the logarithmic function).

The Dynamic Time Warping (DTW) is a more complex algorithm also used to measure the similarity or calculate the distance between temporal sequences with different length. DTW has been applied to temporal sequences of video, audio and graphics data, and speaker recognition and online signature recognition [53]. The method searches for a path through the grid parameterized by the two sequences of the same length ix and iy, such that the distance minimum is defined by:

$$d = \sum_{\substack{m \in ix \\ n \in iy}} d_{mn}(X,Y) \tag{3.10}$$

Another similarity metric is the Cosine Similarity, that measures cosine of the angle between two N-dimensional vectors in an N-dimensional space [61]. The method corresponds to the division between the dot product of the two vectors and the product of the

lengths or magnitudes of the two vectors:

$$similarity(A, B) = \frac{A.B}{\|A\| \, \|B\|} = \frac{\sum_{i=1}^{N} A_i B_i}{\sqrt{\sum_{i=1}^{N} A_i^2} \sqrt{\sum_{i=1}^{N} B_i^2}} \tag{3.11}$$

where $\|x\|$ is the Euclidean norm of vector x.

A cosine value of zero means that the two vectors are orthogonal, with $\pi/2$ radians between each other and have no match, while a cosine value close to one means that the two vectors have a high match between them and the vectors are very similar.

3.3.2.5 Canonical Correlation Analysis

Canonical Correlation Analysis (CCA) is a multivariable statistical method which allows a multichannel data processing approach to infer cross-covariance information between two variables that may have some correlation. The method finds a set of linear combination between the two variables, so that the correlation between the two variables is maximized [11]. It optimizes the recognition procedure because it combines information from multiple channels to improve the SNR [82].

In the context of BCI, CCA was used for the first time to detect SSVEP frequencies in 2007 [38]. CCA is currently one of the most used methods in VEP due to its high efficiency, robustness, simple implementation, low computation cost and because it does not require calibration. CCA is however affected by the interferences of EEG artefacts and spontaneous activities.

Different variants of the CCA methods have been proposed in the context of BCI for target detection:

- Cluster Analysis of CCA coefficient (CACC) proposed by Poryzala *et al.* to realize an asynchronous BCI system [59].
- Phase Constrained CCA (PCCA) proposed by Pan *et al.*, fixing the phases of the sinusoidal references signals according to the visual latency estimated from the calibration data [54].
- Multi-way CCA (MwayCCA) proposed by Zhang *et al.* to find appropriate reference signals for SSVEP detection based on multiple standard CCA processes with the calibration data [81].
- Individual Template-based CCA method (IT-CCA) developed by Bin et al., in [10], using the averaging EEG trials from the calibration data to each individual as VEP reference signals.

In this dissertation, CCA is used for detection of SSVEP and C-VEP, which may present some minor differences in its application, as shown bellow.

CCA-based method for detecting SSVEP

The CCA method calculates the canonical correlation ρ_n between the multi-channel EEG signals matrix $X_{N\times T}$ (N: number of channels and T: time samples) and the reference signals at each stimulus frequency $Y_{2M\times T}$ (M: number of harmonics and T: time samples).

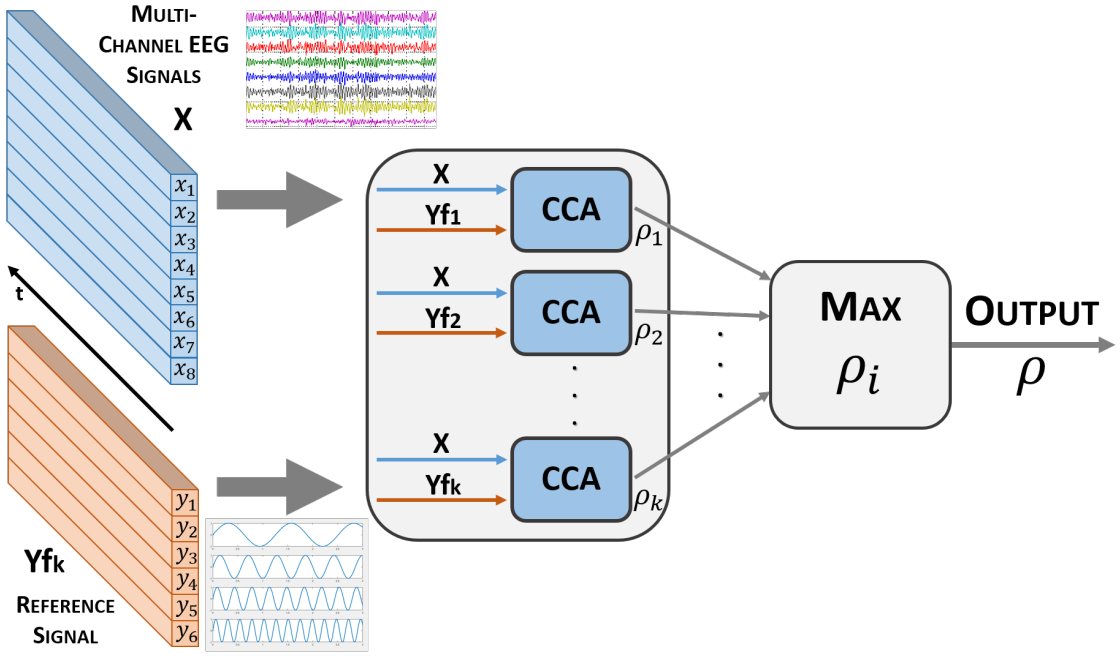

Figure 3.4: CCA-based method for EEG signals analysis in SSVEP. (Fig adapted from [11]).

The reference signals $Y(f_n)$ in the SSVEP detection are a group of sines and cosines waveforms with frequencies containing the frequency of the stimuli f_n and the respective harmonics, defined by:

$$Y(f_n) = \begin{bmatrix} \sin(2\pi \times f_n \times t) \\ \cos(2\pi \times f_n \times t) \\ \dots \\ \sin(2\pi \times N_h \times f_n \times t) \\ \cos(2\pi \times N_h \times f_n \times t) \end{bmatrix}, t = \frac{1}{f_s}, \frac{2}{f_s}, ..., \frac{N_S}{f_s} \tag{3.12}$$

where f_n is the base stimulation frequency, f_s is the sample rate, and N_h is the number of harmonics used [49].

The multi-channel EEG signals and each of the reference signals is used as an input of the CCA method, which is applied to each frequency of the reference signal.

Considering these two multidimensional variables and their linear combinations $x = X^T w_x$ and $y = Y^T w_y$, where w_x and w_y are the weight vectors, this method finds the

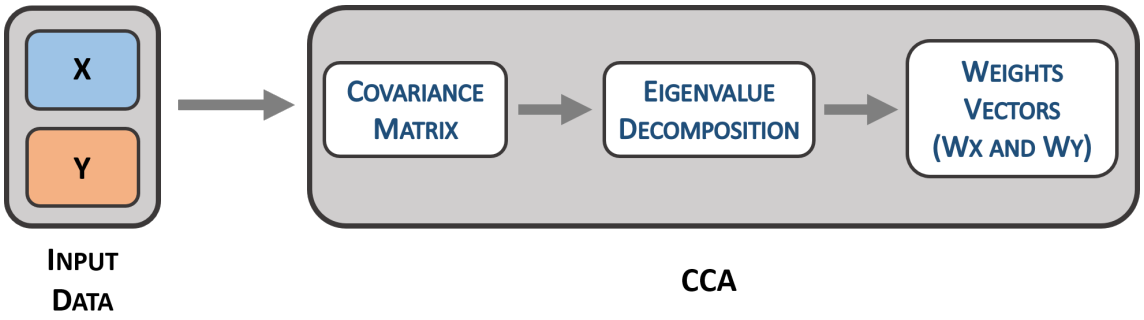

Figure 3.5: Pipeline for the calculation of the weights in the CCA.

vectors w_x and w_y, which maximizes the correlation between the variables x and y solving:

$$\max_{w_x,w_y} \rho(x,y) = \frac{E[xy^T]}{\sqrt{E[xx^T]E[yy^T]}} = \frac{E[w_x^T XY^T w_y]}{\sqrt{E[w_x^T XX^T w_x]E[w_y^T YY^T w_y]}} \tag{3.13}$$

with the operator $E[x]$ representing the average of x data. The optimization problem is solved using a eigenvalue decomposition problem.

The cross-covariance matrix between X and Y is calculated by:

$$K = cov[X,Y] = E[(X - E[X])(Y - E[Y])^T] = E[(X - \mu_x)(Y - \mu_y)^T] = E[XY^T] - \mu_x\mu_y^T \tag{3.14}$$

The classification can be done simply by choosing the highest value of ρ_i to which corresponds the target frequency f_i, that is the reference signal with the maximal correlation. The canonical correlation output ρ can then be used for frequency recognition where ρ_i are the CCA coefficients obtained with the frequency of reference signals being f_1, f_2,... , f_K [11, 49].

$$\rho = \max_i \rho_i, i = 1, 2, ..., K, \tag{3.15}$$

Individual Template CCA-based method for detecting SSVEP and C-VEP

The above approach can be easily adjusted to replace the reference signals by a template, and therefore be used for SSVEP and C-VEP. During the training stage, the user is required to fixate on a reference target, and the recorded EEG will be used as a template for that target. The multichannel EEG data during k stimulus cycles will be acquired as X. After that, it is necessary to average the segments of data from the k cycles of stimulation, producing the variable R containing the multichannel evoked response. The

variable S is the replication of the evoked response R during k times, corresponds to:

$$S = [R, R, ..., R] \tag{3.16}$$

Considering these two multidimensional variables and their linear transformations W_x and W_s, the maximization of the correlation between the variables X and S is obtained from:

$$\rho = \max_{W_x, W_S} \frac{W_x^T X S^T W_S}{\sqrt{W_x^T X X^T W_x . W_S^T S S^T W_S}} \tag{3.17}$$

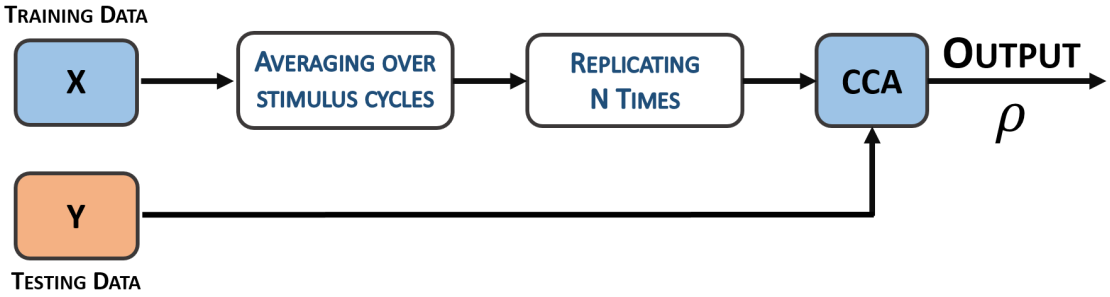

Figure 3.6: Pipeline of the ITCCA-based method for EEG signals analysis in C-VEP.

3.3.2.6 Task-Related Component Analysis

Task-related component analysis (TRCA) method was developed by Tanaka *et al.* in 2013 [71], in the context of the near-infrared spectroscopy (NIRS) data in time-locked activities, such as ERD/ERS. The objective of this method is to optimize the coefficients to show the maximum temporal similarity that exists between the task sessions, using as a starting point a temporal profile of a component related to the task. With TRCA, there are two signals initially considered: 1) task-related signal, $s(t)$; 2) task-unrelated signal, $n(t)$. The TRCA aims to recover the task-related component $s(t)$ of the linear, weighted sum of the multichannel EEG signal, maximizing the reproducibility of the activities during this period, which is observed in:

$$y(t) = \sum_{j=1}^{N_C} w_j x_j(t) = \sum_{j=1}^{N_C} (w_j a_{1,j} s(t) + w_j a_{2,j} n(t)) \tag{3.18}$$

with j being the index of the number of channels (N_C), and a_{1j} and a_{2j} being the coefficients which project the signals to the EEG signal.

The inter-trial covariance between the h_1-trial and the h_2-trial is described by:

$$C_{h_1h_2} = Cov(y^{h1}(t), y^{h2}(t)) = \sum_{j_1,j_2=1}^{N_C} w_{j_1} w_{j_2} Cov(x_{j1}^{(h_1)}(t), x_{j2}^{(h_2)}(t)) \tag{3.19}$$

and the sum of all possible combinations of trials is described as:

$$\sum_{h_1,h_2=1;h_1\neq h_2}^{N_T} C_{h_1h_2} = \sum_{h_1,h_2=1;h_1\neq h_2}^{N_T} \sum_{j_1,j_2=1}^{N_C} w_{j_1} w_{j_2} Cov(x_{j1}^{(h_1)}(t), x_{j2}^{(h_2)}(t)) = \mathbf{w^T S w} \tag{3.20}$$

where $Cov(a, b)$ relates to the covariance between a and b, $j1$ and $j2$ relate to the index of the channels and $h1$ and $h2$ relate to the index of two blocks of the training trials, with the two blocks regarded as task-related.

The matrix $\mathbf{S} = (S_{j_1j_2})_{1\leq j_1,j_2\leq N_C}$ is the sum of all covariance between blocks of the task-related and it is defined by:

$$S_{j_1j_2} = \sum_{h_1,h_2=1;h_1\neq h_2}^{N_T} Cov(x_{j1}^{(h_1)}(t), x_{j2}^{(h_2)}(t)) \tag{3.21}$$

To obtain a finite solution, the variance of $y(t)$ must be equal to 1, defined by:

$$Var(y(t)) = \sum_{j_1,j_2=1}^{N_C} w_{j1} w_{j2} Cov(x_{j1}(t), x_{j2}(t)) = \mathbf{w^T Q w} = 1 \tag{3.22}$$

The spatial covariance matrix Q was obtained calculating the product between the concatenated matrix of all training trials and its transposed [83].

The constrained optimization problem can be solved using

$$\hat{w} = \arg\max_{w} \frac{w^T S w}{w^T Q w} \tag{3.23}$$

The optimal coefficient vector is the largest eigenvalue obtained of the eigenvector of the matrix $Q^{-1}S$ with the spatial covariance matrices Q and S with size $N_C \times N_C$ [71].

The correlation coefficient between the averaged training data for n-th visual stimulus $\overline{\chi}_n^{(m)}$ and the single-trial test data $X^{(m)}$ (both matrices have a size of $N_C \times N_S$, being N_S the number of samples of the EEG signal) is calculated using

$$r_n^{(m)} = \rho\left(\left(X^{(m)}\right)^T w_n^{(m)}, \left(\overline{\chi}_n^{(m)}\right)^T w_n^{(m)}\right) \tag{3.24}$$

where $\rho(a, b)$ is the Pearson's correlation analysis between the signals a and b.

3.4 Performance Evaluation

The performance evaluation was calculated using two different metrics: accuracy and information transfer rate.

Accuracy is computed as the ratio between the number of targets that are correctly identified C, and the set of all selections N.

$$ACC = \frac{C}{N} \tag{3.25}$$

The same formula is used for user-identification, where C represents the number of times users are correctly identified and N is the number of identification attempts.

Information transfer rate (ITR) is commonly applied to calculate the performance evaluation of BCI systems in bit/min, evaluating the communication speed of the system, in the identification of targets. It is given by the product of the number of bits per target and the number of targets per minute that are identified

$$ITR = log_2 \left(N.P^P . \left[\frac{1-P}{N-1} \right]^{1-P} \right) * \left(\frac{60}{T} \right) \tag{3.26}$$

where N is the number of possible selected commands, P is the classification accuracy probability and T is the average target selection time (seconds/selection) [78].

To correctly interpret the results, ITR and accuracy should be presented together, as low values of accuracy can provide a high ITR, if there is a high number of commands to be detected.

3.5 Benchmark Datasets

Two datasets were used to validate the implemented feature extraction methods: SSVEP-dataset and C-VEP-dataset.

3.5.1 SSVEP Benchmark Dataset

The SSVEP dataset allowed the comparison of methods to detect different stimulation frequencies associated to each target.

The SSVEP dataset [74] was recorded from 35 subjects (8 experienced and 27 naive) undergoing a BCI speller task with 40 targets, as shown in Fig. 3.7 with each target representing a letter of the alphabet, a number or a signal. Each target stimulus of the

framework was coded with a frequency and phase modulation, associating a stimulation corresponding to a different frequency between 8Hz and 15.8Hz, spaced by 0.2Hz.

The EEG data was recorded with the Synamps2 EEG system (Compumedics Neuroscan, Australia) at a sampling rate of 1000 Hz, after which the samples were down-sampled to 250 Hz to reduce computational costs and storage. The dataset's data are organized by files, each of which corresponds to a different subject. Each file has a four-dimensional matrix with dimensions of $N_C \times N_S \times N_T \times N_B$, corresponding to $N_C = 64$ channels, $N_S = 1500$ time samples, $N_T = 40$ targets, $N_B = 6$ blocks. Each **block** corresponds to the number of recorded trials per target. A **trial** corresponded to a task including the six seconds recorded for each target.

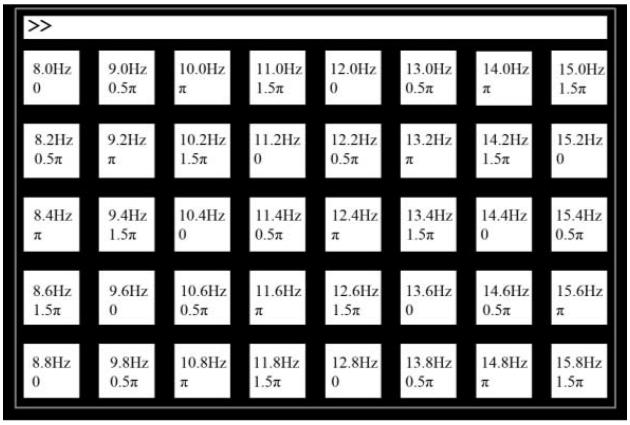

Figure 3.7: Frequency and phase values for all targets using the joint frequency and phase modulation method. (Source: [74]).

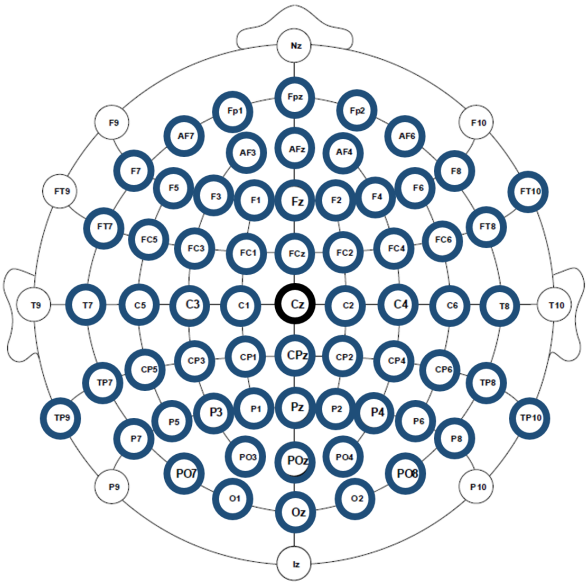

Figure 3.8: 64 electrode recording positions of the international 10-20 extended system used in the SSVEP Benchmark Dataset. The black circle is the ground.

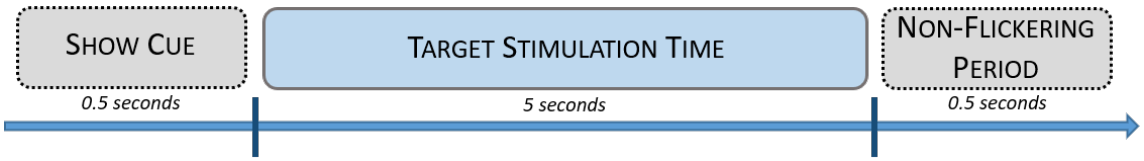

Figure 3.9: Time-course of one trial during the experiment in SSVEP Benchmark Dataset (based in [74]).

Each trial lasted a total of 6 seconds, as shown in Fig. 3.9. Each trial started with a 0.5 seconds target cue, and subjects were asked to change their gaze at the target as soon as possible. After that, all stimuli started to flicker on the screen simultaneously for 5 seconds. Subjects were asked to avoid blinking their eyes during the stimulation. After stimulation, the screen did not flash for 0.5 seconds before starting the next trial. There was a rest period of a few minutes between two consecutive blocks [74].

3.5.2 C-VEP Benchmark Dataset

The C-VEP dataset [77] was used as a benchmark dataset to compare the preprocessing and feature extraction methods presented in Section 3.3.2.

This dataset consists of data from 17 subjects, with normal or corrected-to-normal vision, performing a BCI speller experiment. The interface consists of 32 white circular targets, arranged in an 8x4 matrix, using a stimulus presentation with a high-frequency LCD (120 Hz). Users were seated approximately 60 cm from the monitor.

The m-sequence used to code the targets was 63 bits long, with a 2-bit offset for each of the targets. The original sequence was:

000100001011001010100100111100000110111001100011101011111101101

The identification of different targets in C-VEP based BCIs used different shifts of the presented m-sequence.

The EEG data were recorded with the SynampsRT device (Compumedics Neuroscan, Australia) at a sampling rate of 2000 Hz, with a down-sampling to 200 Hz. The dataset's data are organized by files, each of which corresponds to a different subject. Each file has a four-dimensional matrix with dimensions of $N_C \times N_S \times N_{trials}$, corresponding to the $N_{trials} = 160$ trials (32 targets $\times$ 5 blocks). Each block consisted of the recording of the number of trials per target. A trial corresponded to a task including the 5.25 seconds collected for each target trial consisting of $N_C = 32$ channels and $N_S = 1050$ time samples.

Figure 3.11 shows the time-course of a trial. Each trial started with the presentation of the target to select, highlighted in red. Subjects were asked to redirect their gaze to the target in red and to press a button to start stimulation. After that, all targets were hidden for 1 second. During the next 5.25 seconds, stimulation (10 repetitions of the 31 bit sequence) was performed for each of the targets.

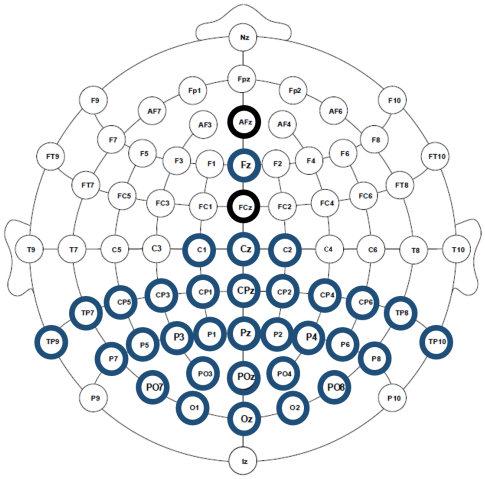

Figure 3.10: Location of 32 electrodes according to the 10-20 system in C-VEP Benchmark Dataset. The ground was AFz channel and the reference was FCz channel. (Based in: [77])

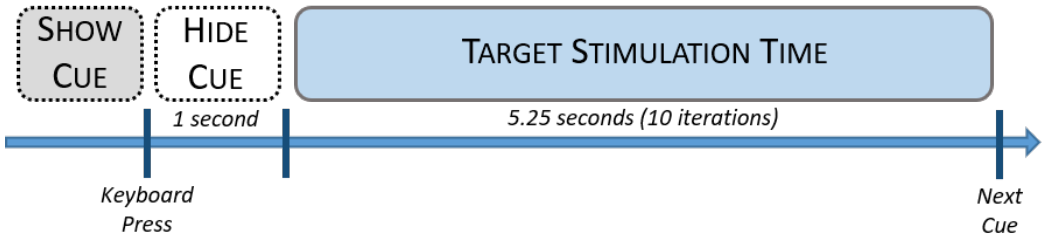

Figure 3.11: Time-course of one trial during the experiment in C-VEP Benchmark Dataset (based in [77]).

4

BCI and User Identification: SSVEP and C-VEP

This chapter presents the work developed in the context of: 1) SSVEP BCI; 2) C-VEP BCI and 3) C-VEP identification. Moreover, we describe our acquisition setup, processing framework and pseudo-online implementation.

In the first stage of the work, public benchmarks datasets (SSVEP-dataset and C-VEP-dataset) were used to validate the methods, which were implemented in Matlab. An extensive set of different methods was implemented and compared, as well as different types of signal normalization. The underlying concepts to generate m-sequences is analyzed, and our own m-sequence for C-VEP is proposed. The correlation between m-sequence complexity and classification accuracy is also explored.

Figure 4.1 shows the modules of the pipeline used to identify users and targets: the EEG acquisition module or benchmark dataset; the normalization and preprocessing module; the first and second derivatives module (optional); the feature extraction module and the threshold-based decision-making module. Since the correlation output value of the feature extraction module is a single variable, classifiers will not be applied, and the decision is only considered through thresholds. The text below each block indicates some of the methods that were applied.

4.1 SSVEP and C-VEP detection

The SSVEP and C-VEP datasets, described in section 3.5, were used to assess the methods. The overall detection pipeline is represented in Fig. 4.1. The methods to detect SSVEP were tested using the SSVEP dataset and also synthetic data (see more information in appendix B).

After analyzing the files of all the subjects in C-VEP Benchmark Dataset, it was possible to detect a failure in the file of subject 11, since target 14 occurred six times, while target 16 only happened four times. Since it was not possible to conclude anything with this subject, it was decided to exclude the data of this subject from the dataset, having used

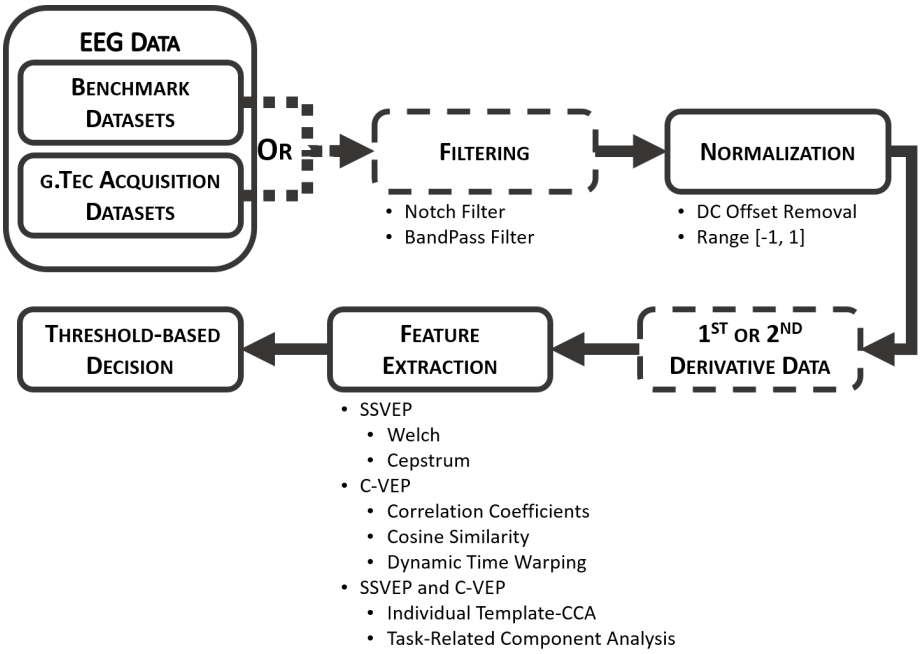

Figure 4.1: Identification Pipeline for BCI and user identification.

the EEG data of the remaining 16 users. To allow data analysis, a script was created to reorganize the trials in the correct order of targets, being stored in a four-dimensional matrix with dimensions of 32 channels × 1050 time samples × 32 targets × 5 blocks. Each block corresponds to the number of recorded trials per target.

The C-VEP dataset for identifying targets has been reorganized so that it can be used in the context of user identification. The new C-VEP dataset for user identification was organized by a file, per each target, encoded by an m-sequence, with a 4-dimensional matrix for each file with dimensions 32 channels × 1050 time samples × 16 subjects × 5 blocks, in which each block consists of the EEG data recorded for a trial for each subject.

4.1.1 Preprocessing

The EEG signal preprocessing stage comprises three sequential steps, as shown in Fig. 4.2.

First, EEG signals were filtered using a 48 to 52 Hz notch filter to attenuate the powerline interference. After that, a bandpass filter was applied depending on the frequencies to be isolated. The bandpass filter applied before normalization in the SSVEP dataset was a third-order Butterworth filter (bandpass) with a minimum cut-off frequency of 5Hz, and a maximum cut-off frequency of 50Hz.

Regarding the data from the C-VEP dataset, the signals were filtered using a filter with a fourth-order Butterworth filter between 4Hz and 31Hz, to attenuate the low-frequency oscillations due to the movements of the electrodes and high-frequency extra physiologic

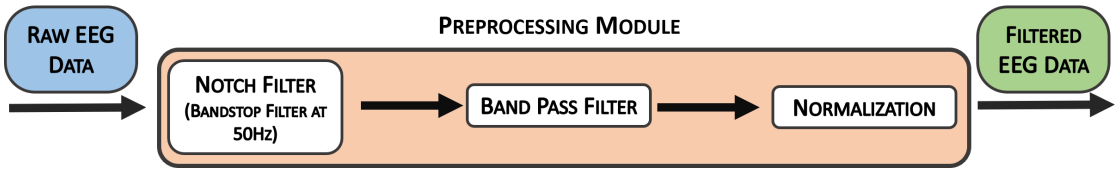

Figure 4.2: Preprocessing module used in SSVEP and C-VEP.

noise. The cut-off frequency of the C-VEP is lower than in the SSVEP since the signal harmonics are not detected because this information is not relevant for the analysis in question.

Finally, EEG signals were normalized using two different methods of normalization. The first method was the DC offset removal defined by:

$$X' = X - mean(X) \tag{4.1}$$

and the second method was the reduce amplitude signal to the value range [-1, 1] defined by:

$$X' = \frac{X}{max(|X|)} \tag{4.2}$$

For the SSVEP dataset, only the DC Offset Removal normalization was used, while for C-VEP dataset both normalizations were used.

4.1.2 Feature Extraction Methods

For the SSVEP paradigm, the Welch, CCA and Cepstrum methods were used, while for the C-VEP paradigm the Correlation Coefficients, Dynamic Time Warping and Cosine Similarity methods were used. The methods ITCCA and TRCA were used for both paradigms. All methods were applied after filtering and normalization.

4.1.2.1 Welch's Method

The welch method was used to increase the robustness of the target frequency estimation. This method required to adjust the EEG data at the input of the method to maximize the resolution of the method.

To take advantage of the Welch method, the concatenation of the largest amount of data from the various channels was made in a single temporal sequence for each trial, using a window with 2048 samples and overlap of 50% of the window. With the use of this window, information was not lost, since the frequency resolution was 0.12 HZ $\left(\frac{F_s}{window} = \frac{250Hz}{2048points} = 0.12Hz\right)$, while the frequency resolution of the benchmark dataset was 0.2 Hz.

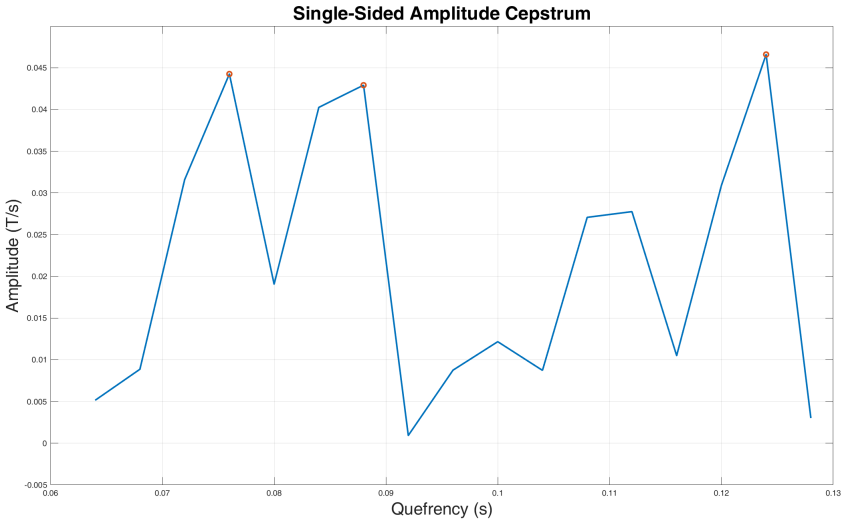

Figure 4.3: Example of a Cepstrum of SSVEPs responses at 8.0 Hz measured at channel Oz.

In the next step, the decision is made, considering the target frequency is deemed to be the central frequency f_c. If the frequency value detected during the Welch method extraction process is in the range between $f_c - \epsilon$ and $f_c + \epsilon$ (with $\epsilon = 0.1$Hz), this target is selected as an answer; otherwise, the target that has obtained the most significant amplitude is selected.

4.1.2.2 Cepstrum

The Cepstrum method was applied in order to identify the fundamental frequency of the SSVEP, taking into account the different harmonics existing in the EEG signal. Initially, a window was applied for each channel to be possible to have a periodic extension of the signal implicit in the discrete Fourier transform. With these signals, it was possible to extract the Cepstrum signal for each channel by applying (3.6). Then, the average signal of the Cepstrum was obtained for each trial. Figure 4.3 shows an example of a Cepstrum obtained from channel Oz.

The cepstrum signal obtained for each trial is analyzed and limited to the values of the quefrency vector between the values of 1/7.8 seconds and 1/16 seconds. The maximum amplitude that gives rise to the identified frequency of the resulting signal is verified in the decision-maker, where the frequency is specified in the same way as in the Welch method, considering f_c as the target frequency to be determined and evaluating whether the frequency detected in Cepstrum signal is in the interval between between $f_c - \epsilon$ and $f_c + \epsilon$ (with $\epsilon = 0.15$Hz).

4.1.2.3 Correlation Coefficients, Dynamic Time Warping and Cosine Similarity

These methods of correlation and similarities between time series aim to maximize the correlation or to minimize the distance that differs between the time series. For each trial, the average of 4 data blocks was used to compare with the test block, creating the template from training data and always testing with unseen data.

The Pearson correlation (3.7) was applied to the individual template with the training EEG and the test EEG was subsequently utilised, creating the matrix of correlation coefficients between the data from train and the test. The element (1,2) of each matrix for all targets (BCI) and all subjects (subject identification) was extracted. The output was the maximum value of the resulting vector.

For the application of the Dynamic Time Warping method, the formula (3.9) was applied to calculate the distance between two-time sequences (each channel) between the training template and the test trial. After that, the average of the distances was calculated and the minimum value of the resulting vector is chosen.

With the Cosine Similarity method, the objective was to compare the similarities by choosing the targets or subjects in which the test data were most similar to the training template. The formula (3.11) was applied to each block of data compared to the template, and then the average of the distances to the channels was applied. The target that has the maximum similarity value was the one selected.

4.1.2.4 CCA

The selected target was extracted based on the CCA output. The reference signal was created, which was constructed considering the equation 3.12, in section 3.3.2. The SSVEP benchmark dataset has 40 targets in total, requiring a reference signal for each of the frequencies f_n, between 8 Hz and 15.8Hz, spaced by 0.2 Hz, defined by:

$$Y(f_n) = \begin{bmatrix} \sin(2\pi \times f_n \times t) \\ \cos(2\pi \times f_n \times t) \\ ... \\ \sin(2\pi \times 4 \times f_n \times t) \\ \cos(2\pi \times 4 \times f_n \times t) \end{bmatrix}, t = \{0, 4ms, 8ms..., 6sec\} \tag{4.3}$$

The next step was the implementation of the CCA shown in Fig. 4.4, with the method inputs being the $X^{(i)}$ corresponding to multi-channel signal from the ith trial, with dimensions N_C channels $\times$ N_S samples and the reference signal, with dimenions 8 harmonics $\times$ N_S samples, and the variables C_{xx} of size $N_C \times N_C$, C_{xy} of size $N_C \times 8$, C_{yx} of size $8 \times N_C$ and C_{yy} of size 8×8. The procedure represented in Fig. 4.4 was replicated for all of the reference signals (40 targets). At last, the canonical correlation output ρ has a

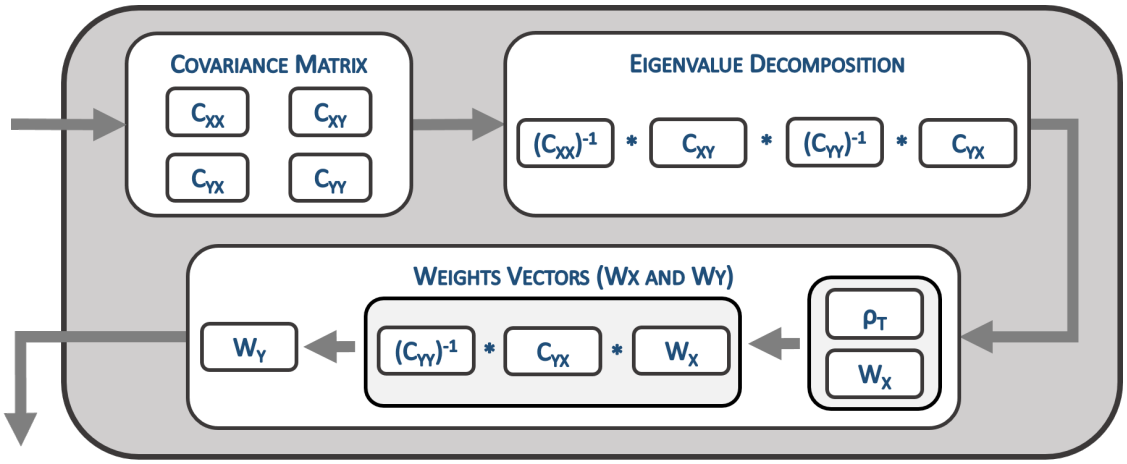

Figure 4.4: Implementation of the CCA and ITCCA algorithm.

dimension of $1 \times N_T$ targets, where the maximum value corresponds to the target that has the highest correlation with the reference signal.

4.1.2.5 ITCCA

The ITCCA method requires an individual template for each target (C-VEP-BCI or SSVEP-BCI) or each user (C-VEP identification). As an individual template, we used the average of the trials of the training blocks for each of the targets (N_C channels $\times N_S$ samples - depending on 'N_C' and 'N_S' of the dataset for the respective paradigm). After that, the method was applied as described in Fig. 4.4, with the inputs being the test multi-channel EEG signal and the individual template signal, both inputs with N_C channels $\times$ N_S samples. At last, the canonical correlation output ρ has a dimension of $1 \times N_T$ targets, where the maximum value corresponds to the target with the highest correlation with the individual template.

4.1.2.6 TRCA

The TRCA was implemented in Matlab following the methodology described in [71]. The implementation of the TRCA method involves the calculation and optimization of weights to maximize the correlation between the various data trials, and for that, it needs to perform the weighted linear sum of the various time series. It should be noted that the necessary inputs for the TRCA method are only the target (BCI) or subject (identification) EEG data.

Initially, in the extraction process for each target or subject, the component related to the task is obtained, and the covariance matrix $S_{N_C \times N_C}$ is built and updated with each

combination between two trials X^i and X^j of a total of B trials of that target, using

$$S = \sum_{i=1}^{B-1} \sum_{j=i+1}^{B} Cov(X^i, X^j) = \sum_{i=1}^{B-1} \sum_{j=i+1}^{B} \left(X^i \times (X^j)^T + X^j \times (X^i)^T \right) \tag{4.4}$$

The EEG signals for all trials of each target are concatenated in a single time series, creating the matrix $U_{N_C \times B*N_S}$. The covariance matrix $Q_{N_C \times N_C}$ is created using $Q = U \times U^T$.

Figure 4.5 presents an example diagram for the implementation of the TRCA method containing three trials of EEG data with N_C channels and N_S samples each for a given target $(X^{(1)}, X^{(2)}, X^{(3)})$. The matrix S was obtained by

$$S = Cov(X^{(1)}, X^{(2)}) + Cov(X^{(1)}, X^{(3)}) + Cov(X^{(2)}, X^{(3)}) \tag{4.5}$$

The EEG data from the three trials were concatenated into a single vector $U_{N_C \times 3N_S} = [X^{(1)} X^{(2)} X^{(3)}]$, to calculate the matrix $Q_{N_C \times N_C}$.

$$Q = \begin{bmatrix} X^{(1)} & X^{(2)} & X^{(3)} \end{bmatrix} . \begin{bmatrix} X^{(1)} \\ X^{(2)} \\ X^{(3)} \end{bmatrix} \tag{4.6}$$

The eigenvalues that maximizes $Q^{-1}S$ are the spatial filters W for each target or user. The decision is made using formula (3.24), i.e., applies the projections to test data and computes its correlation to the projected model data.

4.1.3 EEG Differentiation

Generally, EEG waves recorded based on voltage amplitudes in different channels of the biosignal amplifier are used as input for algorithms to make the respective classification and identification of features [5]. The 1^{st} and 2^{nd} derivatives of the EEG signal is proposed as a implementation step before the feature extraction methods, to explore the dynamics of C-VEP as response the stimulation steps (binary transitions). Particularly, the first derivative has shown improved results, as will be verified in sections 5.1.2.1 and 5.1.3.1. This implementation led to a new differentiated version of some of the methods implemented in the previous section, for example, D-TRCA (Differentiated TRCA) and D-Correlation Coefficients (Differentiated Correlation Coefficients).

The derivatives of the EEG signals were obtained using the finite difference formulas, used as an approximation of the derivative, with:

$$f'(k) = \frac{f(k) - f(k-1)}{h}; \quad f''(k) = \frac{f'(k) - f'(k-1)}{h} \tag{4.7}$$

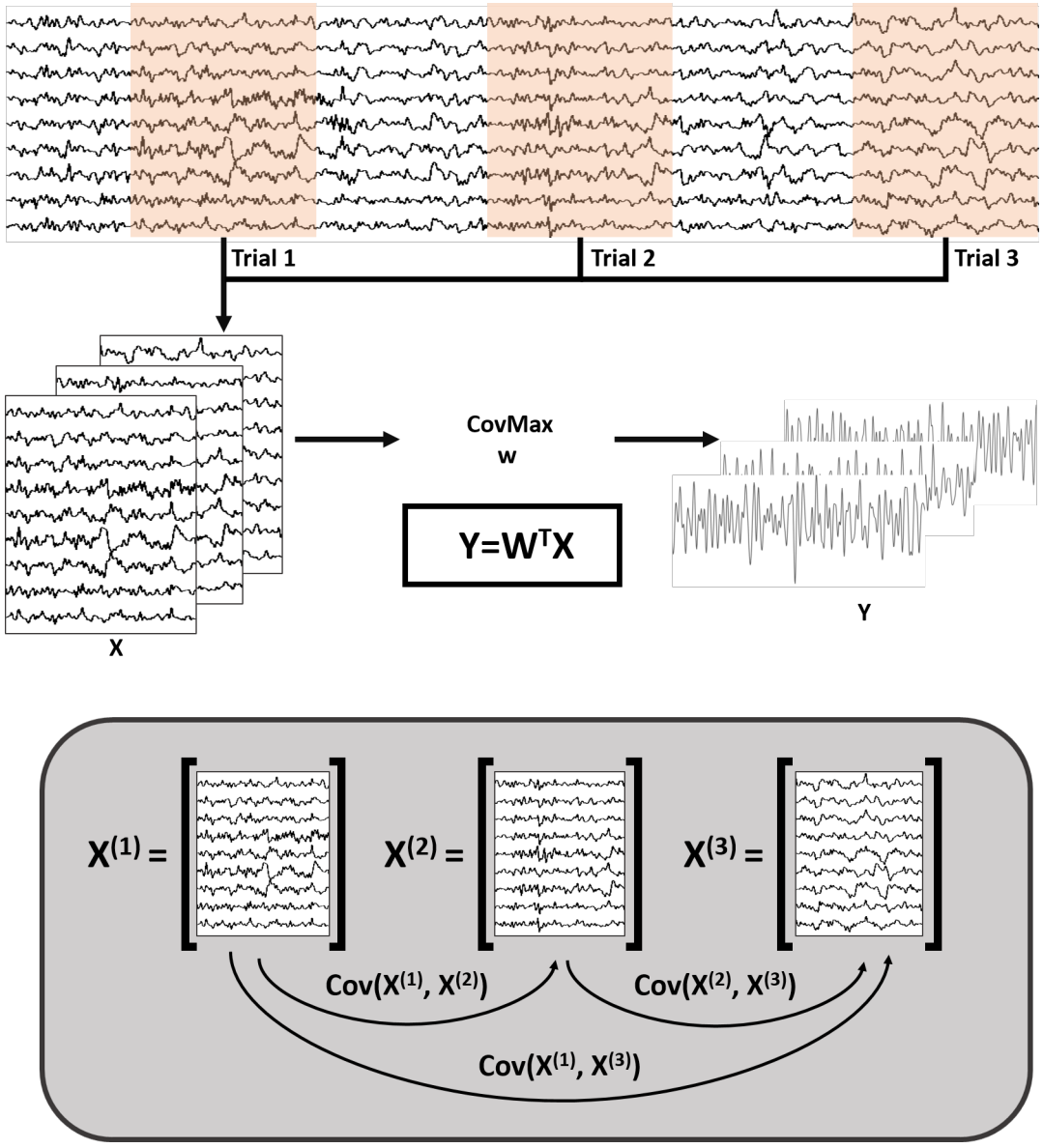

Figure 4.5: Diagram of the TRCA with continuous multi-channel EEG. The shaded areas correspond to the stimulus duration segments corresponding to a target in three different trials. The gray block shows the covariance between the different trials, to create the covariance matrix S.

where h is the value of the sampling period.

4.2 Generation of m-sequences

The creation of our sequence allowed the validation of the logic necessary for the generation of sequences to expand the different codes to be used in C-VEP, not only being dependent on the already existing sequences.

The m-sequences chosen to modulate the targets in the experiment described in section 4.3 have a length of 31 bits. For the creation of a 31-bit m-sequence, there are six possible primitive polynomials of degree 5, defined by

$$\begin{gathered} x^5 + x^2 \\ x^5 + x^3 \\ x^5 + x^3 + x^2 + x \\ x^5 + x^4 + x^3 + x^2 \\ x^5 + x^4 + x^2 + x \\ x^5 + x^4 + x^3 + x \end{gathered} \tag{4.8}$$

Each of these primitive polynomials can generate a different m-sequence, making it possible to have different sequences, considering all the possibilities of initial seed with 5 bits (excluding seeds consisting only of '0' and only '1'). After an analysis of all combinations for the m-sequences and their shifted sequences and the lowest values of the complexities were verified, the coded modulation using the taps of the polynomial $x^5 + x^2$ and the initial seed 01010 were used, creating the m-sequence:

0101011101100011111001101001000

4.3 Experimental Laboratory Setup

This section explain each aspect of the experimental setup, which is composed of the stimulation module, the data acquisition module, the signal processing module and finally, decision-module that selects target (C-VEP BCI) or the user (C-VEP identification). The datasets recorded are referred to as C-VEP-ISR datasets.

4.3.1 Stimulation Module

The C-VEP system requires a strict synchronization between the acquisition data and the stimulus events and the delay between the presentation of the stimuli and the acquisition event needs to be very small and always constant. The stimulation module receives information about the moment of the stimulus presentation using a trigger signal sent by

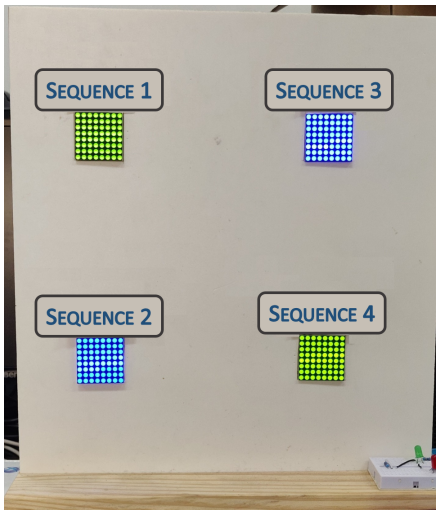

Figure 4.6: Stimulation based on LED matrices.

the EEG recording system. Here, this trigger is sent from Simulink, that embeds an EEG acquisition driver provided by g.tec, that runs in real time (see section 4.3.2.1).

The stimulation module is composed of 4 LED matrices 8x8 (2 yellow-green and 2 blue) and it is controlled by an Adafruit Feather HUZZAH ESP8266[1], as shown in the picture and circuit of the Figs. 4.6 and 4.7. This module generates visual stimuli independent of the use of a computer screen, allowing a greater portability of the system.

Feather HUZZAH ESP8266 has an ESP8266 WiFi microcontroller clocked at 80 MHz and with a 3.3V logic, containing a Tensilica chip core that implements a WiFi stack. The 3.7V Lithium polymer batteries enables the use of this development board in portable projects [2].

Each of the LED matrices flashes according to a pre-programmed binary sequence to be generated directly by the development board. The stimulus alternates between two states: *dark* and *light* (color yellow-green or blue), so a binary sequence can be used as a modulation sequence, where *dark* and *light* represent a bit '0' and '1' in the binary sequence, respectively. The triggers indicating the onsets of the m−sequences were sent from the computer directly to the HUZZAH ESP8266 microcontroller to mark the beginning of each C-VEP response acquisition. The LED matrices are activated via the I2C bus through the generator program for stimuli, which was written in *C*-language.

Since there are only four targets in our setup, it is guaranteed that a sequence with 31 bits and a 7-bit shift for its shifted sequences is sufficiently spaced from the original sequence to ensure identification. For the stimulus modulation, the sequences proposed in [3] were used, as well as our sequences generated in section 4.2.

[1]Adafruit Feather HUZZAH ESP8266: https://learn.adafruit.com/adafruit-feather-huzzah-esp8266/

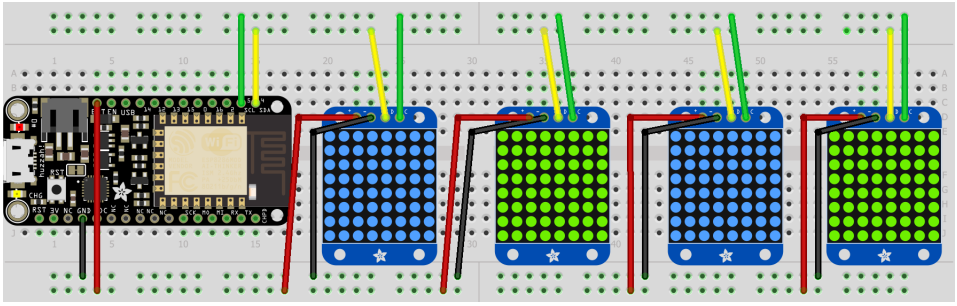

Figure 4.7: Stimulation circuit based on LED matrices.

4.3.2 EEG Recording Systems

The EEG acquisition system is composed of the electrodes, the cap and the bio amplifier. The two systems used are from g.tec (Austria, the Unicorn and the gUSBamp. The experimental setups are shown in Fig. 4.8 and Fig. 4.9. The Unicorn Hybrid Black has the advantage of being portable and has few is a low-cost portable EEG system with eight channels, while the g.USBamp has a 16 channel high-end device with high performance. In appendix E, it is possible to find more details about the two systems.

4.3.2.1 Signal Acquistion with g.USBamp

g.USBamp (g.tec medical engineering GmbH, Austria) is a medical and research-grade device. The system is connected by USB to the PC. It supports 16 DC-coupled wide-range input channels (electrodes) per unit simultaneously sampled biosignal with a 24-bit resolution, allowing a high precision data acquisition [31].

The g.USBamp Simulink block used in the data acquisition on the 'recording' computer allows several hardware configurations: sampling rate, unipolar and bipolar montages, pre-set filters, etc. The g.USBamp acquisition system records the brain's EEG signals using the g.EEGcap, which can be used up to a maximum of 65 active Ag/AgCl electrodes that pre-amplify the EEG signals which are then sent to the system. Figure 4.10a) shows the location of the g.USBamp amplifier electrodes according to the international 10/20 system. The EEG signals were recorded at 256Hz and 512 Hz sample rates in a unipolar way using 12 electrodes. The left or right earlobe was chosen as a reference and the ground electrode placed in the AFz. The channels selected were the Fz, Cz, C3, C4, CPz, Pz, P3, P4, POz, Oz, PO7 and PO8.

The acquisition system performs as a preprocessing step a band-pass filter between 0.5 and 100 Hz to remove high-frequency noise and a notch filter at 50 Hz to reject the power line noise source.

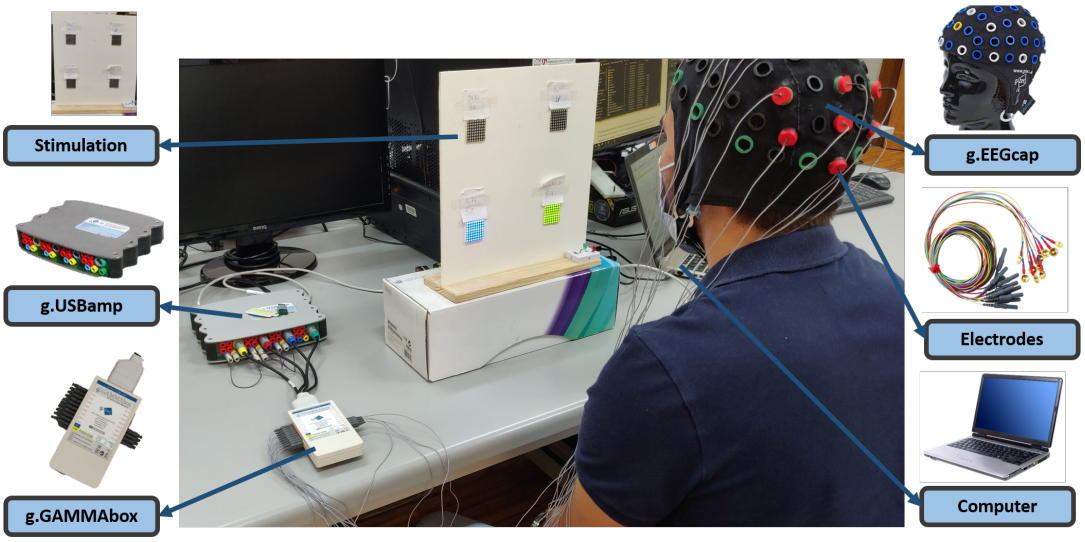

Figure 4.8: Picture of the experimental setup with a user wearing the EEG cap and the g.USBamp amplifier is acquiring the data simultaneous with the occurrence of the stimulation.

4.3.2.2 Signal Acquistion with Unicorn Hybrid Black

Unicorn Hybrid Black allows to read EEG data with 24-bit resolution and sampled with 250 Hz per channel and can be filtered with a notch and band-pass filters to suppress artefacts or to extract certain frequency bands like alpha and beta sub-bands [30].

Unicorn uses Bluetooth data transfer and has its own application (Unicorn Suite Software) and some tools to acquire, view, and store data or perform real-time analysis of brain activity and to calibrate the amplifier electrodes.

Figure 4.10b) shows the location of the Unicorn amplifier electrodes according to the international 10/20 system. The EEG signals were recorded at 250Hz sample rates from 8 electrodes. The electrodes positions of the cap are Fz, C3, Cz, C4, Pz, PO7, Oz and PO8 according to the 10/20 system. The reference and ground EEG electrodes was fixed on the mastoids of the user. The EEG signals was filtered with a 50Hz Notch filter and a 0.5 to 60Hz Bandpass filter.

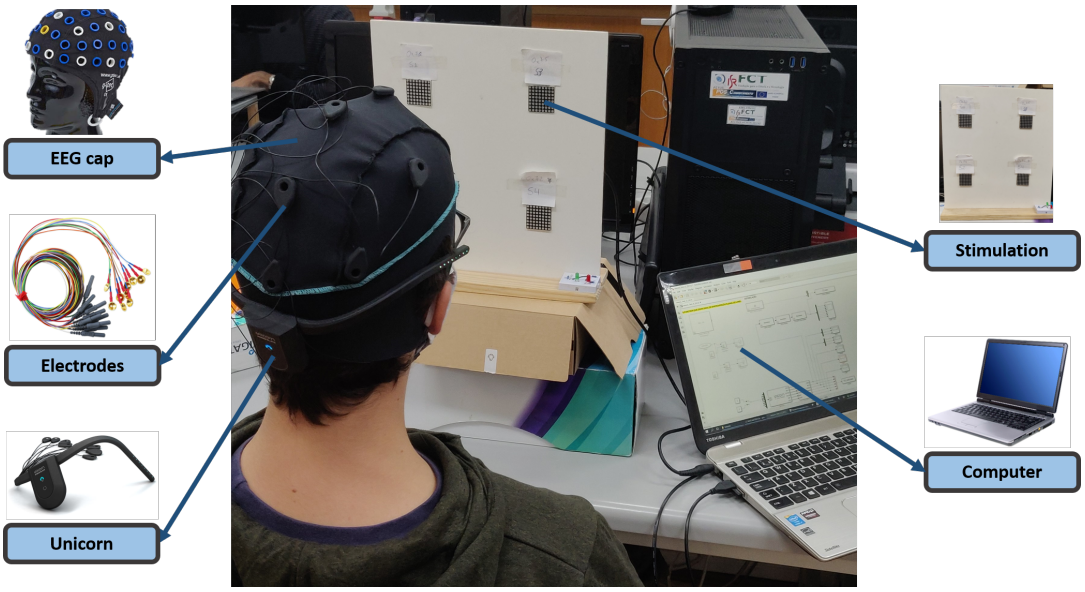

Figure 4.9: Picture of the experimental setup with a user wearing the Unicorn Hybrid Black headset is acquiring the data simultaneous with the occurrence of the stimulation.

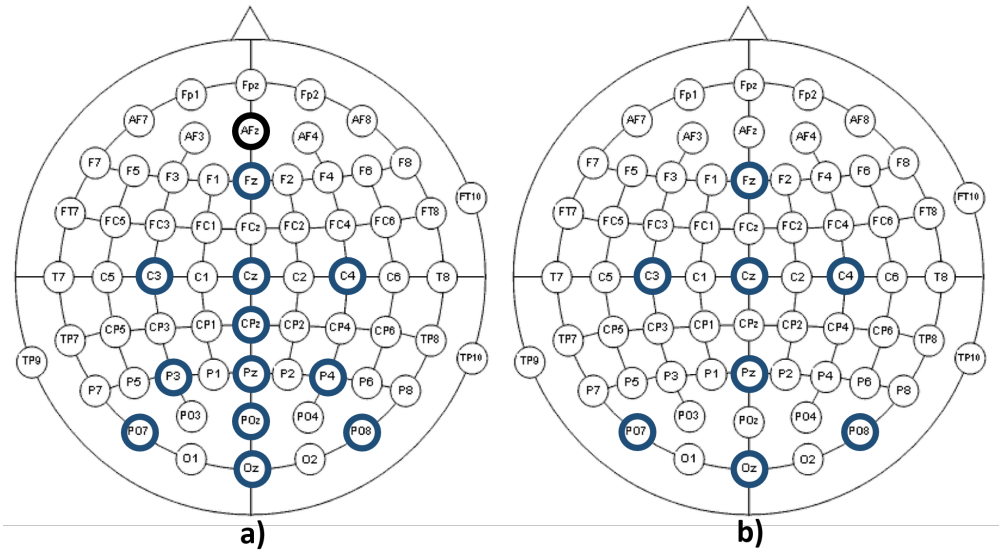

Figure 4.10: Location of electrodes of the EEG amplifiers used in the experiments, according to the international 10/20 system. Blue circles illustrate the channels used in the C-VEP experiments: a) Electrodes in g.USBamp; b) Electrodes in Unicorn.

4.3.3 EEG Data Acquisition and Stimulation Synchronization

The synchronization between the signals collected and the stimulus presentation is obtained through a marker that is transmitted from the Matlab/Simulink to the stimulation microcontroller and at the same time labels the EEG being recorded.

The Callback functions of the Simulink model were used to allow the acquisition to be synchronized with the stimulation, allowing the execution of commands at specific times

points. Therefore, it was possible to send the trigger to start, directly to the EEG amplifier and the stimulation. Three of the existing Callback functions were used: InitFcn, StartFcn and StopFcn. The InitFcn was used to create the connection to serial port between the acquisition computer and the microcontroller; the StartFcn allows sending the flag to start the stimulation at the beginning of the acquisition, and StopFcn allows to stop the stimuli and the simulation when the trial ends.

4.3.4 C-VEP-ISR Datasets

The proposed C-VEP setup allowed to acquire data (C-VEP ISR Datasets) and apply the best detection approaches in a pseudo-online way. We tested the system with m-sequences already used and with our own m-sequences, originating four different C-VEP-ISR Datasets.

Twelve participants enrolled the experiment. During the c-VEP experiments, the users were seated on a comfortable chair in front of the stimulation module, with users sitting approximately 40-50 cm from the stimulation module, and were instructed not to move their neck when changing their eye-gaze among the four LEDs to reduce the electromyographic noise caused during the movement. Each session was separated with breaks of 2-3 minutes during the experimental sessions, to avoid user's eye blinks.

For each of the contexts analyzed with C-VEP (BCI and identification), different datasets were acquired with varying conditions regarding the way users looked at targets. In the acquisitions made to identify targets, all LEDs continued to flash simultaneously, each with the time-shifted m-sequence, with the user focus in a central point of module. During the acquisitions made for the identification of subjects, only one of the LEDs flashed at a time, and it was requested to the users to focus the gaze on that particular LED during these recordings.

During the preliminary acquisitions, the bit time was evaluated, which would allow repeating the binary sequence multiple times, but in such a way that the user does not feel tired, nor makes an effort to gaze to the target. The selected bit time was 25 milliseconds per bit, allowing each sequence of 31 bits to run 0.775 seconds and the stimulation of each target for each trial lasted between 0.775 seconds (1 time) and 7.75 seconds (10 times).

Figure 4.11 shows the experimental time-course during one target acquisition, starting with the indication of the target where the subjects should direct their gaze, followed by the stimulation phase in which all targets adopt their lagged and repeated this sequence ten times during 7.75 seconds. After the stimulation period, subjects could rest for 30 seconds until the next target.

The data processing and storage were performed on a 'recording' computer TOSHIBA laptop (Intel Core i7 2.50 GHz 16.00 GB RAM, Microsoft Windows 7 Home). EEG data were recorded for each of the five sessions of the four targets viewed. The selection of

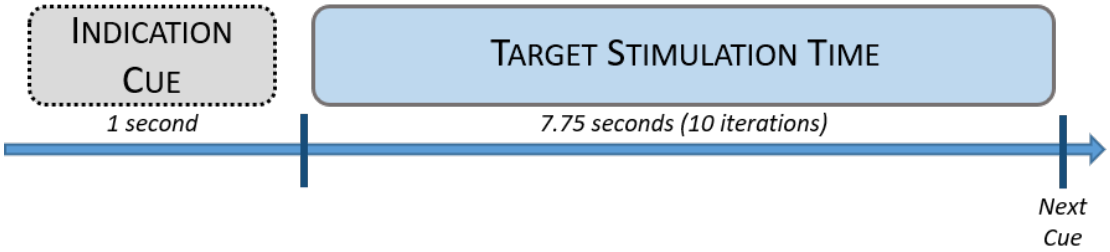

Figure 4.11: Time-course of one target during the experiment in C-VEP-ISR Dataset.

targets during data acquisition was performed randomly to each subject to avoid a bias in the collaboration of participants in the experiment.

The EEG was then cut into 7.75-second epochs starting from the moment of stimulation initiation and labelled and saved with the corresponding cues target. The ISR_C-VEP Dataset contains a data file in MATLAB for each of the participants tested in the experiment, named as subject indices (i.e., S01.mat). For each file, the data generate a 4-dimensional array with dimensions of 12 channels × 3969 time samples × 4 targets × 5 blocks.

4.4 Complexity of Pseudorandom Binary Sequences

To determine which are the best sequences that could be used to code the visual stimulation, we explored complexity measures of the pseudorandomness of binary sequences were evaluated, which is defined as a behaviour similar to random nature, despite presenting a pattern of deterministic mathematical nature. A binary sequence is considered "good" if the values of these parameters are low, depending on the number of bits used, i.e, it is a sequence that allows the identification of subjects with greater accuracy.

The first analysis model used was the sequence distribution formula. Considering the binary sequence with N bits $E_N = (e_1, e_2, ..., e_N) \in \{-1, +1\}^N$, it is possible to defined a well-distribution measure of E_N as:

$$W(En) = \max_{a,b,t} \left| \sum_{j=0}^{t-1} e_{a+jb} \right| \tag{4.9}$$

where the maximum is taken considering all values for a,b and t such that $a, b, t \in \mathbb{N}$ and $1 \leqslant a < a + b(t-1) \leqslant N$ [64].

The second and third methods of analysis assume that S is a binary sequence of n bits, composed of 'zeros' and' ones'. In the second one, Andrei Kolmogorov [35] defines the complexity of S as being the number of bits in the smallest sequence that is capable of generating the sequence S. The number c is the value of complexity, i.e., the number of

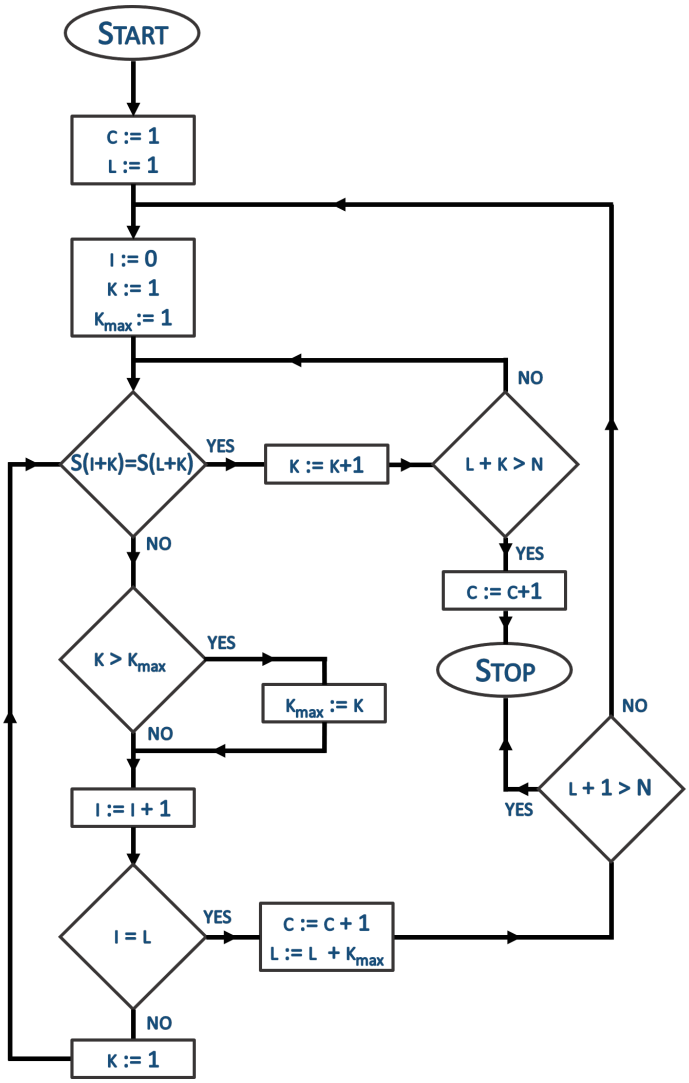

Figure 4.12: Diagram for the algorithm to calculate the Kolmogorov complexity $c(n)$ of a string of length n (figure based in [33]).

iterations required to create the sequence S [33]. Figure 4.12 presents a flowchart of the implemented method to determine the Kolmogorov's complexity.

The third method of analysis is the Lempel-Ziv complexity presented in [37]. This method is the Kolmogorov Complexity computed with a limited set of programs that only allows the recursive copy and insertion in strings [33]. Each bit of the S sequence is analyzed, from left to right. The complexity value is increased by one when a subsequence of consecutive bits that was not found in the analysis previously made is discovered. The analysis using the third method was done using the code provided by [72]. This algorithm evaluates two types of complexity in a sequence [84]:

- Exhaustive - Lower limit of the complexity measurement - based on finding extensions to a sequence, which are not reproducible from that sequence, using a recursive symbol-copying procedure.

- Primitive - Upper limit of the complexity measurement - the sequence decomposition occurs at points where the eigenfunction of a sequence increases in value from the previous one.

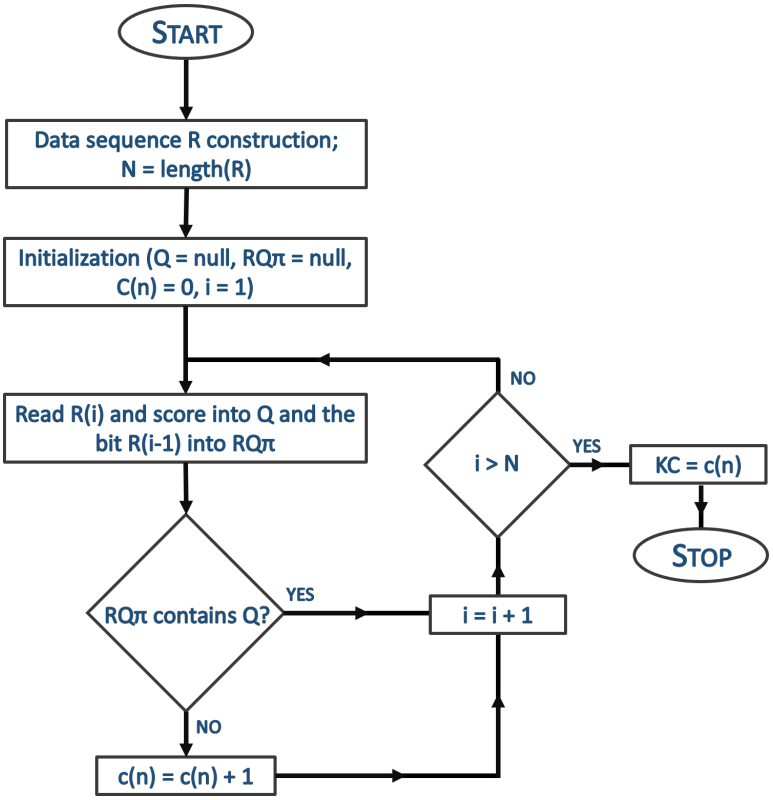

Figure 4.13: Diagram for the algorithm to calculate the Kolmogorov complexity $c(n)$ of a string of length n using the Lempel-Zev algorithm (figure based in [42]).

5

Results and Discussion

This chapter presents the offline results obtained with the SSVEP and C-VEP benchmark datasets and with our own C-VEP datasets. First, all methods are tested on benchmark datasets. Then, EEG signals recorded with our setup is compared using the same detection approaches. Appendix A presents the tables with the most detailed classification results for each user (C-VEP BCI) and each m-sequence (C-VEP identification).

Tests were carried out with the g.USBamp acquisition system, and also with the Unicorn headset. However, due to the excessive existing noise in the recorded signals, it was not possible to obtain consistent results with the Unicorn headset.

5.1 Validation Results

In the first stage of experiments, the public benchmark datasets for SSVEP [74] and C-VEP [77] were tested with the feature extraction methods analyzed in section 3.3.2 and implemented in the section 4.1.2. The goal was to evaluate different feature extraction methods for SSVEP and C-VEP detection to decide the optimal configuration for each one. With the different methods applied, it was possible to study two different perspectives: 1) the best methods to obtain the highest possible accuracy; 2) less computational demanding techniques for identifying targets or subjects in real-time, and test smaller subsets of channels.

For a direct comparison with our wearable EEG system (Unicorn), the methods were applied considering all channels of the public dataset, considering 8 channels from the visual cortex and considering only 8 preset channels, which have the same scalp location as the Unicorn headset, our wearable EEG acquisition system.

Cross-validation was used for assessment of the methods. For the detection methods in which a statistical model was required, the individual template was estimated using leave-one-out cross-validation, thereby ensuring that the results were never obtained from seen data, and providing a reliable metric [7]. With the cross-validation, the data was split in train and test sets. Given that the test data was not used in the training procedure, the performance obtained in that trial can provide an insight into the generalization capabil-

ities of the method. Each dataset is divided into blocks (repetitions of the same target or user). For the SSVEP dataset with 6 data blocks, the validation was performed using 5 blocks for training and 1 test block, while for the C-VEP dataset with 5 data blocks the validation was done with 4 training blocks and one test block.

For the C-VEP paradigm, four analyzes were performed regarding normalization: 1) DC Offset Removal using the entire acquired signal (10 repetitions of the 31 bit sequence); 2) Signal normalized to [-1; 1] across ten repetitions ; 3) DC Offset Removal with the average of the ten acquired repetitions ; 4) Signal normalized to [-1; 1] with the average of the ten acquired repetitions .

Appendix A presents the tables with the most detailed results of the various tests performed for each subject (BCI) and each target (subject identification).

5.1.1 SSVEP-based BCI

Five feature extraction methods were used with the public benchmark dataset for SSVEP: the Welch, Cepstrum, CCA, ITCCA and TRCA.

The mean classification results are shown in table 5.1. The method that performed best accuracy for all subset of channels was the TRCA. The best accuracy was achieved using the 8 occipital channels, with the TRCA. Using only the subset channels corresponding to the channels of the Unicorn, best results were obtained also using the TRCA, reaching 95% accuracy.

It is possible to verify that the methods that have a user model obtained previously (CCA, ITCCA and TRCA) show better results than the Welch and Cepstrum methods, which do not have the training component or use the correlation between channels.

The best results achieved with occipital channels can be explained by two reasons: 1) these channels are part of the visual cortex channels allow to obtain better results since it is in this area that the SSVEP is evoked; 2) the use of electrodes with signals with high contamination due to movement muscle and eye, causing irrelevant features.

The Cepstrum values were low due to the existence of too many signals convolved together to cepstrum to extract correctly. However, a more particular analysis was made, using fewer targets, that is explained in Annex C.

The computational effort of each method was another variable analyzed during the implementation of the methods. Table 5.2 shows the processing time for each feature extraction method. It should be noted that the processing times presented for ITCCA and TRCA exclude the time required for calculating the template. The TRCA method is the most effective since it has the best accuracy results and was found to have a very short processing time, which shows that it can be implemented in devices with lower computation power. The processing time has decreased with the use of just 8 channels,

compared to using the 64 channels.

Table 5.1: Mean classification results in the SSVEP benchmark dataset (based on 5 seconds stimulation) for each method.

	All channels		Visual 8 channels		Unicorn 8 channels	
Method	**Accuracy** [%]	**ITR** [bpm]	**Accuracy** [%]	**ITR** [bpm]	**Accuracy** [%]	**ITR** [bpm]
Welch	34,05	30,10	51,63	49,31	46,02	43,32
Cepstrum	54,75	46,68	30,76	18,32	33,05	21,29
CCA	86,45	102,14	93,95	115,11	77,22	87,85
ITCCA	81,53	94,64	93,74	114,23	80,27	92,26
TRCA	96,55	120,93	**97,36**	**121,63**	95,68	118,12

Table 5.2: Processing time in Matlab, in seconds, for the methods implemented in the SSVEP benchmark dataset.

	All channels	Visual 8 channels	Unicorn 8 channels
Welch	0,36	**0,06**	**0,06**
Cepstrum	62,12	9,51	9,72
CCA	7,20	0,87	0,87
ITCCA	10,00	0,55	0,56
TRCA	0,89	0,16	0,19

5.1.2 C-VEP-based BCI

With the public benchmark dataset used for identification of targets with C-VEP, four feature extraction methods were applied: the ITCCA, the TRCA, the Correlation Coefficients and the Cosine Similarity.

5.1.2.1 C-VEP Benchmark Dataset

Table 5.3 shows the results obtained for the identification of targets by applying the different combinations of signal normalization functions and feature extraction methods, while table 5.4 presents the results obtained for the various combinations with the application of the first derivative of the EEG signals. Table 5.3 shows the best result using a subset of channels corresponding to the channels located in the visual cortex, obtained with the averaged data of ten repetitions , normalized with DC offset removal and applied to the TRCA method (97.66%), close to those presented in [77]. For all channels in the public dataset, it was possible to achieve an accuracy of 94.22% and with the subset corresponding to Unicorn channels, a maximum of 88.48%. Table 5.4 shows the best result

was also obtained using a subset of channels corresponding to the channels located in the visual cortex and as the same method attained with the averaged data of ten repetitions, normalized with [-1; 1] interval (98.79%). For all channels in the public dataset, it was possible to achieve an accuracy of 97.57% and with the subset corresponding to Unicorn channels, a maximum of 91.95%.

The application of the derivative proved to be an excellent improvement for the identification of targets, seen when comparing results between both tables, having improved the results in all tested combinations.

The use of normalization at the interval [-1; 1] allowed to improve the results obtained, as can be seen in both tables, reaching an improvement of 9 percentage points with the application of data from the channels located in the visual cortex to the Correlation Coefficients method.

The effect of using the average of the various ten repetitions of data, comparing with the use of the concatenated signal, greatly improved the performance of the system, with maximal improvements of 30 percentage points being obtained in certain tests, except with the application of the ITCCA method, in that the use of the average dropped the results dramatically. These results were motivated by the small number of signal samples used to create the template to apply the canonical correlation.

Table A.2 shows the best classifications results for each method and each subset of channels with different normalizations. It can be seen that S9 and S15 obtained the best target identification accuracy, especially with TRCA, while S7 was the subject with the lowest mean accuracy values. Table A.3 shows that all participants had improvements in many of the tests performed, with the previously worse result seen for S7 having improved by 30 percentage points.

The comparison between the accuracy values with all channels and only with the visual cortex channels suggests that the evoked potentials are driven by visual stimulation.

Table 5.5 shows the processing time for each method implemented. The Cosine Similarity method has the best processing times when considering only the use of visual channels or the Unicorn channels. When all channels in the dataset are used, the best method is TRCA with a processing time of 36 milliseconds. As would be expected, given the amount of data processed differs with the number of channels used, processing time is lower for 8 channels than for the full set of channels.

Table 5.3: Mean classification results for the C-VEP benchmark dataset for each subject to target identification with different methods of normalization.[a]

	Method	**ITCCA**		**TRCA**		**Correlation Coefficients**		**Cosine Similarity**	
	Normalization	**Acc** [%]	**ITR** [bpm]	**Acc** [%]	**ITR** [bpm]	**Acc** [%]	**ITR** [bpm]	**Acc** [%]	**ITR** [bpm]
All chans	**DC Offset Removal**	60,70	24,75	92,23	45,56	46,76	16,62	49,49	17,19
	Range [-1 1]	61,41	25,15	94,22	47,12	52,42	18,74	50,47	17,66
	DC Offset Removal (Average)	10,16	1,12	92,27	45,07	75,31	34,08	76,84	33,51
	Range [-1 1] (Average)	9,30	0,93	90,70	43,64	80,00	35,69	78,24	34,50
Visual 8chans	**DC Offset Removal**	82,81	38,47	94,14	46,82	66,80	28,32	72,66	30,93
	Range [-1 1]	82,62	38,35	94,57	47,20	75,47	32,82	74,14	31,93
	DC Offset Removal (Average)	62,50	24,36	**97,66**	**49,75**	83,28	39,79	90,27	43,35
	Range [-1 1] (Average)	62,07	23,94	97,54	49,56	91,00	43,98	90,78	43,77
Unicorn 8chans	**DC Offset Removal**	67,97	30,73	80,31	38,88	43,75	15,11	47,77	16,65
	Range [-1 1]	68,16	30,70	80,82	39,12	50,63	18,16	48,05	16,79
	DC Offset Removal (Average)	47,46	16,84	88,48	43,60	74,22	33,54	73,36	31,71
	Range [-1 1] (Average)	47,46	16,70	88,32	43,25	76,50	33,87	73,63	31,84

[a] The term 'All chans' is the label for tests performed using the 31 channels of the dataset. The term 'Visual 8chans' is the label for the use of the 8 channels of the visual cortex used in the dataset (Oz, O1, O2, POz, PO3, PO4, PO7, PO8). The term 'Unicorn 8chans' is the label for the use of the 8 channels of the dataset that correspond to the channels existing in the Unicorn Hybrid Black headset (Fz, C1, Cz, C2, Pz, PO7, PO8 and Oz).

Table 5.4: Mean classification results for the C-VEP benchmark dataset for each subject to target identification with different methods of normalization, using the first derivative of the EEG data. [a]

	Method	**D-ITCCA**		**D-TRCA**		**D-Correlation Coefficients**		**D-Cosine Similarity**	
	Normalization	**Acc [%]**	**ITR [bpm]**	**Acc [%]**	**ITR [bpm]**	**Acc [%]**	**ITR [bpm]**	**Acc [%]**	**ITR [bpm]**
All chans	**DC Offset Removal**	72,27	31,96	96,48	48,79	50,70	18,81	52,14	17,01
	Range [-1 1]	73,24	32,65	97,57	49,68	56,50	20,88	52,89	17,41
	DC Offset Removal (Average)	10,55	1,17	96,56	48,79	79,61	37,28	80,74	34,84
	Range [-1 1] (Average)	9,88	1,09	96,45	48,48	89,26	42,90	81,33	35,28
Visual 8chans	**DC Offset Removal**	88,87	42,68	96,17	48,53	66,56	28,45	73,63	29,86
	Range [-1 1]	89,45	43,11	96,80	48,96	75,51	33,11	74,37	30,36
	DC Offset Removal (Average)	30,05	30,05	98,44	50,57	84,53	40,83	90,98	42,95
	Range [-1 1] (Average)	30,05	30,05	**98,79**	**50,88**	93,44	46,25	91,17	43,11
Unicorn 8chans	**DC Offset Removal**	72,38	33,99	82,50	40,15	48,59	17,63	50,63	16,22
	Range [-1 1]	72,30	34,22	82,85	40,37	55,94	21,07	51,41	16,63
	DC Offset Removal (Average)	56,41	21,90	91,41	45,52	79,18	37,44	77,62	32,60
	Range [-1 1] (Average)	56,48	21,79	91,95	45,80	86,80	41,90	78,13	32,96

Table 5.5: Processing time in Matlab, in seconds, for the methods implemented in the C-VEP benchmark dataset.

	All chans	**Visual 8chans**	**Unicorn 8chans**
ITCCA	0,700	0,103	0,105
TRCA	0,036	0,026	0,027
Correlation Coefficients	0,063	0,031	0,032
Cosine Similarity	0,051	**0,017**	**0,017**

5.1.2.2 C-VEP-ISR Dataset

The tests were experimentally conducted on 13 healthy patients with normal or corrected vision. Table 5.6 presents some information about the participants in the experiment. Ten of the participants were male, and three were female. The mean age of the participants was 22.4 years. Only three participants had previous experience with BCIs.

Table 5.7 shows the results obtained when visual stimuli were modulated by the sequences proposed in [3], for the target identification approach. With these results, it is possible to verify that the method that presents the best results is the TRCA, which can achieve 100% accuracy when using only the four channels, reaching results above 98% for all combinations of methods and normalizations, without the application of the derivative form. Using the derivative form of the EEG data was possible to achieve 97.08% of accuracy using all channels of the system. In general, the use of the form derived from EEG data as preprocessing maintains or improves the results obtained.

The application of normalization in [-1; 1] interval maintained or increased the accuracy of the tests performed, with the most significant improvement being seen in the Correlation Coefficients and Cosine Similarity methods.

The tables A.4 and A.5 present the detailed results for each subject, and the participants that achieved the best results for all the tested methods were the S12 and S13. In these tables, it is possible to verify that the application of the first derivative to the EEG data, improved the results for some subjects and worsened for others (S5, S9 and S11).

The results obtained for target identification approach from the EEG acquired during stimulation modulated by our proposed m-sequences are shown in table 5.8. With this table, it is possible to verify that the best results were obtain with the ITCCA and TRCA method. The best result was possible to achieve with a subset of 8 EEG channels and the application of the ITCCA method with the normalization of the amplitude to [-1, 1] interval, allowing a 98% accuracy target identification. The results obtained after the application of the derivative form showed a heterogeneous effect in all configurations, increasing the accuracy for some individuals, despite the decreasing of accuracy mean for the majority of the methods. For this dataset, the change in the applied normalization method did not change the results significantly, being similar between both methods.

The tables A.6 and A.7 present the detailed results for each participant with the stimulation modulated by our proposed sequence for the target identification approach. It should be noted the results obtained with the subject S3, where it was possible to obtain 100% accuracy for almost all tests performed.

Table 5.6: Information about each participant of the experiment (F-Female, M-Male, Amin-sequence proposed in [3]).

Participant	1	2	3	4	5	6	7	8	9	10	11	12	13
Name	M.I.G.F.	N.A.P.P.	A.P.T.F.	F.J.L.M.	Z.A.G.F.	D.S.P.	T.M.C.B	J.P.O.S	D.M.G	R.S.C.G	R.G.C	L.G.E	R.M.
Age	22	21	22	22	22	23	24	23	23	21	23	23	22
Gender	F	M	F	M	M	M	M	M	M	F	M	M	M
BCI experience	yes	yes	naïve	naïve	naïve	naïve	yes	naïve	naïve	naïve	naïve	naïve	naïve
First PRBS experimented	Our	Our	Amin	Our	Amin	Our	Our	Our	Our	Amin	Amin	Amin	Amin
PRBS experimented	Both	Both	Both	Both	Both	Both	Both	Both	Both	Our	Amin	Amin	Amin

Table 5.7: Mean classification results for the C-VEP-ISR dataset for each subject to target identification with different methods of normalization, using the sequence proposed in [3]. [a]

	Method	ITCCA		TRCA		Correlation Coefficients		Cosine Similarity		D-ITCCA		D-TRCA		D-Correlation Coefficients		D-Cosine Similarity	
	Normalization	**Acc** [%]	**ITR** [bpm]	**Acc** [%]	**ITR** [bpm]	**Acc** [%]	**ITR** [bpm]	**Acc** [%]	**ITR** [bpm]	**Acc** [%]	**ITR** [bpm]	**Acc** [%]	**ITR** [bpm]	**Acc** [%]	**ITR** [bpm]	**Acc** [%]	**ITR** [bpm]
All chan	**DC Offset Removal**	84,55	8,45	98,75	14,04	54,58	2,13	53,18	1,94	87,92	9,52	**97,08**	**13,14**	56,25	2,37	54,58	2,13
	Range [-1 1]	83,64	8,18	99,58	14,56	60,42	3,01	55,91	2,32	88,33	9,65	95,83	12,55	59,58	2,88	60,42	3,01
8 chans	**DC Offset Removal**	88,64	9,76	98,75	14,04	58,75	2,75	56,36	2,39	92,08	10,99	96,67	12,94	58,33	2,68	58,75	2,75
	Range [-1 1]	90,00	10,23	99,58	14,56	64,17	3,66	60,45	3,02	93,33	11,48	95,42	12,37	61,25	3,15	60,00	2,94
4 chans	**DC Offset Removal**	95,00	12,18	**100,00**	**14,90**	66,25	4,04	64,55	3,73	87,50	9,38	93,75	11,65	58,33	2,68	63,33	3,51
	Range [-1 1]	95,45	12,38	98,75	14,04	72,92	5,43	68,64	4,51	89,17	9,94	93,75	11,65	60,82	3,08	62,50	3,36
Unicorn 8chans	**DC Offset Removal**	88,64	9,76	98,33	13,80	57,08	2,49	54,55	2,13	82,50	7,85	95,00	12,18	59,17	2,81	58,33	2,68
	Range [-1 1]	88,64	9,76	98,75	14,04	62,50	3,36	59,55	2,87	85,83	8,85	93,33	11,48	60,83	3,08	60,00	2,94

[a] The term 'All chans' is the label for tests performed using the 12 channels chosen from the g.USBamp. The term '8chans' is the label for the use of the 8 channels of the visual cortex used in the dataset (CPz, Pz, P3, P4, POz, Po7, Oz, PO8). The term '4chans' is the label for the use of the 8 channels of the visual cortex used in the dataset (POz, Po7, Oz, PO8). The term 'Unicorn 8chans' is the label for the use of the 8 channels of the g.USBamp that correspond to the channels existing in the Unicorn Hybrid Black headset (Fz, C1, Cz, C2, Pz, PO7, PO8 and Oz).

Table 5.8: Mean classification results for the C-VEP-ISR dataset for each subject to target identification with different methods of normalization, using our proposed m-sequence. [a]

	Method	ITCCA		TRCA		Correlation Coefficients		Cosine Similarity		D-ITCCA		D-TRCA		D-Correlation Coefficients		D-Cosine Similarity	
	Normalization	**Acc [%]**	**ITR [bpm]**	**Acc [%]**	**ITR [bpm]**	**Acc [%]**	**ITR [bpm]**	**Acc [%]**	**ITR [bpm]**	**Acc [%]**	**ITR [bpm]**	**Acc [%]**	**ITR [bpm]**	**Acc [%]**	**ITR [bpm]**	**Acc [%]**	**ITR [bpm]**
All chans	**DC Offset Removal**	91,50	10,78	96,50	12,86	56,50	2,41	59,00	2,79	85,00	8,59	**97,50**	**13,35**	56,50	2,41	57,00	2,48
	Range [-1 1]	91,50	10,78	95,50	12,40	58,50	2,71	58,50	2,71	81,00	7,43	93,50	11,55	55,50	2,26	56,50	2,41
8 chans	**DC Offset Removal**	97,00	13,10	97,50	13,35	59,50	2,86	59,50	2,86	90,00	10,23	93,50	11,55	58,00	2,63	56,00	2,33
	Range [-1 1]	**98,00**	**13,62**	96,00	12,63	59,00	2,79	57,50	2,55	87,00	9,22	93,50	11,55	56,00	2,33	58,50	2,71
4 chans	**DC Offset Removal**	97,00	13,10	97,00	13,10	65,50	3,90	66,00	4,00	82,50	7,85	88,00	9,54	64,00	3,63	61,50	3,19
	Range [-1 1]	96,00	12,63	96,50	12,86	67,00	4,19	67,50	4,29	82,00	7,71	88,00	9,54	60,50	3,03	62,00	3,28
Unicorn 8chans	**DC Offset Removal**	92,50	11,16	97,50	13,35	59,50	2,86	59,50	2,86	81,50	7,57	88,00	9,54	57,00	2,48	59,50	2,86
	Range [-1 1]	90,00	10,23	97,50	13,35	60,50	3,03	60,00	2,94	78,50	6,77	88,00	9,54	57,50	2,55	56,50	2,41

[a] The term 'All chans' is the label for tests performed using the 12 channels chosen from the g.USBamp. The term '8chans' is the label for the use of the 8 channels of the visual cortex used in the dataset (CPz, Pz, P3, P4, POz, Po7, Oz, PO8). The term '4chans' is the label for the use of the 8 channels of the visual cortex used in the dataset (POz, Po7, Oz, PO8). The term 'Unicorn 8chans' is the label for the use of the 8 channels of the g.USBamp that correspond to the channels existing in the Unicorn Hybrid Black headset (Fz, C1, Cz, C2, Pz, PO7, PO8 and Oz).

5.1.3 C-VEP-based user identification

For the identification of subjects, the different methods of normalization were applied with the feature extraction methods and with the application of the first derivative to the subjects' EEG data. Five feature extraction methods were applied: the ITCCA, TRCA, correlation coefficients, Cosine Similarity and Dynamic Time Warping, which given the processing complexity was only used with the data from the visual cortex channels.

5.1.3.1 C-VEP Benchmark Dataset

Table 5.9 shows the results obtained for subject identification approach, using the modulated m-sequences for the targets in the framework from [77]. In contrast, table 5.10 presents the improved results with the data differentiation before the application of the feature extraction method. The first table shows that the best result was obtained with the subset of channels of the visual cortex, using the TRCA with the average data of the ten repetitions normalized with the DC Offset Removal (91.52%). The best result obtained with the application of the derivative was obtained in the same test, improving the previous result to 94.02%.

The values presented in both tables show that the application of the derivative form allowed to improve all the results, except with the Cosine Similarity method using all EEG channels and with the subset that uses the channels corresponding to the location in Unicorn.

In both tables, is possible to verify that the application of the normalization method in the [-1; 1] interval, in comparison with the DC Offset Removal, allowed to maintain or improve the results with the different feature extraction methods, except in the TRCA method that worsened the results.

The results obtained with the application of the different combinations to the average of the 10 repetitions, comparing with the concatenated data, improved in all tests except with the use of the ITCCA method, allowing to verify what already had the analysis carried out for the target identification. One of the possibilities is the ITCCA method to create a separability in the correct identification. The results with the DTW are low when considering only the eight channels of the visual cortex, which does not happen with the other methods.

The tables A.8 and A.9 show the best results, detailed for each m-sequence of the dataset, for the subject identification approach. Through these values, it is possible to verify which sequences are more efficient in discriminating subjects. The m-sequences that get the best results for all methods were T7, T12, T15, T21, T22 and T28.

The values presented in table 5.11 confirm what is shown in the processing times of the implemented methods of table 5.5 for the target identification. The processing time for the Cosine Similarity method is the lowest, followed by TRCA, using the subset of

eight EEG channels. The ITCCA method showed a high processing time with the results obtained when considering the classification results obtained with the other methods. The DTW method's computational demands were consistent to what is shown in the state of the art, with higher processing times even when compared to other methods processing a higher channel count.

Table 5.9: Mean accuracy classification (%) results for the C-VEP benchmark dataset to each target sequence for user identification with different methods of normalization.[a]

	Method	ITCCA	TRCA	Correlation Coefficients	Cosine Similarity	DTW
All chans	**DC Offset Removal**	57,77	86,48	50,55	50,82	-
	Range [-1 1]	57,77	84,45	52,62	50,82	-
	DC Offset Removal (Average)	15,27	81,72	74,37	72,46	-
	Range [-1 1] (Average)	15,55	76,95	81,95	73,09	-
Visual 8chans	**DC Offset Removal**	66,91	86,6	60,98	63,59	21,76
	Range [-1 1]	67,11	84,14	66,25	64,06	16,45
	DC Offset Removal (Average)	58,71	**91,52**	81,64	82,3	33,09
	Range [-1 1] (Average)	58,6	89,3	87,5	83,36	37,54
Unicorn 8chans	**DC Offset Removal**	57,66	72,54	45,51	44,77	-
	Range [-1 1] (Average)	57,65	69,49	47,15	46	-
	DC Offset Removal (Average)	48,79	82,58	71,29	67,15	-
	Range [-1 1] (Average)	49,11	79,26	77,77	68	-

[a] The term 'All chans' is the label for tests performed using the 31 channels of the dataset. The term 'Visual 8chans' is the label for the use of the 8 channels of the visual cortex used in the dataset (Oz, O1, O2, POz, PO3, PO4, PO7, PO8). The term 'Unicorn 8chans' is the label for the use of the 8 channels of the dataset that correspond to the channels existing in the Unicorn Hybrid Black headset (Fz, C1, Cz, C2, Pz, PO7, PO8 and Oz).

Table 5.10: Mean accuracy classification (%) results for the C-VEP benchmark dataset to each target sequence for user identification with different methods of normalization, using the first derivative of the EEG data. [a]

	Method	D-ITCCA	D-TRCA	D-Correlation Coefficients	D-Cosine Similarity
All chans	**DC Offset Removal**	66,17	91,33	51,09	38,79
	Range [-1 1]	65,08	90,39	53,63	38,59
	DC Offset Removal (Average)	16,68	88,87	77,27	62,85
	Range [-1 1] (Average)	16,02	86,41	84,69	68,98
Visual 8chans	**DC Offset Removal**	70,78	89,69	60,70	63,98
	Range [-1 1]	71,29	85,00	66,09	65,00
	DC Offset Removal (Average)	65,66	**94,02**	82,34	85,31
	Range [-1 1] (Average)	65,74	92,30	88,91	86,00
Unicorn 8chans	**DC Offset Removal**	62,54	73,36	47,15	38,79
	Range [-1 1]	63,09	71,13	49,77	38,59
	DC Offset Removal (Average)	55,39	83,91	76,17	62,85
	Range [-1 1] (Average)	55,94	83,48	81,21	63,13

[a] The term 'All chans' is the label for tests performed using the 31 channels of the dataset. The term 'Visual 8chans' is the label for the use of the 8 channels of the visual cortex used in the dataset (Oz, O1, O2, POz, PO3, PO4, PO7, PO8). The term 'Unicorn 8chans' is the label for the use of the 8 channels of the dataset that correspond to the channels existing in the Unicorn Hybrid Black headset (Fz, C1, Cz, C2, Pz, PO7, PO8 and Oz).

Table 5.11: Processing time in Matlab, in seconds, for the methods implemented in the C-VEP benchmark dataset for user identification.

	All channels	Visual 8 channels	Unicorn 8 channels
ITCCA	0,584	0,106	0,085
TRCA	0,043	0,020	0,022
Correlation Coefficients	0,095	0,053	0,038
Cosine Similarity	0,067	0,020	**0,019**
DTW	-	1,462	-

Figure 5.1 presents a plot of the EEG signals, the first derivative and the second derivative of the signals of the Oz channel of the subjects S14 and S17 of the C-VEP Benchmark Dataset, that evidences the differences between the signals for the same target (T7).

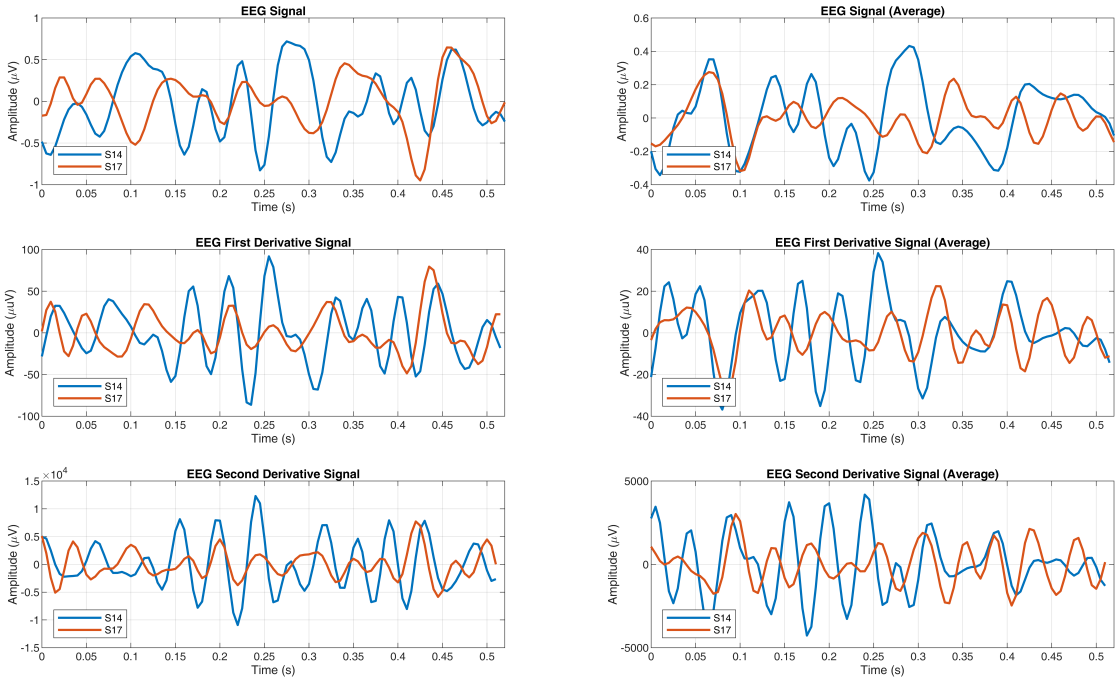

Figure 5.1: Plot of the EEG signal, the first and second derivative of channel Oz with target 7 for the subjects S14 and S17 of the dataset [77]. The graphics on the left use the full EEG signal, while the pictures on the right use the average of the repetitions of the EEG signal.

5.1.3.2 C-VEP-ISR Dataset

Table 5.13 shows the results obtained for the stimulation modulated with the sequences proposed in [3] to the user identification approach.

The best result achieved was with the use of EEG data from a subset consisting of 8 channels, standardized with DC Offset Removal and applied to the TRCA method (91.67%). Although the average of the highest accuracy values was 91.67%, it was possible to achieve 96.67% with the T3 sequence, using a subset of eight channels of the acquisition system, as it is possible to verify in table A.10. The application of the derivative with the same combination allows reaching the best result with a value of 89.17%. The application of the derivative to the ITCCA and TRCA methods decreases the accuracy results, while the methods based on correlation or distance between time-series increase. Meanwhile, the T2 and T3 sequences achieved 93.33% accuracy with the TRCA method.

The application of normalization [-1; 1] interval allowed to improve the accuracy values with all methods except TRCA.

Table 5.12 shows the results obtained for the stimulation modulated with the sequences proposed by us to the user identification approach. The best method achieved an accuracy of 93% for the TRCA using a subset of eight channels of the EEG. In contrast, the application of the derivative form only reached 86% in subject identification accuracy, with the same combination. The application of the derivative form of the EEG to Correlation Coefficients and Cosine Similarity methods increases the results.

The detailed results presented in tables A.12 and A.13 show that it was possible to achieve 96% results with the T2 sequence for a subset with 4 and 8 g.USBamp channels and an accuracy of 90% applying the derivative form and using all channels and a subset of 8 channels.

Table 5.12: Mean accuracy classification (%) results for the C-VEP-ISR dataset to each target sequence for user identification with different methods of normalization, for the sequence in [3].

	Method	ITCCA	TRCA	Correlation Coefficients	Cosine Similarity	D-ITCCA	D-TRCA	D-Correlation Coefficients	D-Cosine Similarity
All chans	**DC Offset Removal**	78,75	90,00	33,75	37,08	74,17	87,92	39,17	40,42
	Range [-1 1]	79,58	87,50	37,92	38,75	71,67	82,92	37,50	37,50
8 chans	**DC Offset Removal**	85,42	**91,67**	36,25	36,25	76,25	**89,17**	42,50	42,92
	Range [-1 1]	85,83	89,17	39,17	37,75	75,00	82,08	42,50	40,83
4 chans	**DC Offset Removal**	82,92	86,67	43,33	42,50	73,33	79,58	42,50	43,75
	Range [-1 1]	82,50	84,58	47,08	44,17	75,83	81,67	43,33	42,92
Unicorn 8chans	**DC Offset Removal**	76,67	86,25	35,83	37,08	70,42	81,25	40,00	40,42
	Range [-1 1]	79,17	84,17	39,17	38,33	69,17	77,50	39,17	38,75

Table 5.13: Mean accuracy classification (%) results for the C-VEP-ISR dataset to each target sequence for user identification with different methods of normalization, for our proposed m-sequence.

	Method	ITCCA	TRCA	Correlation Coefficients	Cosine Similarity	D-ITCCA	D-TRCA	D-Correlation Coefficients	D-Cosine Similarity
All chans	**DC Offset Removal**	84,00	92,00	30,00	29,50	74,00	85,00	38,50	38,50
	Range [-1 1]	84,50	88,50	30,00	30,00	72,00	81,50	38,00	38,50
8 chans	**DC Offset Removal**	88,00	**93,00**	35,50	35,50	72,50	**86,00**	38,50	38,50
	Range [-1 1]	92,00	92,00	34,00	34,00	72,00	82,00	39,00	40,00
4 chans	**DC Offset Removal**	86,50	91,00	42,00	44,00	70,50	74,00	42,00	42,50
	Range [-1 1]	85,50	89,50	42,50	42,00	70,50	69,50	41,00	40,50
Unicorn 8chans	**DC Offset Removal**	82,00	89,50	30,00	30,00	70,50	76,50	38,50	41,00
	Range [-1 1]	80,50	87,50	29,50	28,00	69,50	72,00	39,50	40,50

[a] The term 'All chans' is the label for tests performed using the 12 channels chosen from the g.USBamp. The term '8chans' is the label for the use of the 8 channels of the visual cortex used in the dataset (CPz, Pz, P3, P4, POz, Po7, Oz, PO8). The term '4chans' is the label for the use of the 8 channels of the visual cortex used in the dataset (POz, Po7, Oz, PO8). The term 'Unicorn 8chans' is the label for the use of the 8 channels of the g.USBamp that correspond to the channels existing in the Unicorn Hybrid Black headset (Fz, C1, Cz, C2, Pz, PO7, PO8 and Oz).

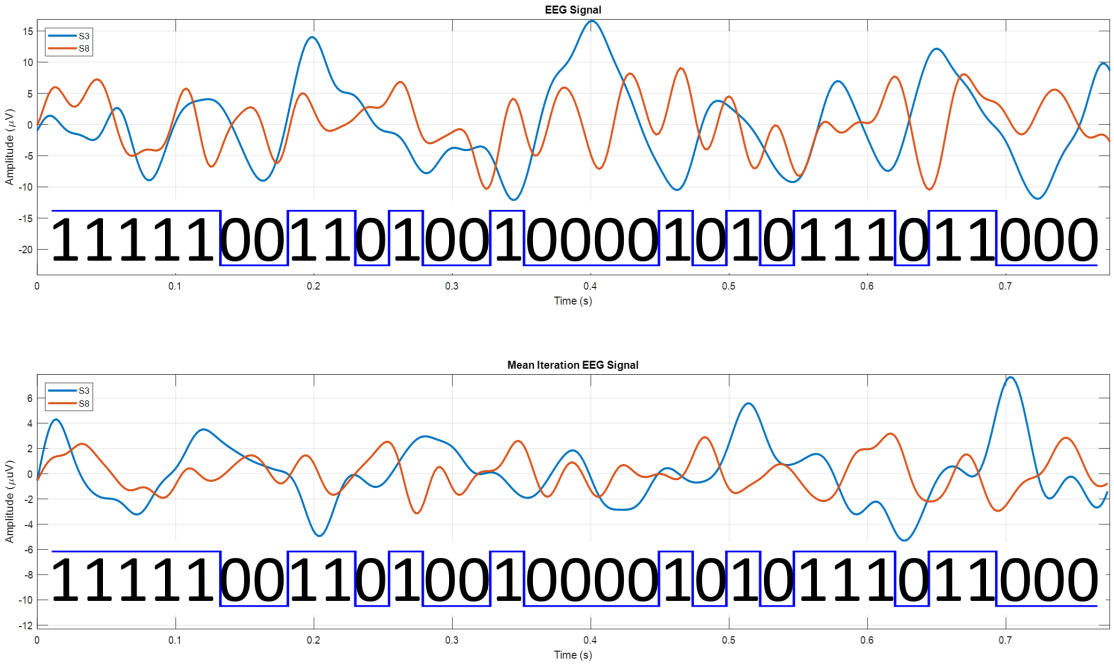

Figure 5.2: EEG signal for one stimulation repetition and for the average of the ten repetitions, acquired from two subjects of the C-VEP-ISR Dataset. The modulated sequence is presented under each plot.

Figure 5.2 shows the signals of the C-VEP responses to one repetition of stimulation and the average of the ten repetitions of stimulus modulated by the sequence shown in the figure of two subjects from the C-VEP-ISR Dataset. With these signals, it is possible to graphically check the differences between the two time series for the results in the user identification.

After all the tests and analysis of the results, it was found that:

- the best feature extraction method was TRCA;
- the application of the derivative made it possible to substantially improve the results in the C-VEP dataset with the ITCCA and TRCA methods, with no significant effect on the results obtained with the C-VEP-ISR dataset;
- the results obtained with the average of the repetitions of the EEG signals allowed to improve the results obtained with the methods except for the ITCCA;
- the normalization of the data with the [-1; 1] interval improves the results with the ITCCA and TRCA methods, not significantly altering the results with the Correlation Coefficients and Cosine Similarity methods.

Table 5.14 presents the parameters used that allowed to obtain the best results with the public dataset and the acquired dataset for the two analyzed approaches (BCI and user identification).

Table 5.14: Parameters for the best results obtained for each dataset and each identification approach.

Dataset	Identif.	M-Seq	Chans	Filters (Hz)	Normaliz.	Mean Rep	Deriv. Form	Feature Extraction Method	Acc (%
C-VEP Dataset	Target	-	Visual Cortex	Bandpass: 4 - 31	Range [-1;1]	Yes	Yes	TRCA	98,79
	Subject	-	Visual Cortex		DC Offset Removal	Yes	Yes	TRCA	94,02
C-VEP ISR Dataset	Target	Amin.	4chans	Notch: 48-52 Bandpass: 1 - 60	DC Offset	No	No	TRCA	100
		Our	8chans		Range [-1;1]	No	No	ITCCA	98
	Subject	Amin.	8chans		DC Offset	No	No	TRCA	91,67
		Our	8chans		DC Offset	No	No	TRCA	93

5.2 Sequences Analysis

In this section, the results obtained with the analysis of the various complexity methods implemented in the previous chapter are analyzed. The objective of implementing these methods was to find a direct relationship between the m-sequences that modulate the stimuli and the results of accuracy in the identification of subjects, to be able to find efficient sequences that would allow reaching values of 100% accuracy.

5.2.1 C-VEP Benchmark Dataset Sequences

Figure 5.3 shows the linear regression between the accuracy values using the ITCCA method with the normalization of the signal amplitude to the range of [-1 1] and the complexity values of the m-sequences calculated in table 5.15 with the Lempel-Ziv Primitive method. This linear regression originated a line with a slope of -0.7155.

The value of the line's slope will depend on the accuracy value obtained for each of the m-sequences. However, although the variables are not directly related, there is a small linearization that can explain the variability of the results obtained for specific sequences.

Table 5.15: Pseudorandomness results for the C-VEP benchmark dataset sequences for subject identification.

	Kolmogorov	**LZ Primitive**	**Distribution**
T1	14	40	9
T2	15	42	7
T3	14	40	8
T4	15	40	7
T5	16	41	7
T6	14	39	7
T7	14	37	7
T8	14	37	7
T9	14	39	7
T10	16	40	7
T11	16	39	7
T12	14	36	7
T13	14	33	9
T14	14	33	7
T15	13	33	5
T16	14	34	7
T17	15	36	9
T18	15	38	9
T19	14	37	9
T20	15	39	7
T21	15	38	7
T22	14	38	7
T23	14	38	7
T24	13	35	9
T25	14	36	7
T26	15	37	7
T27	13	36	7
T28	14	38	7
T29	14	39	7
T30	15	43	8
T31	14	41	8
T32	15	41	8

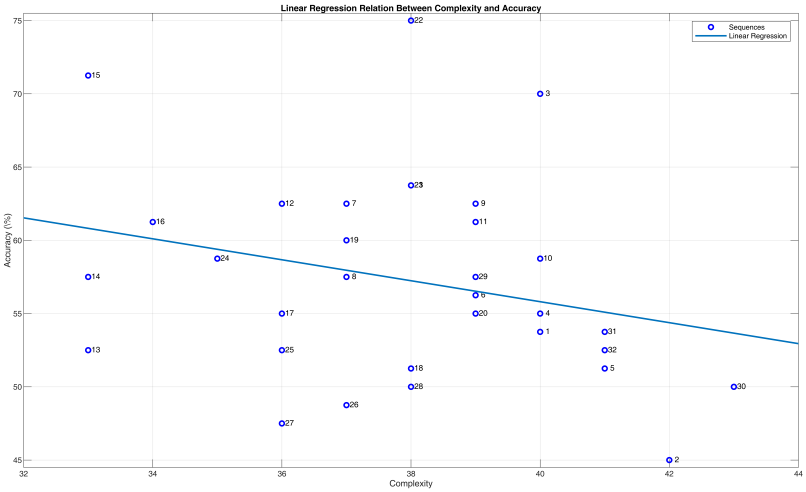

Figure 5.3: Linear regression between the accuracy and the complexity of the sequences used in [77].

Table 5.16: Complexity results for the C-VEP sequences for subject identification in [3].

	Kolmogorov	LZ Primitive	Distribution
S1	10	17	5
S2	8	18	4
S3	9	16	5
S4	9	18	6

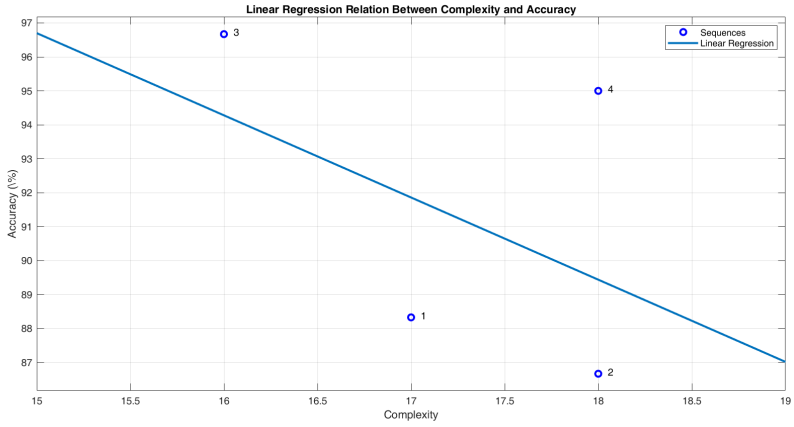

Figure 5.4: Linear regression between the accuracy and the complexity of the sequences used in [3].

5.2.2 C-VEP-ISR Dataset Sequences

Figure 5.4 shows the linear regression between the complexity calculated in table 5.16 and the results obtained from the identification of subjects with the TRCA method. The slope of the linear regression line was -2.42.

The m-sequences have an autocorrelation function approximate to the unit impulse function, and are approximately orthogonal to its time lag sequences, allowing their use in C-VEP BCI systems. Figure 5.5a) shows the autocorrelation of the proposed m-sequence, while fig. 5.5b) shows the autocorrelation of the EEG signals in response to targets modulated with the proposed m-sequence. This result proves the property of the orthogonality, which is established in the response evoked by the m-sequences. The linear regression in Fig. 5.6, between the results of complexity and the accuracy values obtained from the tests performed, shows a slope with a value of -2.

Table 5.17: Complexity results for the C-VEP proposed sequence.

	Kolmogorov	LZ Primitive	Distribution
P1	9	17	5
P2	10	18	5
P3	9	17	5
P4	9	17	4

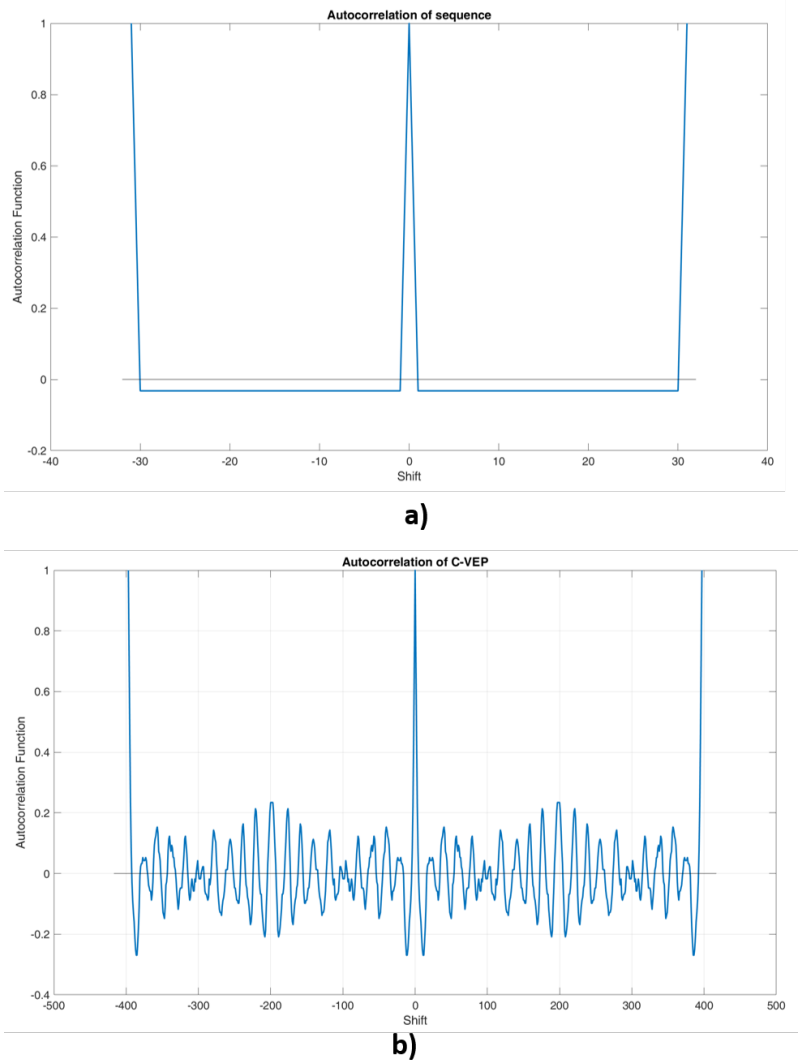

Figure 5.5: a) Autocorrelation of the proposed m-sequence; b) Autocorrelation of the EEG signals acquired for C-VEP-ISR Dataset.

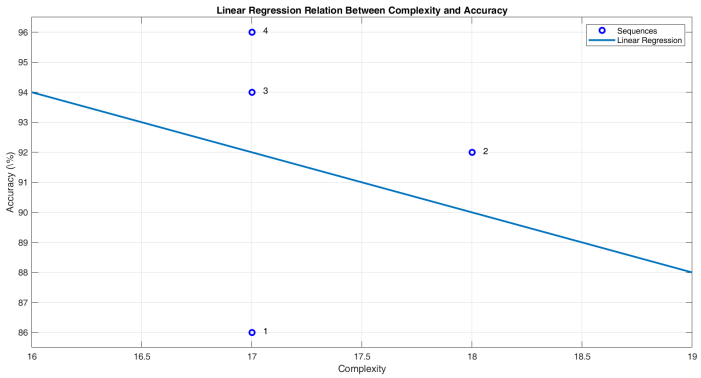

Figure 5.6: Linear regression between the accuracy and the complexity of the propose sequence.

5.2.3 Different Sequences

The average results of accuracy obtained in the identification of subjects in [83] with the ITCCA method were M1: 94.52%, M2: 93.92%, M3: 93.94 M4: 94.96%, M5: 95.48%, M6: 92.76%.

Table 5.18 presents the results of the complexity methods tested for the sequences used in [83], where it is possible to verify that the M3 sequence has the highest Lempel-Ziv complexity value.

Figure 5.7 shows the linear regression between the accuracy values and the complexity values used with the Lempel-Ziv method. The slope of the linear regression function has a value of -0.1771. The obtained results show that there is no statistically significant correlation between the two variables.

Table 5.18: Complexity results for the C-VEP sequences for subject identification in [83].

	Kolmogorov	**LZ Primitive**	**Distribution**
M1	15	37	7
M2	13	40	10
M3	15	43	8
M4	15	41	7
M5	16	37	9
M6	14	40	6

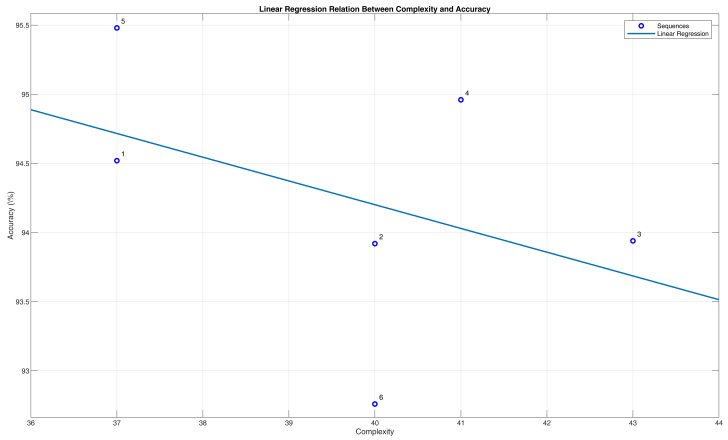

Figure 5.7: Linear regression between the accuracy and the complexity of the sequences used in [83].

6

Conclusions and Future Work

The goal of this dissertation was to develop a stimulation and EEG acquisition framework to implement C-VEP in two different approaches: C-VEP BCI and C-VEP identification. To achieve this objective, several feature extraction methods were applied combined with different data normalizations. First, we applied the algorithms to the C-VEP Benchmark dataset, and then the same methods on our own datasets collected from a group of participants who underwent C-VEP experiments with our laboratory acquisition and framework setup.

Using the results obtained in this experiment, it was possible to conclude that the method that provides the best results was TRCA, achieving a maximum of 100% accuracy in the two application contexts. In addition to that, it was also possible to ascertain that the methods which utilize the spatial correlation of EEG data (TRCA and ITCCA) had a better performance by using the DC Offset Removal normalization. On the other hand, the methods that utilize the correlation or distance between time-series achieved better results using the normalization in the [-1, 1] interval. For some extraction methods, the results were significantly improved with the implementation of the first derivative to the EEG signals, showing that the differentiation of data and the dynamics of C-VEP allows to obtain more discriminative features for the identification of users (C-VEP identification) and targets (C-VEP BCI).

The understanding of the generation of a PBRS and its analysis of complexity allowed us to propose a new sequence for data acquisition. Although the linear regressions estimated between the accuracy values and the sequence complexity values indicate a correlation, the estimates did not prove to be statistically relevant.

Considering the work developed and the results obtained, there are several possibilities for continuing the project to improve the current work, such as:

- Implementation of other types of pseudorandom sequences for stimulation such as gold-code and Barker-code, which enable better ITR results in target identification, because of the smaller number of bits in the sequence compared to the m-sequences;
- Implementation of trinary (base 3) m-sequences where the three digits correspond

to different colours (for example, blue, green and yellow);

- Implementation of an authenticator that uses a different sequence for each subject, allowing to improve the performance in identifying subjects (used only in a user recognition system and not in a user identification approach);
- Use of a larger group of participants to validate the implemented approaches over several sessions;
- Implementation of security layers in the biometric authenticator with the use of encryption cyphers (Vernam Cipher, e.g.) of the binary sequences.

Bibliography

[1] Sarah N Abdulkader, Ayman Atia, and Mostafa Sami M Mostafa. Brain computer interfacing: Applications and challenges. *Egyptian Informatics Journal*, 16(2):213–230, 2015.

[2] Lady Ada. Adafruit Feather HUZZAH ESP8266, 2020.

[3] Daiki Aminaka, Shoji Makino, and Tomasz M Rutkowski. Chromatic and High – frequency cVEP – based BCI Paradigm. *Annual International Conference of the IEEE Engineering in Medicine and Biology Society (EMBC)*, pages 1906–1909, 2015.

[4] Daiki Aminaka, Shoji Makino, and Tomasz M Rutkowski. SVM classification study of code-modulated visual evoked potentials. *2015 Asia-Pacific Signal and Information Processing Association Annual Summit and Conference, APSIPA ASC 2015*, (December):1065–1070, 2016.

[5] Dimitrios Andreou and Riccardo Poli. Comparing EEG, its time-derivative and their joint use as features in a BCI for 2-D pointer control. *Proceedings of the Annual International Conference of the IEEE Engineering in Medicine and Biology Society, EMBS*, 2016-Octob:5853–5856, 2016.

[6] Divya Geethakumari Anil, Krupal Sureshbhai Mistry, Vaibhav Palande, and Kiran George. A Novel Steady-State Visually Evoked Potential (SSVEP) Based Brain Computer Interface Paradigm for Disabled Individuals. *Proceedings - 2017 IEEE International Conference on Healthcare Informatics, ICHI 2017*, pages 421–428, 2017.

[7] Sylvain Arlot and Alain Celisse. A survey of cross-validation procedures for model selection. *Statistics Surveys*, 4:40–79, 2010.

[8] A G Asuero, A Sayago, and A G González. The correlation coefficient: An overview. *Critical Reviews in Analytical Chemistry*, 36(1):41–59, 2006.

[9] Guangyu Bin, Xiaorong Gao, Yijun Wang, Bo Hong, and Shangkai Gao. VEP-based brain-computer interfaces: Time, frequency, and code modulations. *IEEE Computational Intelligence Magazine*, 4(4):22–26, 2009.

[10] Guangyu Bin, Xiaorong Gao, Yijun Wang, Yun Li, Bo Hong, and Shangkai Gao. A high-speed BCI based on code modulation VEP. *Journal of Neural Engineering*, 8(2), 2011.

[11] Guangyu Bin, Xiaorong Gao, Zheng Yan, Bo Hong, and Shangkai Gao. An online multi-channel SSVEP-based brain-computer interface using a canonical correlation analysis method. *Journal of Neural Engineering*, 6(4), 2009.

[12] P. Brunner, L. Bianchi, C. Guger, F. Cincotti, and G. Schalk. Current trends in hardware and software for brain-computer interfaces (BCIs). *Journal of Neural Engineering*, 8(2), 2011.

[13] Giedrius T. Buračas and Geoffrey M. Boynton. Efficient design of event-related fMRI experiments using m-sequences. *NeuroImage*, 16(3 I):801–813, 2002.

[14] Patrizio Campisi and Daria La Rocca. Brain waves for automatic biometric-based user recognition. *IEEE Transactions on Information Forensics and Security*, 9(5):782–800, 2014.

[15] Hui Ling Chan, Po Chih Kuo, Chia Yi Cheng, and Yong Sheng Chen. Challenges and Future Perspectives on Electroencephalogram-Based Biometrics in Person Recognition. *Frontiers in Neuroinformatics*, 12(October):1–15, 2018.

[16] Nesrine Charfi. *Biometric recognition based on hand schape and palmprint modalities.* PhD thesis, 2017.

[17] Yeou-jiunn Chen, Aaron Raymond, Ang See, and Shih-chung Chen. A review and experimental study on application of classifiers and evolutionary algorithms in EEG based brain-machine interface systems. 50(10):8–9, 2014.

[18] Koel Das, Sheng Zhang, Barry Giesbrecht, and Miguel P Eckstein. Using rapid visually evoked EEG activity for person identification. *Proceedings of the 31st Annual International Conference of the IEEE Engineering in Medicine and Biology Society: Engineering the Future of Biomedicine, EMBC 2009*, pages 2490–2493, 2009.

[19] Rig Das, Emanuele Maiorana, and Patrizio Campisi. Visually evoked potential for EEG biometrics using convolutional neural network. *25th European Signal Processing Conference, EUSIPCO 2017*, 2017-Janua:951–955, 2017.

[20] Rig Das, Emanuele Maiorana, and Patrizio Campisi. Motor Imagery for EEG Biometrics Using Convolutional Neural Network. *ICASSP, IEEE International Conference on Acoustics, Speech and Signal Processing - Proceedings*, 2018-April:2062–2066, 2018.

[21] Rig Das, Emanuele Maiorana, Daria La Rocca, and Patrizio Campisi. EEG biometrics for user recognition using visually evoked potentials. *Lecture Notes in Informatics (LNI), Proceedings - Series of the Gesellschaft fur Informatik (GI)*, P-245, 2015.

[22] Rig Das, Emanuela Piciucco, Emanuele Maiorana, and Patrizio Campisi. Visually evoked potentials for EEG biometrie recognition. *2016 1st International Workshop on Sensing, Processing and Learning for Intelligent Machines, SPLINE 2016 - Proceedings*, 2016.

[23] Touradj Ebrahimi, Ulrich Hoffmann, and Jean-marc Vesin. Recent advances in brain-computer interfaces. *2007 IEEE 9Th International Workshop on Multimedia Signal Processing, MMSP 2007 - Proceedings*, (May 2014):17, 2007.

[24] L. A. Farwell and E. Donchin. Talking off the top of your head: toward a mental prosthesis utilizing event-related brain potentials. *Electroencephalography and Clinical Neurophysiology*, 70(6):510–523, 1988.

[25] Felix Gembler, Mihaly Benda, Abdul Saboor, and Ivan Volosyak. A multi-target c-VEP-based BCI speller utilizing n -gram word prediction and filter bank classification. *IEEE International Conference on Systems, Man and Cybernetics (SMC)*, 66:2705–2710, 2019.

[26] Felix Gembler, Piotr Stawicki, Aya Rezeika, Abdul Saboor, and Mihaly Benda. *Symbiotic Interaction*, volume 10727. Springer International Publishing, 2018.

[27] Felix Gembler, Piotr Stawicki, Abdul Saboor, and Ivan Volosyak. Dynamic time window mechanism for time synchronous VEP-based BCIs-Performance evaluation with a dictionary-supported BCI speller employing SSVEP and c-VEP. *PLoS ONE*, 14(6):1–18, 2019.

[28] Felix W Gembler, Aya Rezeika, Mihaly Benda, and Ivan Volosyak. Five Shades of Grey: Exploring Quintary m -Sequences for More User-Friendly c-VEP-Based BCIs. *Computational Intelligence and Neuroscience*, 2020, 2020.

[29] Solomon W Golomb. Shift register sequences - A retrospective account. *Lecture Notes in Computer Science (including subseries Lecture Notes in Artificial Intelligence and Lecture Notes in Bioinformatics)*, 4086 LNCS:1–4, 2006.

[30] G.tec. Unicorn Hybrid Black | The Brain Interface.

[31] G.tec. Brain-Computer Interface. Technical report, 2018.

[32] Christoph Guger, Christoph Kapeller, Hiroshi Ogawa, and Kyousuke Kamada. An electrocorticographic BCI using code-based VEP for control in video applications : a single-subject study. *Frontiers in Systems Neuroscience*, 8(August):1–8, 2014.

[33] F Kaspar and H G Schuster. Easily calculable measure for the complexity of spatiotemporal patterns. *Physical Review A*, 36(2):842–848, 1987.

[34] Ibrahim Kaya. A BCI Gaze Sensing Method Using Low Jitter Code Modulated VEP. 2019.

[35] A. N. Kolmogorov. On tables of random numbers. *Theoretical Computer Science*, 25(4):369–376, 1963.

[36] H. Lasota and R. Mazurek. Application of maximum-length sequences to impulse response measurement of hydroacoustic communications systems. *Hydroacoustics*, 10(June):123–130, 2007.

[37] Abraham Lempel and Jacob Ziv. On the complexity of finite sequences over a finite set. *IEEE Transactions on Information Theory*, 22(1), 1976.

[38] Zhonglin Lin, Changshui Zhang, Wei Wu, and Xiaorong Gao. Frequency recognition based on canonical correlation analysis for SSVEP-Based BCIs. *IEEE Transactions on Biomedical Engineering*, 54(6):1172–1176, 2007.

[39] Yonghui Liu, Qingguo Wei, and Zongwu Lu. A multi-target brain-computer interface based on code modulated visual evoked potentials. *PLoS ONE*, 13(8):1–17, 2018.

[40] D J McFarland and J R Wolpaw. EEG-based brain–computer interfaces. *Current Opinion in Biomedical Engineering*, 4:194–200, 2017.

[41] Dennis J McFarland and Jonathan R Wolpaw. Brain-computer interfaces for communication and control. *Communications of the ACM*, 54(5):60–66, 2011.

[42] Dragutin T. Mihailović, Miloud Bessafi, Sara Marković, Ilija Arsenić, Slavica Malinović-Milićević, Patrick Jeanty, Mathieu Delsaut, Jean Pierre Chabriat, Nusret Drešković, and Anja Mihailović. Analysis of solar irradiation time series complexity and predictability by combining Kolmogorov measures and Hamming distance for La Reunion (France). *Entropy*, 20(8), 2018.

[43] Surej Mouli and Ramaswamy Palaniappan. Eliciting higher SSVEP response from LED visual stimulus with varying luminosity levels. *2016 International Conference for Students on Applied Engineering, ICSAE 2016*, pages 201–206, 2017.

[44] Surej Mouli, Ramaswamy Palaniappan, and Ian P.Sillitoe. Arduino based configurable LED stimulus design for multi-frequency SSVEP-BCI. *Proceedings of the IEEE EMBS UKRI Postgraduate Conference on Biomedical Engineering*, 2014.

[45] Surej Mouli, Ramaswamy Palaniappan, Ian P Sillitoe, and John Q Gan. Performance analysis of multi-frequency SSVEP-BCI using clear and frosted colour LED stimuli. *13th IEEE International Conference on BioInformatics and BioEngineering, IEEE BIBE 2013*, (August 2015), 2013.

[46] Sebastian Nagel, Werner Dreher, Wolfgang Rosenstiel, and Martin Spüler. The effect of monitor raster latency on VEPs, ERPs and Brain–Computer Interface performance. *Journal of Neuroscience Methods*, 295:45–50, 2018.

[47] Masaki; Nakanishi and Yasue Mitsukura. PERIODICITY DETECTION FOR BCI BASED ON PERIODIC CODE MODULATION VISUAL EVOKED POTENTIALS

Masaki Nakanishi , Yasue Mitsukura Keio University Graduate School of Science and Technology. *Science And Technology*, pages 665–668, 2012.

[48] Masaki Nakanishi, Yijun Wang, Xiaogang Chen, Yu Te Wang, Xiaorong Gao, and Tzyy Ping Jung. Enhancing detection of SSVEPs for a high-speed brain speller using task-related component analysis. *IEEE Transactions on Biomedical Engineering*, 65(1):104–112, 2018.

[49] Masaki Nakanishi, Yijun Wang, Yu Te Wang, and Tzyy Ping Jung. A comparison study of canonical correlation analysis based methods for detecting steady-state visual evoked potentials. *PLoS ONE*, 10(10):1–18, 2015.

[50] Hooman Nezamfar, Seyed Sadegh Mohseni Salehi, and Deniz Erdogmus. Stimuli with opponent colors and higher bit rate enable higher accuracy for C-VEP BCI. *2015 IEEE Signal Processing in Medicine and Biology Symposium - Proceedings*, 2016.

[51] Omar B Osman and M Hassan Arbab. Mitigating the effects of granular scattering using cepstrum analysis in terahertz time-domain spectral imaging. *PLoS ONE*, 14(5):1–14, 2019.

[52] R Palaniappan and K V R Ravi. A new method to identify individuals using signals from the brain. *ICICS-PCM 2003 - Proceedings of the 2003 Joint Conference of the 4th International Conference on Information, Communications and Signal Processing and 4th Pacific-Rim Conference on Multimedia*, 3:1442–1445, 2003.

[53] K K Paliwal, Anant Agarwal, and Sarvajit S Sinha. A modification over Sakoe and Chiba's dynamic time warping algorithm for isolated word recognition. *Signal Processing*, 4(4):329–333, 1982.

[54] Jie Pan, Xiaorong Gao, Fang Duan, Zheng Yan, and Shangkai Gao. Enhancing the classification accuracy of steady-state visual evoked potential-based brain-computer interfaces using phase constrained canonical correlation analysis. *Journal of Neural Engineering*, 8(3), 2011.

[55] R B Paranjape, J Mahovsky, L Benedicenti, and Z Koles. The electroencephalogram as a biometric. *Canadian Conference on Electrical and Computer Engineering*, 2:1363–1366, 2001.

[56] U. Parlitz and S. Ergezinger. Robust communication based on chaotic spreading sequences. *Physics Letters A*, 188(2):146–150, 1994.

[57] Montri Phothisonothai. An investigation of using SSVEP for EEG-based user authentication system. *2015 Asia-Pacific Signal and Information Processing Association Annual Summit and Conference, APSIPA ASC 2015*, (December):923–926, 2016.

[58] Emanuela Piciucco, Emanuele Maiorana, Owen Falzon, Kenneth P Camilleri, and Patrizio Campisi. Steady-State Visual Evoked Potentials for EEG-Based Biomet-

ric Identification. *Lecture Notes in Informatics (LNI), Proceedings - Series of the Gesellschaft fur Informatik (GI)*, 2017.

[59] Pawel Poryzala and Andrzej Materka. Cluster analysis of CCA coefficients for robust detection of the asynchronous SSVEPs in brain–computer interfaces. *Biomedical Signal Processing and Control*, 10:201–208, 2014.

[60] Bruno Quintela and Silva Cunha. Biometric authentication using electroencephalograms: a practical study using visual evoked potentials. *Electrónica e Telecomunicações*, 5(2):185–194, 2010.

[61] Faisal Rahutomo, Teruaki Kitasuka, and Masayoshi Aritsugi. Semantic Cosine Similarity. *Semantic Scholar*, 2(4):4–5, 2012.

[62] Hannes Riechmann, Andrea Finke, and Helge Ritter. Using a cVEP-Based Brain-Computer Interface to Control a Virtual Agent. *IEEE Transactions on Neural Systems and Rehabilitation Engineering*, 24(6):692–699, 2016.

[63] J. Sachs, R. Herrmann, M. Kmec, M. Helbig, and K. Schilling. Recent advances and applications of m-sequence based ultra-wideband sensors. *2007 IEEE International Conference on Ultra-Wideband, ICUWB*, (October):50–55, 2007.

[64] András Sárközy. On pseudorandomness of families of binary sequences. *Discrete Applied Mathematics*, 216:670–676, 2017.

[65] Jun Ichi Sato and Yoshikazu Washizawa. Neural decoding of code modulated visual evoked potentials by spatio-temporal inverse filtering for brain computer interfaces. *Proceedings of the Annual International Conference of the IEEE Engineering in Medicine and Biology Society, EMBS*, 2016-Octob(1):1484–1487, 2016.

[66] Zahra Shirzhiyan, Ahmadreza Keihani, Morteza Farahi, Elham Shamsi, Mina Gol-Mohammadi, Amin Mahnam, Mohsen Reza Haidari, and Amir Homayoun Jafari. Introducing chaotic codes for the modulation of code modulated visual evoked potentials (c-VEP) in normal adults for visual fatigue reduction. *PLoS ONE*, 14(3):1–29, 2019.

[67] Martin Spüler, Wolfgang Rosenstiel, and Martin Bogdan. Online Adaptation of a c-VEP Brain-Computer Interface(BCI) Based on Error-Related Potentials and Unsupervised Learning. *PLoS ONE*, 7(12), 2012.

[68] H H Stassen. Computerized recognition of persons by EEG spectral patterns. *Electroencephalography and Clinical Neurophysiology*, 49(1-2):190–194, 1980.

[69] Erich E. Sutter. The visual evoked response as a communication channel. *In: Proc. of IEEE Symposium on Biosensors*, pages 95–100, 1984.

[70] Erich E Sutter. The brain response interface: communication through visually-induced electrical brain responses. *Journal of Microcomputer Applications*, 15(1):31–45, 1992.

[71] Hirokazu Tanaka, Takusige Katura, and Hiroki Sato. Task-related component analysis for functional neuroimaging and application to near-infrared spectroscopy data. *NeuroImage*, 64(1):308–327, 2013.

[72] Quang Thai. calc_lz_complexity, 2020.

[73] Mathuranathan Viswanathan. *Wireless Communication Systems in Matlab: Second Edition*. Independently, 2020.

[74] Yijun Wang, Xiaogang Chen, Xiaorong Gao, and Shangkai Gao. A Benchmark Dataset for SSVEP-Based Brain-Computer Interfaces. *IEEE Transactions on Neural Systems and Rehabilitation Engineering*, 25(10):1746–1752, 2017.

[75] Qingguo Wei, Siwei Feng, and Zongwu Lu. Stimulus Specificity of Brain-Computer Interfaces Based on Code Modulation Visual Evoked Potentials. *PLoS ONE*, pages 1–17, 2016.

[76] Peter D Welch. The Use of Fast Fourier Transform for the Estimation of Power Spectra. *Digital Signal Processing*, (2):532–574, 1975.

[77] Benjamin Wittevrongel, Elia Van Wolputte, and Marc M Van Hulle. Code-modulated visual evoked potentials using fast stimulus presentation and spatiotemporal beamformer decoding. *Scientific Reports*, 7(1):1–10, 2017.

[78] J R Wolpaw, H Ramoser, D J McFarland, and G Pfurtscheller. EEG-based communication: Improved accuracy by response verification. *IEEE Transactions on Rehabilitation Engineering*, 6(3):326–333, 1998.

[79] Erdem Yavuz and Can Eyupoglu. A cepstrum analysis-based classification method for hand movement surface EMG signals. *Medical and Biological Engineering and Computing*, 57(10):2179–2201, 2019.

[80] Ting Yu, Chun Shu Wei, Kuan Jung Chiang, Masaki Nakanishi, and Tzyy Ping Jung. EEG-Based User Authentication Using a Convolutional Neural Network. *International IEEE/EMBS Conference on Neural Engineering, NER*, 2019-March:1011–1014, 2019.

[81] Yu Zhang, Guoxu Zhou, Qibin Zhao, Akinari Onishi, Jing Jin, Xingyu Wang, and Andrzej Cichocki. Multiway Canonical Correlation Analysis for Frequency Components Recognition in SSVEP-Based BCIs. *Neural Information Processing. ICONIP 2011. Lecture Notes in Computer Science*, 7062, 2011.

[82] Zhuo Zhang, Chuanchu Wang, Kai Keng Ang, Aung Aung Phyo Wai, and Cuntai Guan Nanyang. Spectrum and Phase Adaptive CCA for SSVEP-based Brain

Computer Interface. *Proceedings of the Annual International Conference of the IEEE Engineering in Medicine and Biology Society, EMBS*, 2018-July(July):311–314, 2018.

[83] Hongze Zhao, Yijun Wang, Zhiduo Liu, Weihua Pei, and Hongda Chen. Individual identification based on code-modulated visual-evoked potentials. *IEEE Transactions on Information Forensics and Security*, 14(12):3206–3216, 2019.

[84] E Nikolić Đorić, D T Mihailović, N Drešković, and G Mimić. Complexity analysis of the turbulent environmental fluid flow time series. 3(1):1–13, 2013.

A

Detailed Results

The tables presented in this annex refer to the tests performed, showing more detailed results for each subject (BCI) and each target (Subject identification).

1. SSVEP - Target Identification - SSVEP Dataset - Table A.1;
2. C-VEP
   (a) Target Identification
      i. C-VEP Dataset - Tables A.2 and A.3
      ii. C-VEP-ISR Dataset
         A. Aminaka Sequences - Tables A.4 and A.5
         B. Own Sequences - Tables A.6 and A.7
   (b) Subject Identification
      i. C-VEP Dataset - Tables A.8 and A.9
      ii. C-VEP-ISR Dataset
         A. Aminaka Sequences - Tables A.10 and A.11
         B. Own Sequences - Tables A.12 and A.13

Table A.1: Classification accuracy (%) results in the SSVEP benchmark dataset (based on 5 seconds stimulation) for each subject. [a]

Method	Welch			CEPSTRUM			CCA			ITCCA			TRCA		
Subject	All chans	Visual 8chans	Unicorn 8chans	All chans	Visual 8chans	Unicorn 8chans	All chans	Visual 8chans	Unicorn 8chans	All chans	Visual 8chans	Unicorn 8chans	All chans	Visual 8chans	Unicorn 8chans
S1	10,00	25,00	15,42	55,83	27,50	33,33	89,58	92,08	89,58	85,42	93,75	87,92	99,58	99,58	99,58
S2	2,50	34,17	5,83	56,25	43,33	27,08	87,92	94,58	84,17	35,00	93,33	87,50	83,75	98,75	99,17
S3	33,33	75,00	73,33	57,92	30,42	42,08	99,17	**100,00**	**100,00**	96,97	98,33	97,92	99,58	99,58	**100,00**
S4	51,25	41,67	67,50	55,42	41,67	36,25	97,08	97,50	90,83	96,67	97,50	95,42	99,17	95,83	97,50
S5	26,67	71,67	53,33	57,50	28,75	33,75	**100,00**	**100,00**	99,58	**100,00**	**100,00**	99,58	**100,00**	**100,00**	**100,00**
S6	65,83	85,00	83,33	55,83	22,08	33,75	**100,00**	**100,00**	99,58	99,17	99,58	98,75	99,58	99,58	99,58
S7	5,00	14,17	18,33	50,42	26,67	26,67	85,42	98,75	90,83	94,17	99,58	99,17	99,58	99,58	**100,00**
S8	43,75	64,17	63,75	57,50	30,42	31,25	97,92	99,58	86,25	98,33	98,75	89,58	99,17	99,17	99,17
S9	13,75	33,75	23,75	50,83	29,58	27,08	76,25	89,17	60,00	50,00	87,50	56,67	97,92	97,50	92,08
S10	41,25	70,00	66,25	55,83	24,17	33,33	99,17	99,17	99,58	93,33	98,75	98,33	99,17	99,17	98,75
S11	1,67	31,25	30,00	49,58	22,92	26,67	90,42	95,00	38,33	94,17	83,75	58,33	99,17	93,75	78,75
S12	60,42	64,17	64,58	54,17	27,08	30,42	**100,00**	99,58	92,08	97,50	98,75	90,00	98,75	92,08	95,83
S13	11,25	7,92	15,00	53,75	39,58	33,75	94,17	94,17	50,83	98,33	89,58	88,75	97,08	95,00	96,67
S14	43,33	84,58	37,92	58,33	32,08	58,33	96,67	**100,00**	41,25	77,50	97,92	37,08	99,58	99,58	80,83
S15	83,75	92,50	90,83	55,42	27,50	31,67	**100,00**	**100,00**	98,33	95,83	99,58	99,17	**100,00**	**100,00**	**100,00**
S16	3,75	7,50	4,17	46,25	25,83	26,67	37,50	92,08	33,75	48,33	97,92	40,00	**100,00**	**100,00**	97,08
S17	8,75	42,92	26,67	52,08	33,75	28,33	96,25	99,58	85,83	98,33	99,58	94,58	99,58	99,58	99,58
S18	15,00	50,00	27,08	57,92	30,83	35,42	62,08	92,92	67,50	79,58	96,67	80,83	96,67	96,67	96,67
S19	6,25	27,50	35,00	55,42	31,25	30,00	79,58	90,42	82,08	22,50	93,75	73,75	92,92	99,17	90,42
S20	22,08	43,33	43,33	56,25	29,17	31,67	97,08	99,58	97,50	97,92	99,58	99,58	**100,00**	**100,00**	**100,00**
S21	4,58	9,58	5,42	48,75	30,83	28,75	55,42	62,08	41,25	51,67	75,00	56,25	99,17	97,08	99,58
S22	40,00	67,50	59,58	57,92	29,17	35,42	88,75	98,33	60,42	92,08	96,67	61,67	99,58	99,58	97,92
S23	13,75	32,08	24,58	57,92	38,75	33,33	92,08	95,00	84,58	62,92	76,25	67,92	95,00	93,75	92,50
S24	8,75	45,83	15,83	52,08	37,92	33,33	67,08	96,67	35,42	66,67	97,50	26,25	99,17	98,75	99,17
S25	90,42	90,00	93,75	**62,50**	29,17	40,83	99,58	99,58	97,08	98,75	98,33	96,67	98,75	99,58	98,75
S26	93,33	92,08	93,75	60,42	30,00	34,58	99,58	95,83	98,33	99,17	96,25	98,33	99,17	98,75	98,75
S27	5,83	30,83	15,42	51,25	30,00	33,75	90,00	98,75	90,00	87,08	99,58	96,67	99,58	99,58	99,58
S28	12,92	27,50	23,33	57,08	21,25	38,33	79,17	94,58	86,67	80,42	96,25	89,17	99,58	99,17	99,58
S29	5,83	18,75	7,92	53,75	29,17	27,50	46,25	70,83	13,75	62,50	74,58	22,92	98,33	91,25	79,58
S30	50,42	71,25	65,83	50,42	28,75	30,83	98,33	98,75	98,33	94,58	97,92	98,75	99,17	99,17	99,17
S31	82,08	**98,75**	92,50	56,67	34,17	34,17	**100,00**	**100,00**	97,50	99,17	**100,00**	99,58	**100,00**	**100,00**	99,58
S32	61,25	82,92	79,58	50,83	24,58	33,33	97,92	**100,00**	96,67	98,75	**100,00**	98,75	**100,00**	**100,00**	**100,00**
S33	11,67	13,75	13,33	53,75	26,67	30,00	25,42	44,58	17,08	3,75	50,42	27,08	31,25	67,92	63,75
S34	66,25	63,75	78,33	56,25	27,50	32,08	**100,00**	99,17	98,33	97,92	98,33	97,92	99,58	98,75	99,58
S35	95,00	96,25	96,25	54,17	54,17	32,92	**100,00**	**100,00**	99,58	99,17	99,58	98,75	99,58	99,58	99,58
Mean	**34,05**	**51,63**	**46,02**	**54,75**	**30,76**	**33,05**	**86,45**	**93,95**	**77,22**	**81,53**	**93,74**	**80,27**	**96,55**	**97,36**	**95,68**
STD	29,88	28,34	30,43	3,44	6,49	5,71	19,12	11,53	26,15	24,44	10,23	24,24	11,57	5,56	7,88

[a] The term 'All chans' is the label for tests performed using the 64 channels of the dataset. The term 'Visual 8chans' is the label for the use of the 8 channels of the visual cortex used in the dataset (PO4, PO6, PO8, CB1, CB2, O1, O2 and Oz). The term 'Unicorn 8 chans' is the label for the use of the 8 channels of the dataset that correspond to the channels existing in the Unicorn Hybrid Black headset (Fz, C3, Cz, C4, Pz, PO7, PO8 and Oz).

Table A.2: Classification accuracy (%) results for the C-VEP-ISR dataset dataset for each subject to target identification with the best method of normalization. [a]

Method	ITCCA			TRCA			Correlation Coefficients			Cosine Similarity		
Subject	All chans[b]	Visual 8chans[b]	Unicorn 8chans[b]	All chans[c]	Visual 8chans[d]	Unicorn 8chans[d]	All chans[e]	Visual 8chans[e]	Unicorn 8chans[e]	All chans[e]	Visual 8chans[e]	Unicorn 8chans[e]
S1	40,63	71,25	69,38	81,88	93,75	95,63	92,50	94,38	83,13	90,00	95,00	76,25
S2	78,13	98,75	96,88	**100,00**	**100,00**	**100,00**	79,38	91,25	82,50	75,63	91,88	78,75
S3	58,75	93,75	81,25	99,38	**100,00**	99,38	97,50	99,38	96,88	98,75	99,38	97,50
S4	38,13	93,13	78,13	97,50	98,75	98,75	63,13	88,75	58,75	55,00	88,75	51,25
S5	71,88	95,00	96,25	98,75	96,25	96,88	70,00	88,75	77,50	65,63	90,63	72,50
S6	31,25	68,75	6,25	92,50	86,88	35,00	63,75	95,63	22,50	61,25	93,75	23,13
S7	9,38	30,63	5,00	55,63	91,88	33,75	39,38	53,75	32,50	36,88	55,63	34,38
S8	31,88	71,25	26,25	91,25	93,13	90,00	85,00	95,63	82,50	83,13	96,88	81,25
S9	**100,00**	**100,00**	**100,00**	**100,00**	**100,00**	**100,00**	88,13	97,50	93,75	89,38	96,25	95,00
S10	80,63	86,88	94,38	**100,00**	99,38	96,25	78,75	85,00	85,00	78,13	78,13	82,50
S12	77,50	94,38	90,00	**100,00**	**100,00**	**100,00**	87,50	98,13	84,38	83,75	97,50	75,00
S13	86,88	93,13	86,88	97,50	98,13	98,75	93,13	96,25	89,38	91,88	96,88	90,00
S14	73,75	99,38	83,13	**100,00**	**100,00**	98,13	88,13	95,63	93,13	89,38	96,88	90,63
S15	95,63	**100,00**	98,75	**100,00**	**100,00**	**100,00**	99,38	**100,00**	98,75	**100,00**	**100,00**	96,88
S16	15,63	54,38	14,38	93,13	93,75	63,13	79,38	92,50	80,63	81,25	91,25	76,88
S17	81,25	74,38	60,63	**100,00**	99,38	97,50	76,25	83,75	63,13	71,88	83,75	56,25
Mean	**60,70**	**82,81**	**67,97**	**94,22**	**96,95**	**87,70**	**80,08**	**91,02**	**76,52**	**78,24**	**90,78**	**73,63**
STD	27,87	19,07	33,64	11,06	3,83	21,95	14,87	10,71	21,31	16,35	10,67	21,22

[a] The term 'All chans' is the label for tests performed using the 31 channels of the dataset. The term 'Visual 8chans' is the label for the use of the 8 channels of the visual cortex used in the dataset (Oz, O1, O2, POz, PO3, PO4, PO7, PO8). The term 'Unicorn 8chans' is the label for the use of the 8 channels of the dataset that correspond to the channels existing in the Unicorn Hybrid Black headset (Fz, C1, Cz, C2, Pz, PO7, PO8 and Oz).
[b] Normalization using DC Offset Removal (EEG signal with 10 stimulation iterations); [c] Normalization using amplitude signal in the range [-1 1] (EEG signal with 10 stimulation iterations); [d] Normalization using DC Offset Removal (EEG signal with an average of 10 stimulation iterations); [e] Normalization using amplitude signal in the range [-1 1] (EEG signal with an average of 10 stimulation iterations).

Table A.3: Classification accuracy (%) results for the C-VEP benchmark dataset for each subject to target identification with the best method of normalization, using the first derivative of the EEG data. [a]

Method	D-ITCCA			D-TRCA			D-Correlation Coefficients			D-Cosine Similarity		
Subject	All chans[c]	Visual 8chans[c]	Unicorn 8chans[c]	All chans[c]	Visual 8chans[e]	Unicorn 8chans[e]	All chans[e]	Visual 8chans[e]	Unicorn 8chans[e]	All chans[e]	Visual 8chans[e]	Unicorn 8chans[e]
S1	61,25	78,75	81,88	94,38	97,50	98,13	96,88	97,50	93,13	95,00	97,50	81,88
S2	93,13	99,38	98,13	**100,00**	**100,00**	**100,00**	93,75	95,00	97,50	85,63	95,00	87,50
S3	71,25	95,63	83,75	**100,00**	**100,00**	97,50	98,75	97,50	99,38	99,38	97,50	98,75
S4	61,88	96,88	87,50	98,75	**100,00**	99,38	95,00	98,75	97,50	83,75	96,88	76,25
S5	90,00	96,25	98,13	**100,00**	**100,00**	**100,00**	88,13	95,00	93,75	66,25	86,88	74,38
S6	56,25	82,50	5,00	94,38	93,75	37,50	85,63	**100,00**	25,00	51,25	94,38	21,88
S7	18,75	48,13	8,75	84,38	95,63	65,00	38,13	55,63	39,38	33,75	52,50	35,63
S8	35,63	72,50	16,88	93,13	95,63	93,75	90,00	95,00	87,50	83,75	94,38	81,25
S9	**100,00**	**100,00**	**100,00**	**100,00**	**100,00**	**100,00**	99,38	99,38	**100,00**	97,50	98,75	99,38
S10	87,50	96,88	93,75	99,38	99,38	98,75	78,75	81,25	86,88	70,63	72,50	75,00
S12	90,00	96,88	98,75	**100,00**	**100,00**	**100,00**	96,88	**100,00**	96,88	85,63	**100,00**	75,63
S13	96,25	96,25	92,50	98,75	98,75	98,75	96,25	98,13	96,25	95,00	96,25	93,13
S14	84,38	99,38	90,63	**100,00**	**100,00**	99,38	96,25	98,13	99,38	91,25	97,50	98,13
S15	99,38	**100,00**	**100,00**	**100,00**	**100,00**	**100,00**	98,75	**100,00**	**100,00**	97,50	**100,00**	96,25
S16	27,50	78,13	14,38	97,50	**100,00**	84,38	82,50	92,50	90,00	80,63	90,00	84,38
S17	98,75	93,75	86,88	**100,00**	**100,00**	98,75	93,13	91,25	86,25	84,38	88,75	70,63
Mean	**73,24**	**89,45**	**72,30**	**97,54**	**98,79**	**91,95**	**89,26**	**93,44**	**86,80**	**81,33**	**91,17**	**78,13**
STD	26,11	13,74	35,74	4,09	1,97	16,57	14,47	10,78	21,29	17,48	11,98	20,98

[a] The term 'All chans' is the label for tests performed using the 64 channels of the dataset. The term 'Visual 8chans' is the label for the use of the 8 channels of the visual cortex used in the dataset (PO4, PO6, PO8, CB1, CB2, O1, O2 and Oz). The term 'Unicorn 8 chans' is the label for the use of the 8 channels of the dataset that correspond to the channels existing in the Unicorn Hybrid Black headset (Fz, C3, Cz, C4, Pz, PO7, PO8 and Oz).
[b] Normalization using DC Offset Removal (EEG signal with 10 stimulation iterations); [c] Normalization using amplitude signal in the range [-1 1] (EEG signal with 10 stimulation iterations); [d] Normalization using DC Offset Removal (EEG signal with an average of 10 stimulation iterations); [e] Normalization using amplitude signal in the range [-1 1] (EEG signal with an average of 10 stimulation iterations).

Table A.4: Classification accuracy (%) results for the C-VEP-ISR dataset for each subject to target identification with different methods of normalization using the sequence proposed in [3]. [a]

Methods	ITCCA				TRCA				Correlation Coefficients				Cosine Similarity			
Subject	All chans[b]	8 chans[c]	4 chans[c]	Unicorn 8chans[c]	All chans[c]	8 chans[c]	4 chans[b]	Unicorn 8chans[c]	All chans[c]	8 chans[c]	4 chans[c]	Unicorn 8chans[c]	All chans[c]	8 chans[c]	4 chans[c]	Unicorn 8chans[c]
S1	80,00	80,00	95,00	80,00	**100,00**	**100,00**	**100,00**	**100,00**	50,00	50,00	50,00	55,00	55,00	55,00	50,00	55,00
S2	**100,00**	**100,00**	**100,00**	**100,00**	**100,00**	**100,00**	**100,00**	**100,00**	50,00	50,00	80,00	65,00	40,00	50,00	80,00	60,00
S3	35,00	50,00	80,00	**100,00**	**100,00**	**100,00**	**100,00**	**100,00**	65,00	75,00	**100,00**	75,00	65,00	75,00	85,00	70,00
S4	55,00	75,00	90,00	65,00	95,00	95,00	**100,00**	95,00	35,00	35,00	35,00	35,00	35,00	35,00	35,00	35,00
S5	90,00	95,00	**100,00**	90,00	**100,00**	**100,00**	**100,00**	**100,00**	55,00	70,00	85,00	60,00	55,00	70,00	85,00	60,00
S6	85,00	**100,00**	90,00	90,00	**100,00**	**100,00**	**100,00**	95,00	75,00	75,00	75,00	80,00	80,00	75,00	75,00	85,00
S7	**100,00**	**100,00**	95,00	70,00	**100,00**	**100,00**	**100,00**	95,00	60,00	65,00	70,00	60,00	55,00	65,00	70,00	50,00
S8	**100,00**	**100,00**	**100,00**	**100,00**	**100,00**	**100,00**	**100,00**	**100,00**	60,00	75,00	95,00	65,00	60,00	65,00	90,00	60,00
S9	85,00	90,00	100,00	80,00	**100,00**	**100,00**	**100,00**	**100,00**	40,00	25,00	20,00	40,00	35,00	20,00	20,00	45,00
S11	**100,00**	**100,00**	**100,00**	**100,00**	**100,00**	**100,00**	**100,00**	**100,00**	55,00	60,00	65,00	55,00	45,00	60,00	65,00	50,00
S12	**100,00**	**100,00**	**100,00**	**100,00**	**100,00**	**100,00**	**100,00**	**100,00**	95,00	**100,00**	**100,00**	85,00	90,00	95,00	**100,00**	85,00
S13	**100,00**	**100,00**	**100,00**	95,00	**100,00**	**100,00**	**100,00**	**100,00**	85,00	90,00	**100,00**	75,00	80,00	90,00	**100,00**	75,00
Mean	**85,83**	**90,83**	**95,83**	**89,17**	**99,58**	**99,58**	**100,00**	**98,75**	**60,42**	**64,17**	**72,92**	**62,50**	**57,92**	**62,92**	**71,25**	**60,83**
STD	19,98	14,84	6,07	12,05	1,38	1,38	0,00	2,17	16,77	20,70	25,37	14,51	17,38	20,36	23,99	14,84

Table A.5: Classification accuracy (%) results for the C-VEP-ISR dataset for each subject to target identification with different methods of normalization using the first derivative of the EEG data, with the sequence proposed in [3].[a]

Method	D-ITCCA				D-TRCA				D-Correlation Coefficients				D-Cosine Similarity			
Subject	All chans[c]	8 chans[c]	4 chans[c]	Unicorn 8chans[c]	All chans[b]	8 chans[b]	4 chans[b]	Unicorn 8chans[b]	All chans[b]	8 chans[b]	4 chans[b]	Unicorn 8chans[b]	All chans[c]	8 chans[c]	4 chans[c]	Unicorn 8chans[c]
S1	**100,00**	**100,00**	**100,00**	**100,00**	**100,00**	**100,00**	**100,00**	**100,00**	80,00	85,00	85,00	80,00	85,00	80,00	90,00	90,00
S2	**100,00**	**100,00**	**100,00**	**100,00**	**100,00**	**100,00**	**100,00**	**100,00**	80,00	80,00	**95,00**	85,00	75,00	80,00	**95,00**	75,00
S3	**100,00**	**100,00**	**100,00**	**100,00**	**100,00**	**100,00**	**100,00**	**100,00**	75,00	90,00	**95,00**	85,00	75,00	85,00	**95,00**	75,00
S4	70,00	75,00	70,00	65,00	95,00	90,00	95,00	**100,00**	50,00	40,00	35,00	45,00	45,00	40,00	40,00	45,00
S5	70,00	85,00	95,00	80,00	**100,00**	**100,00**	**100,00**	**100,00**	25,00	35,00	45,00	30,00	35,00	35,00	45,00	40,00
S6	75,00	85,00	65,00	65,00	70,00	70,00	55,00	80,00	60,00	55,00	50,00	60,00	75,00	55,00	50,00	65,00
S7	65,00	85,00	55,00	55,00	**100,00**	**100,00**	75,00	65,00	50,00	50,00	45,00	50,00	50,00	50,00	45,00	50,00
S8	**100,00**	**100,00**	**100,00**	**100,00**	**100,00**	**100,00**	**100,00**	**100,00**	75,00	85,00	90,00	75,00	60,00	80,00	90,00	60,00
S9	80,00	90,00	85,00	80,00	**100,00**	**100,00**	**100,00**	**100,00**	25,00	25,00	15,00	35,00	25,00	20,00	15,00	35,00
S11	**100,00**	**100,00**	**100,00**	**100,00**	**100,00**	**100,00**	**100,00**	**100,00**	25,00	30,00	10,00	35,00	30,00	30,00	15,00	30,00
S12	**100,00**	**100,00**	**100,00**	95,00	**100,00**	**100,00**	**100,00**	**100,00**	85,00	85,00	85,00	70,00	85,00	85,00	85,00	75,00
S13	**100,00**	**100,00**	**100,00**	90,00	**100,00**	**100,00**	**100,00**	95,00	85,00	75,00	80,00	80,00	85,00	80,00	85,00	80,00
Mean	**88,33**	**93,33**	**89,17**	**85,83**	**97,08**	**96,67**	**93,75**	**95,00**	**59,58**	**61,25**	**60,83**	**60,83**	**60,42**	**60,00**	**62,50**	**60,00**
STD	14,19	8,50	15,79	15,79	8,28	8,50	13,56	10,61	23,05	23,55	29,85	20,09	21,65	23,27	29,47	18,82

[a] The term 'All chans' is the label for tests performed using the 12 channels chosen from the g.USBamp. The term '8chans' is the label for the use of the 8 channels of the visual cortex used in the dataset (CPz, Pz, P3, P4, POz, Po7, Oz, PO8). The term '4chans' is the label for the use of the 8 channels of the visual cortex used in the dataset (POz, Po7, Oz, PO8). The term 'Unicorn 8chans' is the label for the use of the 8 channels of the g.USBamp that correspond to the channels existing in the Unicorn Hybrid Black headset (Fz, C1, Cz, C2, Pz, PO7, PO8 and Oz).

[b] Normalization using DC Offset Removal (EEG signal with 10 stimulation iterations); [c] Normalization using amplitude signal in the range [-1 1] (EEG signal with 10 stimulation iterations).

Table A.6: Classification accuracy (%) results for the C-VEP-ISR benchmark dataset for each subject to identify targets with different methods of normalization, with the our proposed m-sequence. [a]

Method	ITCCA				TRCA				Correlation Coefficients				Cosine Similarity			
Subject	All chans[c]	8 chans[c]	4 chans[c]	Unicorn 8chans[b]	All chans[b]	8 chans[b]	4 chans[b]	Unicorn 8chans[b]	All chans[c]	8 chans[b]	4 chans[c]	Unicorn 8chans[c]	All chans[b]	8 chans[b]	4 chans[c]	Unicorn 8chans[c]
S1	**100,00**	**100,00**	**100,00**	**100,00**	**100,00**	**100,00**	**100,00**	**100,00**	55,00	60,00	60,00	55,00	55,00	60,00	60,00	55,00
S2	95,00	**100,00**	**100,00**	**100,00**	**100,00**	**100,00**	**100,00**	**100,00**	65,00	70,00	80,00	70,00	65,00	70,00	80,00	70,00
S3	**100,00**	**100,00**	**100,00**	**100,00**	**100,00**	**100,00**	**100,00**	**100,00**	75,00	85,00	**95,00**	75,00	75,00	80,00	**95,00**	75,00
S4	70,00	**100,00**	95,00	90,00	85,00	95,00	**100,00**	**100,00**	70,00	65,00	50,00	70,00	70,00	60,00	50,00	70,00
S5	90,00	**100,00**	100,00	85,00	90,00	90,00	90,00	95,00	40,00	50,00	55,00	50,00	50,00	50,00	55,00	50,00
S6	70,00	80,00	75,00	80,00	90,00	90,00	80,00	80,00	50,00	40,00	40,00	50,00	55,00	45,00	50,00	55,00
S7	**100,00**	**100,00**	**100,00**	85,00	**100,00**	**100,00**	**100,00**	**100,00**	60,00	60,00	80,00	60,00	65,00	60,00	75,00	60,00
S8	**100,00**	**100,00**	**100,00**	**100,00**	**100,00**	**100,00**	**100,00**	**100,00**	60,00	65,00	90,00	65,00	50,00	65,00	90,00	60,00
S9	90,00	**100,00**	**100,00**	85,00	**100,00**	**100,00**	**100,00**	**100,00**	30,00	25,00	30,00	25,00	25,00	25,00	35,00	25,00
S10	**100,00**	**100,00**	**100,00**	100.00	**100,00**	**100,00**	**100,00**	**100,00**	80,00	75,00	90,00	85,00	80,00	80,00	85,00	80,00
Mean	**91,50**	**98,00**	**97,00**	**92,50**	**96,50**	**97,50**	**97,00**	**97,50**	**58,50**	**59,50**	**67,00**	**60,50**	**59,00**	**59,50**	**67,50**	**60,00**
STD	11,41	6,00	7,48	7,83	5,50	4,03	6,40	6,02	14,67	16,50	21,82	15,88	14,97	15,72	19,14	14,83

Table A.7: Classification accuracy (%) results for the C-VEP-ISR benchmark dataset for each subject to identify targets with different methods of normalization, using the first derivative of the EEG data, with the our proposed m-sequence. [a]

Method	D-ITCCA				D-TRCA				D-Correlation coefficients				D-Cosine Similarity			
Subject	All chans[b]	8 chans[b]	4 chans[b]	Unicorn 8chans[b]	All chans[b]	8 chans[b]	4 chans[b]	Unicorn 8chans[b]	All chans[b]	8 chans[b]	4 chans[b]	Unicorn 8chans[b]	All chans[c]	8 chans[c]	4 chans[c]	Unicorn 8chans[b]
S1	**100,00**	**100,00**	**100,00**	95,00	**100,00**	**100,00**	**100,00**	**100,00**	55,00	50,00	65,00	60,00	55,00	55,00	55,00	65,00
S2	95,00	95,00	**100,00**	90,00	**100,00**	**100,00**	**100,00**	**100,00**	75,00	80,00	85,00	75,00	65,00	75,00	80,00	70,00
S3	**100,00**	**100,00**	**100,00**	**100,00**	**100,00**	**100,00**	**100,00**	**100,00**	**100,00**	**100,00**	**100,00**	**100,00**	**100,00**	**100,00**	95,00	**100,00**
S4	70,00	85,00	95,00	80,00	95,00	70,00	80,00	65,00	65,00	65,00	65,00	65,00	60,00	55,00	70,00	70,00
S5	65,00	80,00	80,00	70,00	95,00	**100,00**	95,00	80,00	60,00	65,00	70,00	65,00	65,00	70,00	75,00	70,00
S6	65,00	65,00	25,00	55,00	85,00	65,00	70,00	70,00	50,00	35,00	35,00	45,00	35,00	30,00	30,00	45,00
S7	85,00	90,00	30,00	45,00	**100,00**	**100,00**	35,00	65,00	45,00	45,00	45,00	45,00	55,00	50,00	40,00	50,00
S8	**100,00**	**100,00**	**100,00**	**100,00**	**100,00**	**100,00**	**100,00**	**100,00**	55,00	75,00	90,00	55,00	60,00	80,00	90,00	55,00
S9	70,00	85,00	**100,00**	80,00	**100,00**	**100,00**	**100,00**	**100,00**	5,00	5,00	10,00	5,00	5,00	10,00	20,00	5,00
S10	**100,00**	**100,00**	95,00	**100,00**	**100,00**	**100,00**	**100,00**	**100,00**	55,00	60,00	75,00	55,00	65,00	60,00	65,00	65,00
Mean	**85,00**	**90,00**	**82,50**	**81,50**	**97,50**	**93,50**	**88,00**	**88,00**	**56,50**	**58,00**	**64,00**	**57,00**	**56,50**	**58,50**	**62,00**	**59,50**
STD	15,00	10,95	28,13	18,58	4,61	13,05	20,27	15,20	22,70	24,92	25,87	23,04	22,92	24,19	24,00	23,07

[a] The term 'All chans' is the label for tests performed using the 12 channels chosen from the g.USBamp. The term '8chans' is the label for the use of the 8 channels of the visual cortex used in the dataset (CPz, Pz, P3, P4, POz, Po7, Oz, PO8). The term '4chans' is the label for the use of the 8 channels of the visual cortex used in the dataset (POz, Po7, Oz, PO8). The term 'Unicorn 8chans' is the label for the use of the 8 channels of the g.USBamp that correspond to the channels existing in the Unicorn Hybrid Black headset (Fz, C1, Cz, C2, Pz, PO7, PO8 and Oz).

[b] Normalization using DC Offset Removal (EEG signal with 10 stimulation iterations); [c] Normalization using amplitude signal in the range [-1 1] (EEG signal with 10 stimulation iterations).

Table A.8: Classification accuracy (%) results for the C-VEP benchmark dataset to each target sequence for subject identification. [a]

Methods	ITCCA			TRCA			Corr Coef			Cosine Similarity			DTW
Sequence	All chans[c]	Visual 8chans[c]	Unicorn 8chans[c]	All chans[b]	Visual 8chans[d]	Unicorn 8chans[d]	All chans[e]	Visual 8chans[e]	Unicorn 8chans[e]	All chans[e]	Visual 8chans[e]	Unicorn 8chans[e]	Visual 8chans[e]
T1	55,00	56,25	48,75	83,75	93,75	86,25	77,50	77,50	72,50	66,25	72,50	60,00	38,75
T2	50,00	52,50	50,00	83,75	92,50	83,75	81,25	83,75	77,50	73,75	78,75	72,50	32,50
T3	71,25	76,25	65,00	91,25	96,25	83,75	83,75	88,75	80,00	75,00	85,00	68,75	**52,50**
T4	57,50	75,00	60,00	86,25	96,25	88,75	86,25	88,75	78,75	76,25	83,75	67,50	43,75
T5	52,50	68,75	55,00	87,50	90,00	85,00	81,25	90,00	78,75	77,50	91,25	71,25	45,00
T6	53,75	73,75	62,50	90,00	93,75	86,25	75,00	85,00	70,00	70,00	83,75	61,25	35,00
T7	62,50	**78,75**	57,50	98,75	93,75	88,75	92,50	93,75	86,25	78,75	83,75	71,25	36,25
T8	57,50	65,00	52,50	91,25	91,25	78,75	81,25	86,25	80,00	75,00	82,50	78,75	33,75
T9	65,00	68,75	61,25	88,75	91,25	77,50	81,25	86,25	73,75	67,50	78,75	68,75	38,75
T10	57,50	70,00	58,75	83,75	92,50	81,25	85,00	**96,25**	81,25	76,25	91,25	72,50	27,50
T11	61,25	60,00	55,00	87,50	90,00	78,75	83,75	87,50	78,75	72,50	87,50	65,00	31,25
T12	63,75	71,25	68,75	90,00	91,25	85,00	88,75	93,75	86,25	81,25	88,75	73,75	31,25
T13	52,50	63,75	55,00	88,75	90,00	85,00	81,25	91,25	73,75	66,25	77,50	67,50	33,75
T14	56,25	67,50	48,75	86,25	92,50	82,50	81,25	87,50	82,50	71,25	83,75	72,50	42,50
T15	67,50	76,25	67,50	81,25	93,75	81,25	87,50	90,00	80,00	83,75	90,00	71,25	50,00
T16	60,00	70,00	62,50	88,75	87,50	81,25	76,25	86,25	72,50	71,25	85,00	67,50	46,25
T17	58,75	65,00	62,50	80,00	86,25	85,00	86,25	93,75	83,75	82,50	86,25	72,50	40,00
T18	56,25	67,50	53,75	83,75	90,00	75,00	83,75	90,00	82,50	72,50	83,75	63,75	36,25
T19	56,25	76,25	61,25	91,25	96,25	90,00	78,75	85,00	73,75	71,25	83,75	67,50	32,50
T20	52,50	55,00	53,75	86,25	96,25	90,00	87,50	93,75	80,00	76,25	88,75	72,50	40,00
T21	70,00	76,25	63,75	87,50	95,00	87,50	86,25	93,75	82,50	76,25	**93,75**	71,25	35,00
T22	70,00	75,00	65,00	83,75	88,75	82,50	90,00	93,75	90,00	80,00	90,00	75,00	37,50
T23	62,50	65,00	62,50	88,75	92,50	87,50	78,75	90,00	81,25	72,50	85,00	61,25	41,25
T24	53,75	71,25	56,25	88,75	90,00	81,25	82,50	82,50	76,25	75,00	76,25	68,75	40,00
T25	53,75	65,00	53,75	86,25	86,25	81,25	71,25	81,25	70,00	67,50	78,75	58,75	31,25
T26	51,25	60,00	51,25	88,75	87,50	68,75	68,75	71,25	65,00	57,50	66,25	58,75	28,75
T27	60,00	52,50	53,75	73,75	78,75	70,00	78,75	82,50	77,50	71,25	78,75	63,75	31,25
T28	51,25	61,25	52,50	85,00	**98,75**	83,75	86,25	87,50	72,50	68,75	77,50	60,00	31,25
T29	58,75	73,75	61,25	90,00	96,25	87,50	76,25	85,00	70,00	71,25	87,50	58,75	37,50
T30	51,25	62,50	58,75	78,75	93,75	73,75	81,25	85,00	76,25	72,50	82,50	70,00	40,00
T31	53,75	61,25	50,00	81,25	86,25	85,00	80,00	88,75	76,25	67,50	86,25	65,00	41,25
T32	45,00	66,25	56,25	86,25	90,00	80,00	82,50	83,75	78,75	73,75	78,75	65,00	38,75
Mean	**57,77**	**67,11**	**57,66**	**86,48**	**91,52**	**82,58**	**81,95**	**87,50**	**77,77**	**73,09**	**83,36**	**67,58**	**37,54**
STD	6,24	7,18	5,48	4,50	3,97	5,23	5,12	5,20	5,38	5,29	5,80	5,25	5,87

[a] The term 'All chans' is the label for tests performed using the 31 channels of the dataset. The term 'Visual 8chans' is the label for the use of the 8 channels of the visual cortex used in the dataset (Oz, O1, O2, POz, PO3, PO4, PO7, PO8). The term 'Unicorn 8chans' is the label for the use of the 8 channels of the dataset that correspond to the channels existing in the Unicorn Hybrid Black headset (Fz, C1, Cz, C2, Pz, PO7, PO8 and Oz).

[b] Normalization using DC Offset Removal (EEG signal with 10 stimulation iterations); [c] Normalization using amplitude signal in the range [-1 1] (EEG signal with 10 stimulation iterations); [d] Normalization using DC Offset Removal (EEG signal with an average of 10 stimulation iterations); [e] Normalization using amplitude signal in the range [-1 1] (EEG signal with an average of 10 stimulation iterations).

Table A.9: Classification accuracy (%) results for the C-VEP benchmark dataset to each target sequence for subject identification, using the first derivative of the EEG data. [a]

Methods	D-ITCCA			D-TRCA			D-Correlation Coefficients			D-Cosine Similarity		
Sequence	All chans[b]	Visual 8chans[c]	Unicorn 8chans[c]	All chans[c]	Visual 8chans[d]	Unicorn 8chans[d]	All chans[e]	Visual 8chans[e]	Unicorn 8chans[e]	All chans[e]	Visual 8chans[e]	Unicorn 8chans[e]
T1	65,00	65,00	53,75	83,75	91,25	87,50	80,00	86,25	80,00	60,00	80,00	50,00
T2	58,75	65,00	53,75	92,50	90,00	83,75	85,00	88,75	82,50	73,75	84,00	63,75
T3	82,50	82,50	73,75	95,00	97,50	82,50	85,00	92,50	80,00	73,75	89,00	70,00
T4	61,25	76,25	71,25	93,75	95,00	88,75	87,50	87,50	83,75	67,50	86,00	65,00
T5	66,25	68,75	61,25	91,25	92,50	86,25	95,00	**96,25**	93,75	75,00	96,00	71,25
T6	66,25	72,50	68,75	95,00	91,25	90,00	77,50	78,75	71,25	62,50	75,00	51,25
T7	78,75	78,75	76,25	**100,00**	97,50	92,50	90,00	90,00	83,75	77,50	90,00	67,50
T8	67,50	78,75	60,00	86,25	98,75	82,50	85,00	88,75	80,00	67,50	86,00	61,25
T9	67,50	72,50	61,25	86,25	95,00	80,00	78,75	86,25	76,25	56,25	83,00	58,75
T10	70,00	66,25	63,75	86,25	95,00	78,75	85,00	92,50	85,00	75,00	91,00	70,00
T11	66,25	66,25	62,50	91,25	93,75	76,25	90,00	93,75	82,50	75,00	93,00	71,25
T12	72,50	**83,75**	72,50	95,00	95,00	83,75	91,25	90,00	86,25	78,75	88,00	68,75
T13	58,75	68,75	65,00	88,75	96,25	87,50	88,75	88,75	81,25	66,25	86,00	58,75
T14	63,75	68,75	63,75	95,00	97,50	82,50	85,00	86,25	82,50	70,00	83,00	63,75
T15	68,75	80,00	68,75	95,00	92,50	75,00	93,75	97,50	83,75	71,25	93,00	71,25
T16	73,75	72,50	68,75	96,25	95,00	80,00	83,75	90,00	75,00	60,00	83,00	51,25
T17	61,25	71,25	61,25	87,50	91,25	92,50	91,25	92,50	92,50	77,50	89,00	67,50
T18	63,75	66,25	65,00	90,00	91,25	83,75	90,00	98,75	83,75	71,25	**98,00**	68,75
T19	63,75	70,00	57,50	90,00	98,75	92,50	92,50	91,25	87,50	77,50	88,00	68,75
T20	63,75	68,75	65,00	87,50	93,75	86,25	86,25	91,25	83,75	73,75	88,00	71,25
T21	80,00	80,00	67,50	92,50	95,00	83,75	88,75	92,50	85,00	80,00	90,00	68,75
T22	77,50	78,75	63,75	88,75	93,75	78,75	85,00	90,00	82,50	76,25	90,00	63,75
T23	68,75	72,50	67,50	90,00	92,50	90,00	85,00	87,50	85,00	62,50	85,00	53,75
T24	62,50	78,75	63,75	88,75	96,25	86,25	75,00	82,50	75,00	62,50	80,00	57,50
T25	63,75	63,75	62,50	87,50	88,75	83,75	77,50	82,50	73,75	58,75	80,00	51,25
T26	65,00	56,25	55,00	78,75	92,50	83,75	76,25	82,50	67,50	66,25	80,00	61,25
T27	63,75	66,25	60,00	86,25	88,75	72,50	78,75	82,50	82,50	60,00	79,00	60,00
T28	55,00	65,00	60,00	92,50	95,00	81,25	81,25	86,25	70,00	56,25	83,00	55,00
T29	66,25	75,00	62,50	88,75	96,25	90,00	80,00	88,75	78,75	76,25	86,00	71,25
T30	60,00	66,25	61,25	93,75	92,50	81,25	83,75	91,25	85,00	68,75	85,00	57,50
T31	56,25	67,50	51,25	83,75	92,50	80,00	80,00	87,50	78,75	71,25	86,00	72,50
T32	58,75	68,75	50,00	95,00	96,25	81,25	77,50	83,75	80,00	58,75	81,00	57,50
Mean	**66,17**	**71,29**	**63,09**	**90,39**	**94,02**	**83,91**	**84,69**	**88,91**	**81,21**	**68,98**	**86,06**	**63,13**
STD	6,61	6,32	6,16	4,40	2,65	4,98	5,40	4,50	5,69	7,19	5,08	7,03

[a] The term 'All chans' is the label for tests performed using the 31 channels of the dataset. The term 'Visual 8chans' is the label for the use of the 8 channels of the visual cortex used in the dataset (Oz, O1, O2, POz, PO3, PO4, PO7, PO8). The term 'Unicorn 8chans' is the label for the use of the 8 channels of the dataset that correspond to the channels existing in the Unicorn Hybrid Black headset (Fz, C1, Cz, C2, Pz, PO7, PO8 and Oz).
[b] Normalization using DC Offset Removal (EEG signal with 10 stimulation iterations); [c] Normalization using amplitude signal in the range [-1 1] (EEG signal with 10 stimulation iterations); [d] Normalization using DC Offset Removal (EEG signal with an average of 10 stimulation iterations); [e] Normalization using amplitude signal in the range [-1 1] (EEG signal with an average of 10 stimulation iterations).

Table A.10: Classification accuracy (%) results for the C-VEP-ISR dataset dataset to each target sequence for subject identification, with the sequence from [3]. [a]

Method	ITCCA				TRCA				Correlation Coefficients				Cosine Similarity			
Sequence	All chans[b]	8 chans[b]	4 chans[c]	Unicorn 8chans[b]	All chans[c]	8 chans[c]	4 chans[b]	Unicorn 8chans[c]	All chans[b]	8 chans[b]	4 chans[c]	Unicorn 8chans[b]	All chans[b]	8 chans[b]	4 chans[b]	Unicorn 8chans[b]
T1	78,33	83,33	75,00	85,00	90,00	88,33	86,67	91,67	38,33	38,33	41,67	35,00	40,00	36,67	41,67	36,67
T2	78,33	85,00	76,67	78,33	85,00	86,67	80,00	80,00	36,67	41,67	48,33	38,33	38,33	43,33	40,00	35,00
T3	85,00	88,33	**91,67**	83,33	**96,67**	**96,67**	93,33	95,00	45,00	40,00	**51,67**	46,67	46,67	40,00	**50,00**	46,67
T4	76,67	86,67	86,67	70,00	88,33	95,00	86,67	78,33	31,67	36,67	46,67	36,67	30,00	35,00	45,00	35,00
Mean	**79,58**	**85,83**	**82,50**	**79,17**	**90,00**	**91,67**	**86,67**	**86,25**	**37,92**	**39,17**	**47,08**	**39,17**	**38,75**	**38,75**	**44,17**	**38,33**
STD	3,20	1,86	6,92	5,83	4,25	4,25	4,71	7,20	4,77	1,86	3,61	4,49	5,94	3,20	3,82	4,86

Table A.11: Classification accuracy (%) results for the C-VEP-ISR benchmark dataset to each target sequence for subject identification with different methods of normalization, using the first derivative of the EEG data, with the sequence from [3]. [a]

Methods	D-ITCCA				D-TRCA				D-Correlation Coefficients				D-Cosine Similarity			
Sequence	All chans[b]	8 chans[b]	4 chans[c]	Unicorn 8chans[b]	All chans[c]	8 chans[c]	4 chans[b]	Unicorn 8chans[c]	All chans[b]	8 chans[b]	4 chans[c]	Unicorn 8chans[b]	All chans[b]	8 chans[b]	4 chans[b]	Unicorn 8chans[b]
T1	85,00	**86,67**	80,00	85,00	91,67	88,33	85,00	93,33	33,33	35,00	45,00	33,33	30,00	35,00	38,33	30,00
T2	66,67	70,00	70,00	63,33	91,67	**93,33**	78,33	75,00	30,00	33,33	36,67	30,00	33,33	36,67	36,67	31,67
T3	66,67	70,00	78,33	66,67	90,00	**93,33**	85,00	80,00	46,67	**51,67**	48,33	46,67	48,33	50,00	**53,33**	50,00
T4	78,33	78,33	75,00	66,67	78,33	81,67	78,33	76,67	46,67	50,00	43,33	50,00	50,00	50,00	46,67	50,00
Mean	**74,17**	**76,25**	**75,83**	**70,42**	**87,92**	**89,17**	**81,67**	**81,25**	**39,17**	**42,50**	**43,33**	**40,00**	**40,42**	**42,92**	**43,75**	**40,42**
STD	7,86	6,91	3,82	8,53	5,57	4,79	3,33	7,20	7,59	8,37	4,25	8,50	8,85	7,11	6,71	9,60

[a] The term 'All chans' is the label for tests performed using the 12 channels chosen from the g.USBamp. The term '8chans' is the label for the use of the 8 channels of the visual cortex used in the dataset (CPz, Pz, P3, P4, POz, Po7, Oz, PO8). The term '4chans' is the label for the use of the 8 channels of the visual cortex used in the dataset (POz, Po7, Oz, PO8). The term 'Unicorn 8chans' is the label for the use of the 8 channels of the g.USBamp that correspond to the channels existing in the Unicorn Hybrid Black headset (Fz, C1, Cz, C2, Pz, PO7, PO8 and Oz).
[b] Normalization using DC Offset Removal (EEG signal with 10 stimulation iterations); [c] Normalization using amplitude signal in the range [-1 1] (EEG signal with 10 stimulation iterations).

Table A.12: Classification accuracy (%) results for the C-VEP benchmark dataset to each target sequence for subject identification, using our propose sequence[a]

Methods	ITCCA				TRCA				Correlation Coefficients				Cosine Similarity			
Sequence	All chans[c]	8 chans[c]	4 chans[c]	Unicorn 8chans[c]	All chans[b]	8 chans[b]	4 chans[b]	Unicorn 8chans[b]	All chans[b]	8 chans[b]	4 chans[b]	Unicorn 8chans[b]	All chans[c]	8 chans[c]	4 chans[c]	Unicorn 8chans[c]
T1	76,00	86,00	80,00	78,00	88,00	88,00	86,00	86,00	20,00	28,00	32,00	20,00	20,00	30,00	32,00	22,00
T2	88,00	92,00	92,00	88,00	94,00	**96,00**	**96,00**	94,00	26,00	34,00	**48,00**	30,00	26,00	32,00	**50,00**	26,00
T3	92,00	94,00	92,00	86,00	92,00	94,00	88,00	92,00	40,00	38,00	42,00	40,00	38,00	38,00	48,00	38,00
T4	82,00	**96,00**	82,00	76,00	94,00	94,00	94,00	86,00	34,00	42,00	46,00	30,00	34,00	42,00	46,00	34,00
Mean	**84,50**	**92,00**	**86,50**	**82,00**	**92,00**	**93,00**	**91,00**	**89,50**	**30,00**	**35,50**	**42,00**	**30,00**	**29,50**	**35,50**	**44,00**	**30,00**
STD	6,06	3,74	5,55	5,10	2,45	3,00	4,12	3,57	7,62	5,17	6,16	7,07	6,98	4,77	7,07	6,32

Table A.13: Classification accuracy (%) results for the C-VEP-ISR benchmark to each target sequence for subject identification with different methods of normalization, using the first derivative of the EEG data, with our proposed m-sequence. [a]

Methods	D-ITCCA				D-TRCA				D-Correlation Coefficients				D-Cosine Similarity			
Sequence	All chans[b]	8 chans[b]	4 chans[b]	Unicorn 8chans[b]	All chans[b]	8 chans[b]	4 chans[b]	Unicorn 8chans[b]	All chans[c]	8 chans[c]	4 chans[c]	Unicorn 8chans[c]	All chans[c]	8 chans[c]	4 chans[b]	Unicorn 8chans[b]
T1	68,00	60,00	66,00	62,00	80,00	80,00	72,00	68,00	40,00	42,00	46,00	42,00	40,00	40,00	46,00	46,00
T2	70,00	78,00	66,00	72,00	**90,00**	**90,00**	70,00	78,00	32,00	34,00	38,00	32,00	30,00	36,00	38,00	34,00
T3	78,00	76,00	70,00	78,00	86,00	86,00	76,00	80,00	50,00	**52,00**	46,00	48,00	52,00	48,00	**52,00**	50,00
T4	**80,00**	76,00	80,00	70,00	84,00	88,00	78,00	80,00	30,00	28,00	34,00	36,00	32,00	36,00	34,00	34,00
Mean	**74,00**	**72,50**	**70,50**	**70,50**	**85,00**	**86,00**	**74,00**	**76,50**	**38,00**	**39,00**	**41,00**	**39,50**	**38,50**	**40,00**	**42,50**	**41,00**
STD	5,10	7,26	5,72	5,72	3,61	3,74	3,16	4,97	7,87	9,00	5,20	6,06	8,65	4,90	6,98	7,14

[a] The term 'All chans' is the label for tests performed using the 12 channels chosen from the g.USBamp. The term '8chans' is the label for the use of the 8 channels of the visual cortex used in the dataset (CPz, Pz, P3, P4, POz, Po7, Oz, PO8). The term '4chans' is the label for the use of the 8 channels of the visual cortex used in the dataset (POz, Po7, Oz, PO8). The term 'Unicorn 8chans' is the label for the use of the 8 channels of the g.USBamp that correspond to the channels existing in the Unicorn Hybrid Black headset (Fz, C1, Cz, C2, Pz, PO7, PO8 and Oz).

[b] Normalization using DC Offset Removal (EEG signal with 10 stimulation iterations); [c] Normalization using amplitude signal in the range [-1 1] (EEG signal with 10 stimulation iterations).

B

SSVEP Synthetic Data

The EEG signals acquired with the SSVEP paradigm contain the target frequency identified in the frequency domain [17]. To validate the implementation of the algorithms of the EEG signal processing methods, files were generated using synthetic data that made it possible to carry out tests to confirm the correct construction of the different methods. The use of synthetic data has the advantage of manipulating the amplitudes of the different signals that constitute a real EEG signal (fundamental, harmonics and noise).

These data files were created for the validation of the Cepstrum method, particularly, since there is not much information on the use of this method in an SSVEP framework with a high number of targets such as that presented in [74].

To guarantee the greatest possible equality with the study datasets [74], tested in the chapter 4, an algorithm was created to organize a four-dimensional matrix, with dimensions of the matrix similar to a subject's data file. The output signal for each of the targets were obtained by sampling the sum of sinusoidal functions of the fundamental frequency and and the signals constituted by five harmonics of the respective frequency. After several tests with only noise-free data, the noise was introduced in the form of a vector with standard normal distribution pseudorandom values, which were added to each sample of each channel, for each of the simulated trials.

In the following figures, it is possible to see the graphics for an example of one of the synthetic data files created, for the target with a frequency of 12 Hz. In figure B.1, a null value was used for the amplitude of the noise signal that is added, while the fundamental signal has an amplitude equal to 2 and the amplitude of the harmonics is equal to 1. In figure B.2, the noise signal that is added has an amplitude of 1.4. In both figures, it is possible to find the original signal at the fundamental frequency (a)) and its respective FFT (c)), as well as the contaminated signal (b)) and its respective FFT (d)).

Through the graphs of the signals represented as a function of time and the graphs of the respective FFT, it is possible to validate the synthetic data and the desired target frequencies, thus proving the correct construction of the synthetic data that were used to test the methods used in the SSVEP paradigm.

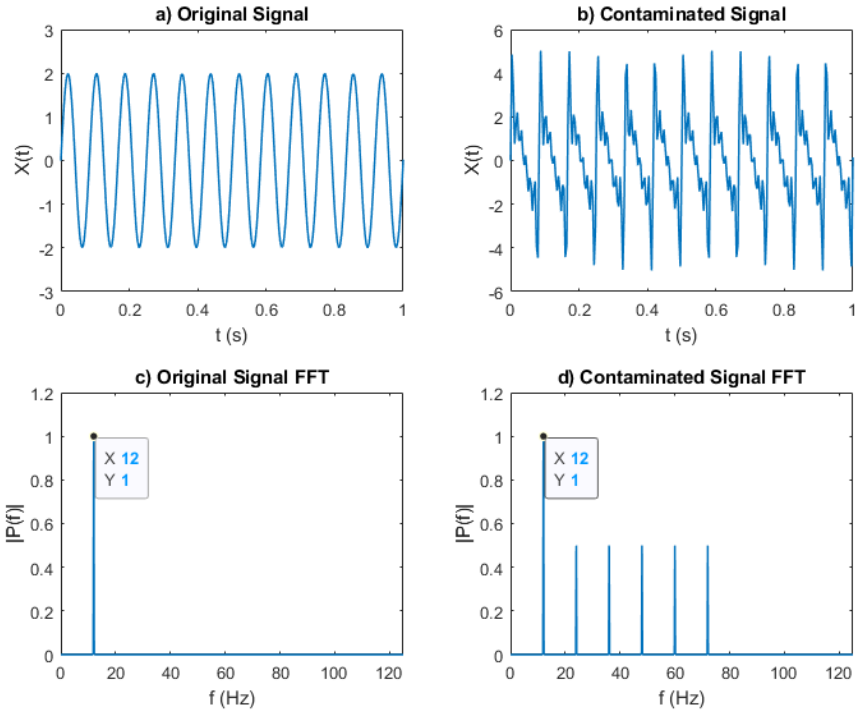

Figure B.1: Synthetic data for a frequency of 12 Hz, without noise component.

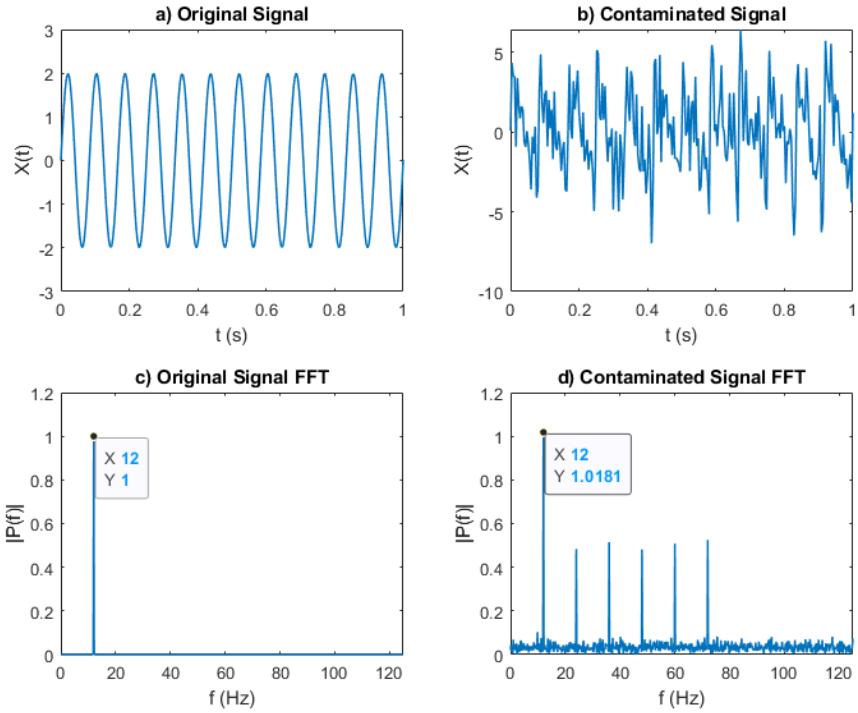

Figure B.2: Synthetic data for a frequency of 12 Hz, with noise component.

C

Analysis of Cepstrum Results

In tables A.1 and 5.1 of chapter 5 are presented the results of the various processing methods applied, including the Cepstrum method. In those results, it appears that the average accuracy values for 40 different targets, with Cepstrum, are 54.75% with the use of all channels in the dataset and between 30% and 35% for the other tested scenarios (8 channels of the visual cortex - PO4, PO6, PO8, CB1, CB2, O1, O2 and Oz and 8 channels corresponding to the channels of the Unicorn Hybrid Black headset - Fz, C3, Cz, C4, Pz, PO7, PO8 and Oz).

Due to this fact, an intensive analysis of frequencies that were not detected by the Cepstrum method was carried out and it is possible to verify that these results are due to 2 reasons: 1) the 0.2 Hz interval between the target frequencies used in the experiment; 2) the effect of the non-linear distortion caused by the non-linearity of the Infinite impulse response filter (IIR) used in the pre-processing stage of EEG data. To solve this problem, a finite impulse response filter (FIR) with higher-order was used, since it does not introduce distortion due to the linear phase response.

Table C.1 resulted from the analysis performed on some subjects with a different number of targets, where it is possible to conclude that Cepstrum is a fast method and that guarantees high accuracy values for the identification of targets, to be implemented in real-time for more practical applications, with a set of commands, as long as the number of targets is reduced and the interval between frequencies is high enough for the method to be able to detect correctly. For 5 different targets it was possible to obtain values of accuracy higher than 85% in all the scenarios and with the 4 subjects tested.

Figure C.1 shows the plots resulting from processing one of the channels for one of the trials acquired from subject 9. In these plots, it is possible to visualize the signal resulting from the acquisition in the time domain during the 6 seconds of stimulation, the respective FFT and the signal resulting from the application of Cepstrum. In this example, where stimulation was performed at a frequency of 10Hz, Cepstrum can identify a frequency of 7.812Hz, that is, a difference of 0.188 Hz to the target frequency.

Table C.1: Classification accuracy (%) results for the offline mode in the SSVEP benchmark dataset (based on 5 seconds stimulation) with Cepstrum method for 4 different subjects.

Subject	Nº targets	Frequencies (Hz)	All chans	Visual 8chans	Unicorn 8chans
S5	**20**	8; 8,4; 8,8; 9,2; 9,6; 10; 10,4; 10,8; 11,2; 11,6; 12; 12,4; 12,8; 13,2; 13,6; 14; 14,4; 14,8; 15,2; 15,6	83,33%	41,67%	45,83%
S15			78,33%	37,50%	44,17%
S20			85,00%	38,33%	47,50%
S35			84,17%	39,17%	43,33%
S5	**14**	8; 8,6; 9,2; 9,8; 10,4; 11; 11,6; 12,2; 12,8; 13,4; 14; 14,6; 15,2; 15,8	94,05%	38,10%	55,95%
S15			95,24%	48,81%	57,14%
S20			95,24%	44,05%	60,71%
S35			91,67%	34,52%	55,95%
S5	**10**	8; 8,8; 9,6; 10,4; 11,2; 12; 12,8; 13,6; 14,4; 15,2	98,33%	56,67%	60,00%
S15			100,00%	56,67%	71,67%
S20			95,00%	45,00%	70,00%
S35			100,00%	45,00%	71,67%
S5	**8**	8; 9; 10; 11; 12; 13; 14; 15	97,92%	85,42%	89,58%
S15			97,42%	85,42%	79,17%
S20			100,00%	79,17%	77,08%
S35			100,00%	77,08%	85,42%
S5	**5**	8; 9; 10; 11; 12	100,00%	90,00%	96,67%
S15			100,00%	90,00%	93,33%
S20			100,00%	83,33%	83,33%
S35			100,00%	90,00%	90,00%

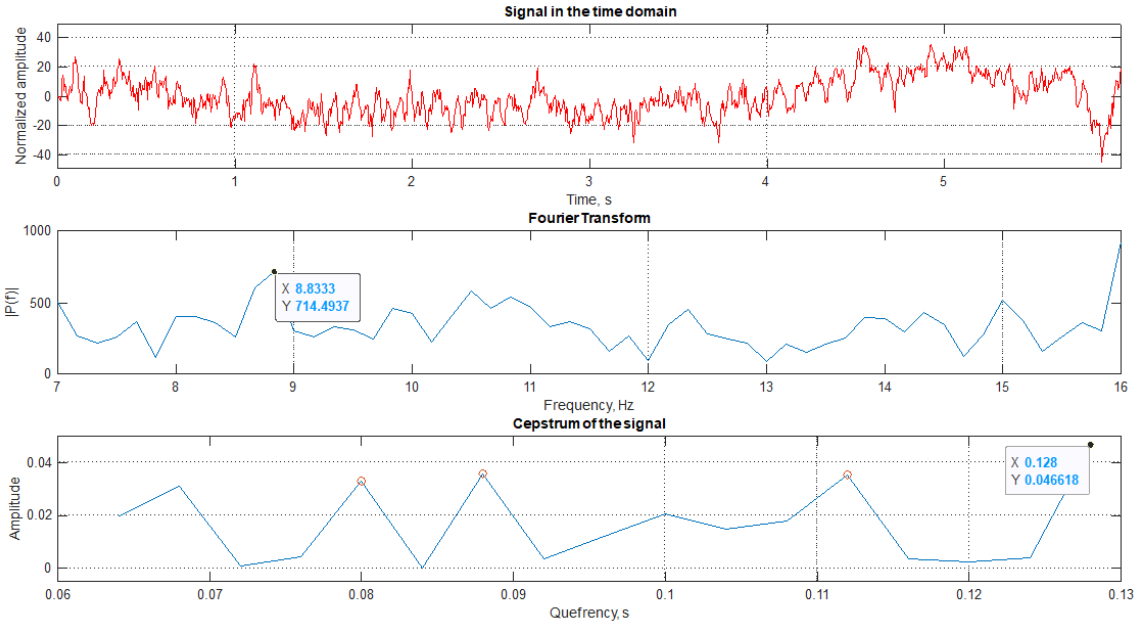

Figure C.1: Time-domain signal resulting from the Oz channel of the international 10/20 system during a trial conducted on subject 9 for target 1 and respective FFT and analysis of Cepstrum.

D

International 10/20 System and Brain Signal Frequency Bands

EEG is a complementary diagnostic examination that by placing electrodes on the scalp will allow, through various leads between these electrodes, the detection, amplification, recording and interpretation of patterns of electrical activity associated with the cerebral cortex. Brain electrical activity is in the order of millionths of Volts (μV). This activity is amplified to be picked up by scalp electrodes. The electrical potential captured in the scalp reflects the electrical activity of a given area (height, depth and width).

The International 10/20 system is an international method to describe the location of scalp electrodes and it is based on the relationship between the location of an electrode and the respective area of the cerebral cortex. The numbers '10' and '20' in the name of the system refers to the that that the distance between adjacent electrodes are 10% or 20% of the total front to back or left to right distance, the letters identify the lobe and the number identify the hemisphere location in the skull.

The letters covers the following lobes:

- 'F' - Frontal;
- 'T' - Temporal;
- 'C' - Central (used only for identification purposes);
- 'P' - Parietal;
- 'O' - Occipital.

The 'z' zero in the electrode refers to an electrode placed on the mid line of the skull, while even numbers (2,4,6,8) refers to electrodes positioned on the right hemisphere and odd numbers (1,3,5,7) refers to electrodes positioned on the left hemisphere.

The skull was divided in four anatomical landmarks used for the essential electrode positioning:

- Nasion - point between the forehead and the nose;

- Inion - lowest point of the skull from the back of the head;
- Pre aurical left point - point anterior to the left ear;
- Pre aurical right point - point anterior to the right ear.

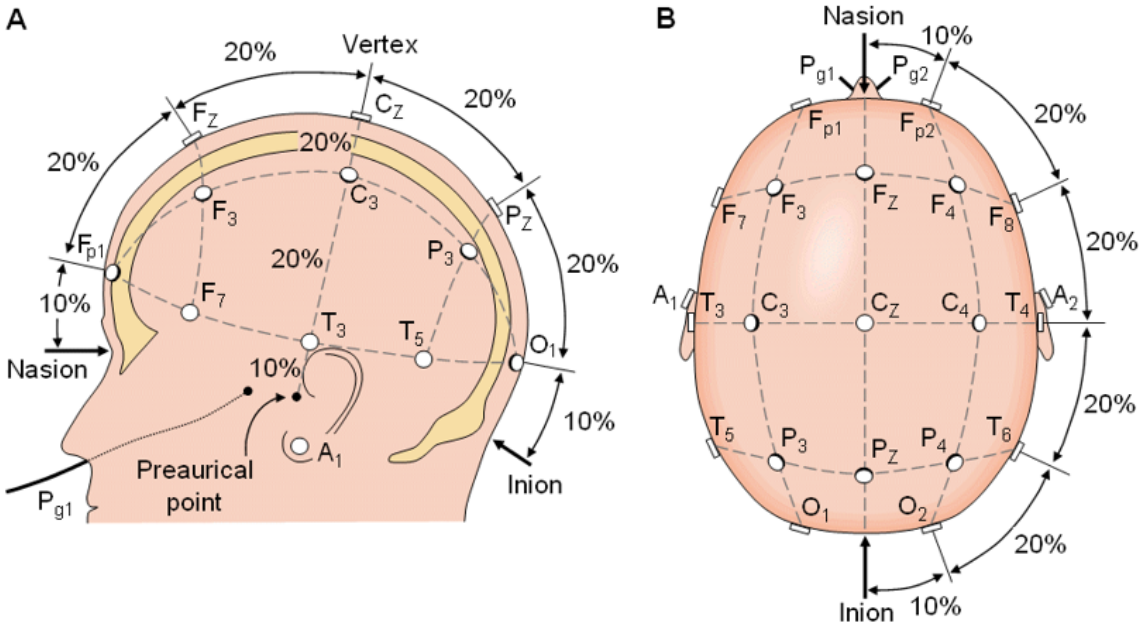

Figure D.1: Map of the 10/20 Electrode Placement System. [1]

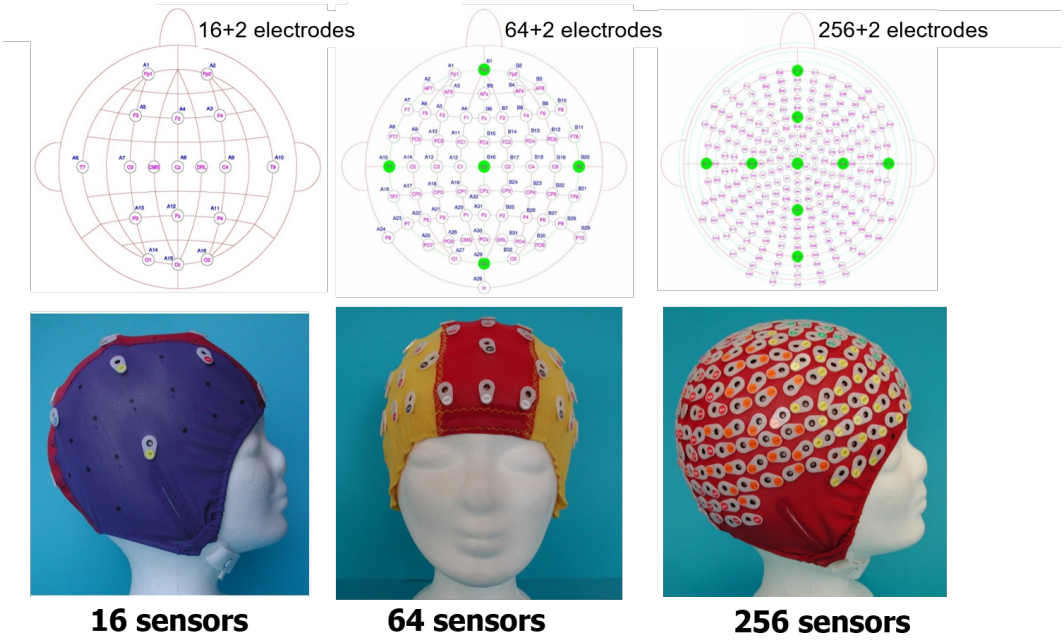

Figure D.2: Map with the Electrodes Placement System and the EEG cap for 16, 64 and 256 sensors.

[1] `https://alivelearn.net/?p=664`

The rhythmic activity of a EEG is divided into bands separated by frequency and the brain waves can be represented by six typical bands based on the frequency range between 1 and 100 Hz with an amplitude between 10 and 200 μV.

Principal Brain Waves				
Brain Wave	**Location**	**Mental State**	**Amplitude (μV)**	**Frequency (Hz)**
Delta δ	Everywhere	Reduced consciousness or during sleep	100-150	<4
Theta θ	Temporal and Parietal	During emotional stress	40-80	4-7.9
Alpha α	Occipital and Parietal	Associated to mental relaxation and have a reduce amplitude during mental imagery	50-100	8-12
Mu μ	Frontal	Associated to intension of movement	-	8-13
Beta β	Parietal and Frontal	Consciously alert, thinking activities	10-20	14-25
Gamma γ	Originated in the thalamus	Associated with attention, perception and cognition	$\simeq$10	25-100

Table D.1: Principal brain waves.

E

Headsets

E.0.1 Unicorn Hybrid Black

The Unicorn Hybrid Black (g.tec) is a high-quality wearable EEG-headset for brain-computer interface (BCI) applications to perfectly acquire brain waves, with the correct positions of EEG electrodes for real brain wave recordings. It is possible to many people without the BCI knowledge the ability to acquire and process brain signals, from only display the signals, to design and control attached devices or interact with computer programs or applications, toys, for example, with his own software from g.tec.

Users can not only acquire EEG data from eight Unicorn Hybrid EEG Electrodes (8 positions on the head (FZ, C3, CZ, C4, PZ, PO7, OZ, PO8, in the international 10/20 system), but also may analyze and process the data with the Unicorn Suite, the main software environment. Reference and ground EEG electrodes are fixed on the mastoids of the user for perfect noise reduction. Unicorn Hybrid EEG electrodes are patented and allows to record dry or with gel and therefore enables the usage for many different BCI applications. The electrodes are placed per default on the:

- sensorimotor cortex to realize motor imagery-based BCIs,
- over the central, parietal and occipital areas for P300 paradigms
- over the parietal regions for steady-state visual evoked potential (SSVEP) and code-based VEP paradigms.

In order to provide perfect noise reduction, reference and ground EEG electrodes are fixed on the mastoids of the user.

The Unicorn Brain Interface is wearable and extremely lightweight to reduce movement artefacts. It fits perfectly to different head shapes and keeps the device in position. This guarantees the solid contact of the electrode to the scalp which is key for high-quality EEG recordings.

Figure E.1: Unicorn Hybrid Black Amplifier from g.tec. Source: G.tec

E.0.2 g.USBamp

g.USBamp is a high-performance and high-accuracy biosignal amplifier and acquisition/processing system from g.tec (Austria). With g.USBamp, it is possible to record activity from the brain, eyes, heart, muscles and more – including respiration, galvanic skin response, temperature and other physiological and physical parameters.

g.USBamp has a total of 4 independent grounds guarantee that there is no interference between the recorded signals. The amplifier connects easily to the USB port on your PC/notebook and can be used for data recording. It is also possible to build a multi-channel system with more than 16 channels using multiple g.USBamp devices. A synchronization cable guarantees that all devices are sampling at exactly the same frequency.

Figure E.2: gUSBamp amplifier board from g.tec [1]

[1] `https://www.mathworks.com/hardware-support/gtec.html`